

**ELECTROCHEMICAL INVESTIGATION OF  
PHENOL AND CHLOROPHENOL DERIVATIVES**

BY

Nurudeen Adewale Odewunmi

A Thesis Presented to the  
DEANSHIP OF GRADUATE STUDIES

**KING FAHD UNIVERSITY OF PETROLEUM & MINERALS**

DHAHRAN, SAUDI ARABIA

1963 ١٣٨٣

In Partial Fulfillment of the  
Requirements for the Degree of

**MASTER OF SCIENCE**

In

CHEMISTRY

JUNE 2012

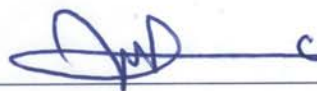
# KING FAHD UNIVERSITY OF PETROLEUM & MINERALS

DHAHRAN 31261, SAUDI ARABIA

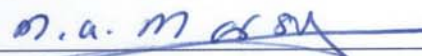
## DEANSHIP OF GRADUATE STUDIES

This thesis, written by Nurudeen Adewale Odewunmi under the direction of his thesis advisor and approved by his thesis committee, has been presented to and accepted by the Dean of Graduate Studies, in partial fulfillment of the requirements for the degree of **MASTER OF SCIENCE in CHEMISTRY**.

Thesis Committee



Dr. Abdel-Nasser Kawde (Advisor)



Dr. Mohamed. Ali Morsy (Member)



Dr. Nouri M. Hassan (Member)



Dr. Abdullah J. Al-Hamdan  
Department Chairman



Dr. Salam A. Zummo  
Dean of Graduate Studies

28/8/12

Date



DEDICATED

TO MY

IMMEDIATE AND EXTENDED FAMILY

## ACKNOWLEDGEMENTS

Glory is to Allah, the sustainers of the Universe. The first without beginning and the last without an end. Who has made me a Muslim. I pray to Allah to make my feet firm in the path of Islam and to continue to guide and guard me in all my endeavors and not to leave me to myself for a twinkle of an eye. I do extend my gratitude to King Fahd University of Petroleum and Minerals for giving me the opportunity to study my Master degree.

My sincere appreciation goes to my advisor, Dr. Abdel-Nasser Kawde, for his support in term of advices, time, encouragement and moral values that made me to overcome the challenges that Research Assistant faces in the Kingdom. Also to my committee members, Dr. Nouri Muhammed Hassan and Dr. Mohammad Ali Morsy for providing me with their valuable comments and feedback to improve my work.

I would like also to appreciate the chemistry department, beginning with the chairman Dr. Abdullah J. Al-Hamdan, all the Faculty, the technical staff, my colleagues in the laboratory and the department.

Dr. Kawde and I would like to express our gratitude to Center of Excellence in Nanotechnology (CENT) for funding the current research (CoRE-NT-07).

My sincere appreciations go to the Nigerian community, African and Asian communities for their support.

Thank you all, May Allah rewards you abundantly.

## TABLE OF CONTENTS

<b>ACKNOWLEDGEMENTS .....</b>	<b>iv</b>
<b>TABLE OF CONTENTS .....</b>	<b>v</b>
<b>LIST OF TABLES .....</b>	<b>ix</b>
<b>LIST OF FIGURES .....</b>	<b>x</b>
<b>THESIS ABSTRACT (ENGLISH) .....</b>	<b>xxiv</b>
<b>THESIS ABSTRACT (ARABIC) .....</b>	<b>xxv</b>
<b>NOMENCLATURE.....</b>	<b>xxvi</b>
<b>CHAPTER 1 .....</b>	<b>1</b>
<b>1.0 INTRODUCTION.....</b>	<b>1</b>
1.1 ANALYTICAL CHEMISTRY .....	1
1.2 ELECTROANALYTICAL TECHNIQUES.....	3
1.2.1 Polarography .....	6
1.2.2 Voltammetry .....	6
1.2.2.1 Normal Pulse Voltammetry .....	6
1.2.2.2 Differential Pulse Voltammetry .....	8
1.2.2.3 Square Wave Stripping Voltammetry .....	10
1.2.2.4 Cyclic Voltammetry .....	13

1.3 ELECTROANALYTICAL CELL IN VOLTAMMETRY .....	16
1.3.1 Reference Electrodes .....	16
1.3.2 Counter or Auxiliary Electrodes .....	16
1.3.3 Working Electrodes .....	16
1.3.3.1 Mercury Electrodes .....	17
1.3.3.2 Carbon Electrodes .....	17
1.3.3.2.1 Glassy or Virteous Carbon Electrodes (GCE) .....	17
1.3.3.2.2 Carbon Paste Electrodes (CPE) .....	18
1.3.3.2.3 Glassy Carbon Paste Electrodes (GCPE).....	18
1.3.3.2.4 Graphite Pencil Electrodes (GPE) .....	18
1.3.3.3 Modified Electrodes (MEs).....	22
1.4 PHENOLS.....	22
1.4.1 Significance of Chlorophenols.....	22
1.5 OBJECTIVES .....	25
<b>CHAPTER 2.....</b>	<b>26</b>
<b>2.0 LITERATURE REVIEW .....</b>	<b>26</b>
2.1 ANALYTICAL DETERMINATION OF PHENOLIC COMPOUNDS.....	26
2.2 ELECTROANALYTICAL DETERMINATION OF PHENOLIC COMPOUNDS	
.....	29
2.2.1 Attempts to Alleviate Fouling Effect on Solid Electrodes.....	32
2.2.2 Electro-oxidation of Chlorophenols .....	34

<b>CHAPTER 3 .....</b>	<b>36</b>
<b>3.0 RESEARCH METHODOLOGY .....</b>	<b>36</b>
3.1 CHEMICALS AND REAGENTS PREPARATIONS .....	37
3.1.1 Chemicals.....	37
3.1.2 Reagents Preparations .....	39
3.1.2.1 Supporting Electrolyte Solutions .....	39
3.1.2.2 Preparations of Standard Solutions .....	42
3.2 EXPERIMENTAL SET-UP .....	43
3.2.1 Electrode Materials .....	43
3.2.2 Potentiostat /galvanostat Units.....	43
3.3 PROCEDURES AND STRATEGIES .....	46
3.3.1 Electrochemical Optimization .....	47
3.3.2 Analytical Performance .....	48
<b>CHAPTER 4 .....</b>	<b>49</b>
<b>4.0 RESULTS AND DISCUSSIONS .....</b>	<b>49</b>
4.1 ELECTROCHEMICAL INVESTIGATION OF PHENOL AND CHLOROPHENOL DERIVATIVES .....	49
4.1.1 Proof of Concept Using Square Wave Stripping Adsorptive Voltammetry (SWSV) Technique for Electrochemical Investigation of Phenol and Chlorophenol Derivatives.....	50

4.1.2	Electrochemical Investigation at Different pHs Using Cyclic Voltammetry and Square Wave Stripping Voltammetry.....	53
4.1.2.1	Investigation Using Cyclic Voltammetry (CV) .....	53
4.1.2.2	Investigation Using Square Wave Stripping Voltammetry (SWSV).....	64
4.1.3	Confirmation of Fouling on Glassy Carbon Electrode (GCE) by Cyclic Voltammetry and Square Wave Stripping Voltammetry .....	74
4.1.4	Electrochemical Investigation at Different Accumulation Potentials Using Cyclic Voltammetry and Square Wave Stripping Voltammetry .....	84
4.1.4.1	Investigation Using Cyclic Voltammetry .....	84
4.1.4.2	Investigation Using Square Wave Stripping Voltammetry .....	92
4.2	ANALYTICAL DETERMINATION OF 2-CHLOROPHENOL .....	103
4.2.1	Electrochemical Optimization of Peak One (P1) of 2-Chlorophenol .....	106
4.2.2	Electrochemical Optimization of Peak Two (P2) of 2-Chlorophenol .....	112
4.2.3	Analytical Performance of Peak One (P1) and Peak Two (P2) .....	121
4.2.4	Calibration Curves for Peak One (P1) and Peak Two (P2) .....	121
<b>CHAPTER 5</b>	.....	<b>126</b>
<b>5.0</b>	<b>CONCLUSIONS AND FUTURE PROSPECTIVES .....</b>	<b>126</b>
5.1	CONCLUSIONS.....	126
5.2	FUTURE PROSPECTIVES .....	127
<b>REFERENCES</b>	.....	<b>129</b>
<b>VITAE</b>	.....	<b>134</b>



## LIST OF TABLES

Table 3.1: Properties of Phenol and Chlorophenols Derivatives. ....	38
Table 3.2: Compositions for Various pHs of 0.1M Phosphate Buffer Solutions for 100ml Solution. ....	40
Table 4.1: Electro-decomposition Potentials, Experimental and Calculated $pK_a$ Values of Phenol and Chlorophenol Derivatives. ....	51
Table 4.2: Optimum pH, $[A^-]$ and Their Corresponding $E_p$ of Cyclic Voltammetry Technique for Phenol and Chlorophenol Derivatives. ....	62
Table 4.3: Optimum pH, $[A^-]$ and Their Corresponding $E_p$ of Square Wave Stripping Voltammetry Technique for Phenol and Chlorophenol Derivatives. ....	72
Table 4.4: Optimized Conditions for Peak One (P1) and Peak Two (P2) of 2- Chlorophenol. ....	120

## LIST OF FIGURES

Figure 1.1: Analytical chemistry methods of analyses (2). .....	2
Figure 1.2: Classifications of interfacial electrochemical methods (4). .....	5
Figure 1.3: Excitation signal for normal pulse voltammetry (3). .....	7
Figure 1.4: Excitation signal for differential pulse voltammetry (3). .....	9
Figure 1.5: Square wave voltammetry waveform (6). .....	11
Figure 1.6: Square wave stripping voltammograms for $i_f$ (C), $i_r$ (B) and net current (A) (6). .....	12
Figure 1.7: Potential-time excitation signals in cyclic voltammetric experiment (8). ....	14
Figure 1.8: Typical cyclic voltammogram, where $ip^c$ and $ip^a$ show the peak cathodic and anodic current respectively for a reversible reaction (8). .....	15
Figure 1.9: Schematic diagrams of (A) carbon paste electrode (CPE) and graphite pencil electrode (GPE) (12). .....	20
Figure 1.10: SEM images of (A) 0.4 – 12 $\mu m$ GCP particle size (B) 20 – 50 $\mu m$ GCP particle size and (C) CP (11). .....	21
Figure 1.11: Chemical structures of phenol and the five basic types of chlorophenols. .	24
Figure 2.1: SEM micrographs of: (A) polyphenol-covered GC electrode; (B) GC substrate (57). .....	31

Figure 3.1: Single distilled, double distilled and ultrapure water systems .....	41
Figure 3.2: (A) Experimental set-up and (B) Electrochemical cell. ....	45
Figure 4.1: (A) Plot of phenols and their corresponding oxidation peak potentials (B) Plot of phenols and their corresponding experimental and calculated $pK_a$ values. ....	52
Figure 4.2: (A) Cyclic voltammograms of 30 $\mu$ M phenol at +0.40 V accumulation potential, 60s accumulation time in 0.1 M PBS at different pHs. (a) 5.00, (b) 6.00, (c) 7.00, (d) 8.00 and (e) 9.00. (B) Corresponding plots showing the peak heights (1) and the peak shift (2) in the electro-decomposition potentials. ....	56
Figure 4.3: (A) Cyclic voltammograms of 30 $\mu$ M 2-chlorophenol at +0.40 V accumulation potential, 60s accumulation time in 0.1 M PBS at different pHs. (a) 5.00, (b) 6.00, (c) 7.00, (d) 8.00 and (e) 9.00. (B) Corresponding plots showing the peak heights (1) and the peak shift (2) in the electro- decomposition potentials. ....	57
Figure 4.4: (A) Cyclic voltammograms of 30 $\mu$ M 2,4-dichlorophenols at +0.40 V accumulation potential, 60s accumulation time in 0.1 M PBS at different pHs. (b) 5.00, (b) 6.00, (c) 7.00, (d) 8.00 and (e) 9.00. (B) Corresponding plots showing the peak heights (2) and the peak shift (2) in the electro- decomposition potentials. ....	58

Figure 4.5: (A) Cyclic voltammograms of 30  $\mu\text{M}$  2,6-dichlorophenols at +0.40 V accumulation potential, 60s accumulation time in 0.1 M PBS at different pHs. (a) 5.00, (b) 6.00, (c) 7.00, (d) 8.00 and (e) 9.00. (B) Corresponding plots showing the peak heights (1) and the peak shift (2) in the electro-decomposition potentials. .... 59

Figure 4.6: (A) Cyclic voltammograms of 30  $\mu\text{M}$  2,4,6-trichlorophenol at +0.40 V accumulation potential, 60s accumulation time in 0.1 M PBS at different pHs. (a) 5.00, (b) 6.00, (c) 7.00, (e) 8.00 and (e) 9.00. (B) Corresponding plots showing the peak heights (1) and the peak shift (2) in the electro-decomposition potentials. .... 60

Figure 4.7: (A) Cyclic voltammograms of 30  $\mu\text{M}$  Pentachlorophenol at +0.40 V accumulation potential, 60s accumulation time in 0.1 M PBS at different pHs. (a) 5.00, (b) 6.00, (c) 7.00, (d) 8.00 and (e) 9.00. (B) Corresponding plots showing the peak heights (1) and the peak shift (2) in the electro-decomposition potentials. .... 61

Figure 4.8: Chart of the pH effect and the corresponding  $\text{pK}_a$  by Cyclic Voltammetry. 63

Figure 4.9: (A) Square wave stripping voltammograms of 30  $\mu\text{M}$  phenol at +0.40 V accumulation potential, 60s accumulation time in 0.1 M PBS at different pHs. (a) 5.00, (b) 6.00, (c) 7.00, (d) 8.00 and (e) 9.00. (B) Corresponding plots showing the peak area (1) and the peak shift (2) in the electro-decomposition potentials. .... 66

Figure 4.10: (A) Square wave stripping voltammograms of 30  $\mu\text{M}$  2-chlorophenol at +0.40 V accumulation potential, 60s accumulation time in 0.1 M PBS at different pHs. (a) 5.00, (b) 6.00, (c) 7.00, (d) 8.00 and (e) 9.00. (B) Corresponding plots showing the peak area (1) and the peak shift (2) in the electro-decomposition potentials. .... 67

Figure 4.11: (A) Square wave stripping voltammograms of 30  $\mu\text{M}$  2,4-dichlorophenol at +0.40 V accumulation potential, 60s accumulation time in 0.1 M PBS at different pHs. (a) 5.00, (b) 6.00, (c) 7.00, (e) 8.00 and (e) 9.00. (B) Corresponding plots showing the peak area (1) and the peak shift (2) in the electro-decomposition potentials. .... 68

Figure 4.12: (A) Square wave stripping voltammograms of 30 $\mu\text{M}$  2,6-dichlorophenol at +0.40 V accumulation potential, 60s accumulation time in 0.1 M PBS at different pHs. (a) 5.00, (b) 6.00, (c) 7.00, (d) 8.00 and (e) 9.00. (B) Corresponding plots showing the peak area (1) and the peak shift (2) in the electro-decomposition potentials. .... 69

Figure 4.13: (A) Square wave stripping voltammograms of 30  $\mu\text{M}$  2,4,6-trichlorophenol at +0.40 V accumulation potential, 60s accumulation time in 0.1 M PBS at different pHs. (a) 5.00, (b) 6.00, (c) 7.00, (d) 8.00 and (e) 9.00. (B) Corresponding plots showing the peak area (1) and the peak shift (2) in the electro-decomposition potentials. .... 70

Figure 4.14: (A) Square wave stripping voltammograms of 30  $\mu\text{M}$  Pentachlorophenol sodium salt at +0.40 V accumulation potential, 60s accumulation time in 0.1

M PBS at different pHs. (a) 5.00, (b) 6.00, (c) 7.00, (d) 8.00 and (e) 9.00.

(B) Corresponding plots showing the peak area (1) and the peak shift (2) in electro-decomposition potentials. .... 71

Figure 4.15: Chart of the pH effect and the corresponding  $pK_a$  by Square Wave Stripping Voltammetry. .... 73

Figure 4.16: (A) Cyclic voltammograms (B) Square wave stripping voltammograms for 30  $\mu$ M phenol at +0.40V accumulation potential, 60s accumulation time in 0.1M PBS pH 9.00 (a) blank, (b) first scan, (c) second scan without polishing and (d) rescan in the blank solution without polishing right after scanning in 30 $\mu$ M phenol. (Note, c in A is same as d in B) ..... 77

Figure 4.17: (A) Cyclic voltammograms (B) Square wave stripping voltammograms for 30  $\mu$ M 2-chlorophenol at +0.40V accumulation potential, 60s accumulation time in 0.1M PBS pH 7.00 (a) blank, (b) first scan, (c) second scan without polishing and (d) rescan in the blank solution without polishing right after scanning in 30 $\mu$ M 2-chlorophenol. (Note, C in A is same as d in B) ..... 78

Figure 4.18: (A) Cyclic voltammograms (B) Square wave stripping voltammograms for 30  $\mu$ M 2,4-dichlorophenol at +0.40 V accumulation potential, 60s accumulation time in 0.1M PBS pH 7.00 (a) blank, (b) first scan, (c) second scan without polishing and (d) rescan in the blank solution without polishing right after scanning in 30  $\mu$ M 2,4-dichlorophenol. (Note, c in A is same as d in B) ..... 79

Figure 4.19: (A) Cyclic voltammograms (B) Square wave stripping voltammograms for 30  $\mu\text{M}$  2,6-dichlorophenol at +0.40 V accumulation potential, 60s accumulation time in 0.1 M PBS pH 6.00 (a) blank, (b) first scan, (c) second scan without polishing and (d) rescan in the blank solution without polishing after scanning with 30 $\mu\text{M}$  2,6- dichlorophenol. (Note, c in A is same as d in B) ..... 80

Figure 4.20: (A) Cyclic voltammograms (B) Square wave stripping voltammograms for 30  $\mu\text{M}$  2,4,6-trichlorophenol at +0.40 V accumulation potential, 60s accumulation time in 0.1 M PBS pH 6.00 (a) blank, (b) first scan, (c) second scan without polishing and (d) rescan in the blank solution without polishing right after scanning with 30 $\mu\text{M}$  2,4,6- trichlorophenol. (Note, c in A is same as d in B) ..... 81

Figure 4.21: (A) Cyclic voltammograms (B) Square wave stripping voltammograms for 30  $\mu\text{M}$  pentachlorophenol at +0.40 V accumulations potential, 60s accumulation time in 0.1 M PBS pH 5.00 (a) blank, (b) first scan (c) second scan without polishing. .... 82

Figure 4.22: Cyclic voltammograms for 5 cycles at +0.40 V accumulation potential, 60s accumulation time in 0.1 M PBS at corresponding optimized pH for (A) 2-chlorophenol, pH 7.00, (B) Pentachlorophenol sodium salt, pH 5.00 and (C) Hydroquinone, pH 7.00..... 83

Figure 4.23: Cyclic voltammograms for 30  $\mu\text{M}$  phenol showing the signal behavior at different accumulation potentials (a) blank at 400 mV, (b) 400mV, (c) 500

mV, (d) 600 mV, (e) 700 mV, (f) 800 mV, (g) 900 mV (h) 1000 mV.

Working conditions: scan rate, 100 mV/s; sample interval, 2 mV and

accumulation time, 60 s in 0.1 M PBS at pH 9.00..... 86

Figure 4.24: Cyclic voltammograms of 30  $\mu$ M 2-chlorophenol showing the signal

behavior at different accumulation potentials (a) blank at 400 mV, (b)

400mV, (c) 500 mV, (d) 600 mV, (e) 700 mV, (f) 800 mV, (g) 900 mV (h)

1000 mV. Working conditions: scan rate, 100 mV/s; sample interval, 2 mV

and accumulation time, 60 s in 0.1 M PBS at pH 7.00. .... 87

Figure 4.25: Cyclic voltammograms of 30  $\mu$ M 2,4-dichlorophenols showing the signal

behavior at different accumulation potentials (a) blank at 400 mV, (b)

400mV, (c) 500 mV, (d) 600 mV, (e) 700 mV, (f) 800 mV, (g) 900 mV (h)

1000 mV. Working conditions: scan rate, 100 mV/s; sample interval, 2 mV

and accumulation time, 60 s in 0.1 M PBS at pH 7.00. .... 88

Figure 4.26: Cyclic voltammograms of 30  $\mu$ M 2,6-dichlorophenols showing the signal

behavior at different accumulation potentials (a) blank at 400 mV, (b)

400mV, (c) 500 mV, (d) 600 mV, (e) 700 mV, (f) 800 mV, (g) 900 mV (h)

1000 mV. Working conditions: scan rate, 100 mV/s; sample interval, 2 mV

and accumulation time, 60 s in 0.1 M PBS at pH 6.00. .... 89

Figure 4.27: Cyclic voltammograms of 30 $\mu$ M 2,4,6-trichlorophenols showing the signal

behavior at different accumulation potentials (a) blank at 400 mV, (b)

400mV, (c) 500 mV, (d) 600 mV, (e) 700 mV, (f) 800 mV, (g) 900 mV (h)



1000 mV. Working conditions: scan rate, 100 mV/s; sample interval, 2 mV  
and accumulation time, 60 s in 0.1 M PBS at pH 6.00. .... 90

Figure 4.28: Cyclic voltammograms of 30  $\mu$ M pentachlorophenol sodium salt showing  
the signal behavior at different accumulation potentials (a) blank at 500 mV,  
(b) 500mV, (c) 600 mV, (d) 700 mV, (e) 800 mV, (f) 900 mV, (g) 1000 mV.  
Working conditions: scan rate, 100 mV/s; sample interval, 2 mV and  
accumulation time, 60 s in 0.1 M PBS at pH 5.00. .... 91

Figure 4.29: Square wave stripping voltammograms for 30  $\mu$ M phenol showing the signal  
behavior at different accumulation potentials (a) blank at 400 mV, (b)  
400mV, (c) 500 mV, (d) 600 mV, (e) 700 mV, (f) 800 mV, (g) 900 mV (h)  
1000 mV. Working conditions: amplitude, 25 mV; frequency 15 Hz;  
increment, 8 mV and accumulation time, 60 s in 0.1M PBS at pH 9.00. .... 94

Figure 4.30: Square wave stripping voltammograms of 30  $\mu$ M 2-chlorophenol showing  
the signal behavior at different accumulation potentials (a) blank at 400 mV,  
(b) 400mV, (c) 500 mV, (d) 600 mV, (e) 700 mV, (f) 800 mV, (g) 900 mV  
(h) 1000 mV. Working conditions: amplitude, 25 mV; frequency 15 Hz;  
increment, 8 mV and accumulation time, 60 s in 0.1M PBS at pH 7.00. .... 95

Figure 4.31: Square wave stripping voltammograms of 30  $\mu$ M 2,4-dichlorophenols  
showing the signal behavior at different accumulation potentials (a) blank at  
400 mV, (b) 400mV, (c) 500 mV, (d) 600 mV, (e) 700 mV, (f) 800 mV, (g)  
900 mV (h) 1000 mV. Working conditions: amplitude, 25 mV; frequency 15

Hz; increment, 8 mV and accumulation time, 60 s in 0.1M PBS at pH	
7.00.....	96

Figure 4.32: Square wave stripping voltammograms of 30 $\mu$ M 2,6-dichlorophenols	
showing the signal behavior at different accumulation potentials (a) blank at	
400 mV, (b) 400mV, (c) 500 mV, (d) 600 mV, (e) 700 mV, (f) 800 mV, (g)	
900 mV (h) 1000 mV. Working conditions: amplitude, 25 mV; frequency 15	
Hz; increment, 8 mV and accumulation time, 60 s in 0.1M PBS at pH	
6.00.....	97

Figure 4.33: Square wave stripping voltammograms of 30 $\mu$ M 2,4,6-trichlorophenol	
showing the signal behavior at different accumulation potentials (a) blank at	
400 mV, (b) 400mV, (c) 500 mV, (d) 600 mV, (e) 700 mV, (f) 800 mV, (g)	
900 mV (h) 1000 mV. Working conditions: amplitude, 25 mV; frequency 15	
Hz; increment, 8 mV and accumulation time, 60 s in 0.1M PBS at pH	
6.00.....	98

Figure 4.34: Square wave stripping voltammograms of 30 $\mu$ M pentachlorophenol sodium	
salt showing the signal behavior at different accumulation potentials (a)	
blank at 500 mV, (b) 500mV, (c) 600 mV, (d) 700 mV, (e) 800 mV, (f) 900	
mV, (g) 1000 mV. Working conditions: amplitude, 25 mV; frequency 15	
Hz; increment, 8 mV and accumulation time, 60 s in 0.1M PBS at pH	
5.00.....	99

Figure 4.35: Effect of accumulation potential on the studied phenol and chlorophenol derivatives using square wave stripping voltammetry at +0.40 V and +1.00 V.....	100
Figure 4.36: Scheme I and II showing the oxidation and reduction pathways of phenol and 2-chlorophenol. ....	101
Figure 4.37: Scheme III, IV, V and VI showing the oxidation and reduction pathways of 2,4-dichlorophenol, 2,6-dichphenol, 2,4,6-trichlorophenol and pentachlorophenol sodium salt. ....	102
Figure 4.38: Square wave stripping voltammograms of 30 $\mu$ M 2-chlorophenol showing the signal behavior at different accumulation potentials: (a) 100 mV, (b) 200 mV, (c) 300 mV, (d) 400 mV, (e) 500 mV, (f) 600 mV, (g) 700 mV, (h) 800 mV, (i) 900 mV, (j) 1000 mV, (k) 1100 mV and (l) 1200 mV for 60s accumulation time in 0.1 M PBS at pH 7.00. Other working conditions, as in Figure 4.30. ....	104
Figure 4.39: Corresponding plot showing the peak heights and accumulation potentials of 2-chlorophenol. ....	105
Figure 4.40: (A) Square wave stripping voltammograms for 30 $\mu$ M 2-chlorophenol in 0.1 M of pH 7.00 PBS at different amplitudes: (a) 15 mV, (b) 25 mV, (c) 50 mV, (d) 75 mV and (e) 100 mV. Working conditions: accumulation time 60s; accumulation potential, +0.40 V; pulse width, 8 mV and frequency, 15 Hz. (B) Corresponding plots of Current ( $\mu$ A) vs. Amplitude (mV). ....	107

Figure 4.41: (A) Square wave stripping voltammograms for 30 $\mu$ M 2-chlorophenol in 0.1 M PBS of pH 7.00 at 50 mV amplitude for different frequencies: (a) 15 Hz, (b) 25 Hz, (c) 50 Hz, (d) 75 Hz, (e) 100 Hz and (f) 125 Hz. Other working conditions as in Figure 4.40. (B) Corresponding plots of Current ( $\mu$ A) vs. Frequency (Hz). ..... 108

Figure 4.42: (A) Square wave stripping voltammograms for 30  $\mu$ M 2-chlorophenol in 0.1 M PBS of pH 7.00 at 100 Hz frequency for different pulse widths: (a) 2 mV, (b) 4 mV, (c) 6 mV, (d) 8 mV and (e) 10 mV. Other working conditions as in Figure 4.40. (B) Corresponding plots of Current ( $\mu$ A) vs. Increment, pulse width (mV)..... 109

Figure 4.43: (A) Square wave stripping voltammograms for 30  $\mu$ M 2-chlorophenol in 0.1 M PBS of pH 7.00 at 8 mV pulse width for different accumulation times: (a) 15 s, (b) 30 s, (c) 60 s, (d) 90 s and (e) 120 s. Other working conditions as in Figure 4.40. (B) Corresponding plots of Current ( $\mu$ A) vs. Accumulation time (s). ..... 110

Figure 4.44: (A) Square wave stripping voltammograms for 20  $\mu$ M 2-chlorophenol in 0.1 M PBS of pH 7.00 at 8mV pulse width for different accumulation times: (a) 15 s, (b) 30 s, (c) 60 s, (d) 90 s and (e) 120 s. Other working conditions as in Figure 4.40. (B) Corresponding plot of Current ( $\mu$ A) vs. Accumulation time (s). ..... 111

Figure 4.45: (A) Square wave stripping voltammograms of 30  $\mu$ M 2-chlorophenol at +1.10 V accumulation potential 0.1 M PBS at different pHs. (a) 5.00, (b)

6.00, (c) 7.00, (d) 8.00 and (e) 9.00. Working conditions: accumulation time, 60 s; amplitude, 25 mV; pulse width, 8 mV and frequency, 15 Hz. (B) Corresponding plots showing the peak area (1) and the peak shift (2) in the electro-decomposition potentials against the pHs..... 114

Figure 4.46: (A) Square wave stripping voltammograms for 30  $\mu$ M 2-chlorophenol in 0.1 M PBS of pH 5.00 for different frequency values: (a) 15 Hz, (b) 25 Hz, (c) 50 Hz, (d) 75 Hz, (e) 100 Hz and (f) 125 Hz. Other working conditions as in Figure 4.45. (B) Corresponding plots of Current ( $\mu$ A) vs. Frequency (Hz).  
.....115

Figure 4.47: (A) Square wave stripping voltammograms for 30  $\mu$ M 2-chlorophenol at 100 Hz frequency for different amplitudes: (a) 15 mV, (b) 25 mV, (c) 50 mV, (d) 75 mV, (e) 100 mV (f) 125 mV and (g) 150 mV. Other working conditions as in Figure 4.45. (B) Corresponding plots of Current ( $\mu$ A) vs. Amplitude (mV)..... 116

Figure 4.48: (A) Square wave stripping voltammograms for 30  $\mu$ M 2-chlorophenol at 100 mV amplitude for different pulse width: (a) 2 mV, (b) 4 mV, (c) 6 mV, (d) 8 mV, and (e) 10 mV. Other working conditions as in Figure 4.45. (B) Corresponding plots of Current ( $\mu$ A) vs. Increment, pulse width (mV).... 117

Figure 4.49: (A) Square wave stripping voltammograms for 30  $\mu$ M 2-chlorophenol at 8 mV pulse width for different accumulation times: (a) 15 s, (b) 30 s, (c) 60 s, (d) 90 s and (e) 120s. Other working conditions as in Figure 4.45. (B) Corresponding plot of Current ( $\mu$ A) vs. accumulation time (s)..... 118

Figure 4.50: (A) Square wave stripping voltammograms for 10  $\mu\text{M}$  2-chlorophenol at 8 mV pulse width for different accumulation times: (a) 15 s, (b) 30 s, (c) 60 s, (d) 90 s and (e) 120 s. Other working conditions as in Figure 4.45. (B) Corresponding plot of Current ( $\mu\text{A}$ ) vs. accumulation time (s)..... 119

Figure 4.51: (A) Square wave stripping Voltammograms for analytical performance of seven repeated measurements for 30  $\mu\text{M}$  2-chlorophenol of Peak One (P1 at +0.40 V) in 0.1 M PBS pH 7.00. Working conditions: accumulation time, 60 s; amplitude, 50 mV; pulse width, 8 mV and frequency, 100 Hz. (B) Square wave stripping Voltammograms for analytical performance of seven repeated measurements for 30  $\mu\text{M}$  2-chlorophenol of Peak Two (P1 at +1.10 V) in 0.1 M PBS pH 5.00. Working conditions: accumulation time, 60 s; amplitude, 100 mV; pulse width, 8 mV and frequency, 100 Hz. .... 123

Figure 4.52: (A) Square wave stripping Voltammograms for 2-chlorophenol at different concentrations for Peak One (P1 at +0.40 V) in 0.1 M PBS pH 7.00 (a) blank, (b) 10  $\mu\text{M}$ , (c) 20  $\mu\text{M}$ , (d) 25  $\mu\text{M}$ , (e) 35  $\mu\text{M}$ , (f) 40  $\mu\text{M}$ , (g) 50  $\mu\text{M}$ , (h) 55  $\mu\text{M}$  and (i) 60  $\mu\text{M}$ . Working conditions: accumulation time, 60 s; amplitude, 50 mV; pulse width, 8 mV and frequency, 100 Hz. (B) Voltammograms for 2-chlorophenol at different concentration for peak two (P2 at +1.10V) in 0.1 M PBS pH 5.00 (a) blank, (b) 2  $\mu\text{M}$ , (c) 3  $\mu\text{M}$ , (d) 4  $\mu\text{M}$ , (e) 5  $\mu\text{M}$ , (f) 6  $\mu\text{M}$ , (g) 7  $\mu\text{M}$ , (h) 9  $\mu\text{M}$  and (i) 11  $\mu\text{M}$ . Working conditions: accumulation time, 60 s; amplitude, 100 mV; pulse width, 8 mV and frequency, 100 Hz. .... 124

Figure 4.53: Corresponding plots for calibration curves (A) Peak One (P1) and (B) Peak  
Two (P2). ..... 125

## THESIS ABSTRACT (ENGLISH)

**Name:** Nurudeen Adewale Odewunmi  
**Title:** Electrochemical Investigation of Phenol and Chlorophenol Derivatives  
**Major:** Chemistry  
**DATE:** June, 2012

Phenol and chlorophenol derivatives were electrochemically investigated on the surface of glassy carbon electrode (GCE) by cyclic voltammetry (CV) and square wave adsorptive stripping voltammetry (SWASV) at optimum pH of 0.1 M phosphate buffer solutions. The obtained results indicated that phenol, 2-chlorophenol, 2,4-dichlorophenol, 2,6-dichlorophenol, 2,4,6-trichlorophenol and pentachlorophenol, with no exception, exhibit fouling effects as a result of first oxidized irreversible phenoxy radical products. At the same time, phenol and all studied chlorophenol derivatives, except pentachlorophenol, showed isomerization peaks. Such peaks were obtained all at once at a single scan via the selection of the right value for accumulation potential. The typical oxidation peak of 2-chlorophenol was obtained by fixing the accumulation potential at +0.40 V, where the isomerize peaks were obtained with relatively much higher signals by accumulation at +1.10 V. Both peaks were optimized for possible analytical determination. Detection limits of 18.99  $\mu\text{M}$  (2.44 ppm) and 1.11  $\mu\text{M}$  (140 ppb) were obtained from monitoring the conventional and the isomerize peak respectively. Relative standard deviation of 1.84% and 1.31% for seven repeated measurement at the same concentration were obtained for the conventional and isomerized peaks of 2-chlorophenol respectively. The current study proved that the well-known phenol surface passivation/fouling effect is no longer a failure, and can be useful for more sensitive electroanalytical determination of phenol and phenol derivatives.

Master of Science Degree  
King Fahd University of Petroleum and Minerals  
Dhahran, Saudi Arabia

June, 2012



## ملخص الرسالة

**الاسم:** نور الدين ادويل اودينو

**عنوان الدراسة:** الدراسة الكهروكيميائية للفينول ومشتقات الكلوروفينول

**التخصص:** الكيمياء

**تاريخ التخرج:** يونيو - 2012

تم في هذه الرسالة دراسة وبحث الخواص الالكتروكيميائية للفينول ومشتقات الكلوروفينول على أسطح أقطاب الكربون الزجاجي (GCE) بواسطة الفولتامترية الدائرية وفولتامترية الامتزاز الكشطية رباعية الموجة في محلول 0.1 مولاري من محلول الفوسفات المنظم. وأشارت النتائج أن الفينول، و مركب احادي الكلوروفينول 2-كلوروفينول ومركب ثنائي 2, 4 الكلوروفينول ومركب ثنائي 2, 6 الكلوروفينول و ايضا مركب ثلاثي 2, 4, 6 الكلوروفينول ومركب خماسي الكلوروفينول أظهرت تأثير ، دون استثناء، يحمل آثار تلوث نتيجة لأول منتجات فينوكسي أكسدة راديكالية. في الوقت نفسه، الفينول ومشتقاتها التي تم دراستها اظهرت قمم ايزومرية. تم الحصول على ذروة الأكسدة النموذجية من مركب احادي الكلوروفينول 2-كلوروفينول عن طريق تحديد إمكانات التراكم في 0.40+ فولت، حيث تم الحصول على القمم الايزوميرية مع إشارات نسبيا أعلى بكثير من تراكم عند 1.10+ فولت.. تم الحصول على حدود كشف 18.99 ميكرومولار (2.44 جزء في المليون) و 1.11 ميكرومولار (140 جزء في البليون). الانحراف المعياري النسبي 1.84% 1.31% لعدد سبعة تحاليل لنفس التركيز للقمم التقليدية والايزومريزم على التوالي. أثبتت الدراسة الحالية تطوير طريقة ممتازة لتحليل الفينول ومشتقات الكلوروفينول.

**ماجستير العلوم**

**جامعة الملك فهد للبترول والمعادن**

**الظهران - المملكة العربية السعودية**

## NOMENCLATURE

$K_a$	Acid Dissociation Constant
$pK_a$	$-\log_{10} k_a$
$[A^-]$	Anion Concentration
Acc. Pot.	Accumulation Potential
Amp.	Amplitude
BP	Boiling Point
Freq.	Frequency
Cal.	Calculated
$E_p$	Electro-decomposition Potential
Exp.	Experimental
FID	Flame Ionization Detector
LPME	Liquid Phase Microextraction
Mol. Wt.	Molecular Weight
MS	Mass Spectroscopy
MP	Melting Point
NA	Not Available
Opt.	Optimum

P1 and P2

Peak One and Peak Two

Sp. Gr.

Specific Gravity

## **CHAPTER 1**

### **1.0 INTRODUCTION**

#### **1.1 ANALYTICAL CHEMISTRY**

Analytical chemistry is the study of the separation, identification and the quantification of the chemical components of natural and artificial materials (1). However, all the procedures involved in analytical chemistry can be classified into two namely; classical and instrumentation methods (2) as shown in Figure 1.1.

Separations are achieved in classical methods (wet chemistry) by the use of techniques such as precipitation, extraction and distillation, identifications by color, odor or melting points and quantifications by weight and volume measurements. Instrumentation on the other hand, utilizes different electron modes. Transfer of electrons for electroanalytical, electron excitations for spectroscopy and interaction of electrons for chromatography.

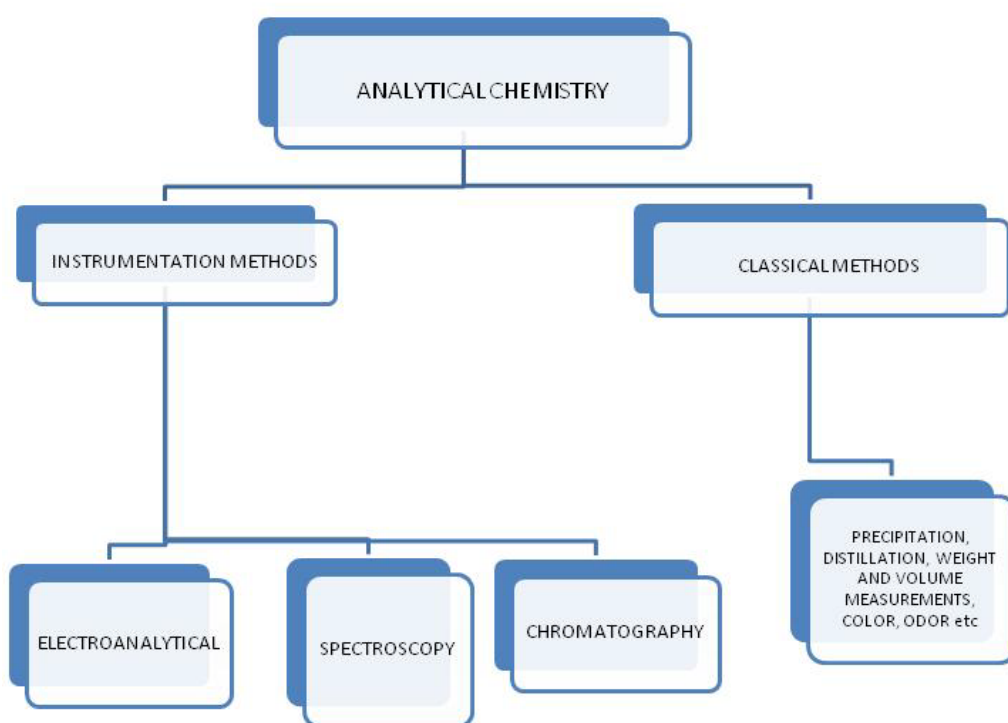


**Figure 1.1:** Analytical chemistry methods of analyses (2).

## 1.2 ELECTROANALYTICAL TECHNIQUES

Electroanalytical techniques are concerned with the measurements of electrical quantities such as potentials and currents in the solution of electrochemical cells containing the analyte (3). They are categorized based on the aspect of electrical quantity that are controlled and measured, and the phenomena of the electrode interactions. However, in contrast to the other analytical techniques where many chemical measurements involve only homogenous bulk solutions, electrochemical reactions take place in both bulk solutions and at the electrode - solution interface (4).

Besides, the interfacial electrochemical technique is divided into static and dynamic techniques. In static technique, current does not allow to flow through the solution during potential measurement of the solution, while in dynamic current is allowed to flow through the solution for the measurements of both current and potential (4). A detail classification of the interfacial electrochemical technique is highlighted in Figure 1.2.

However, voltammetry as a dynamic interfacial and a controlled potential electroanalytical technique is the most useful branch of the electrochemistry owing to the fact that it is used for simultaneous determinations of many analytes with a great sensitivity and very large useful dynamic and linear range concentration for organic species as well as inorganic counterparts. Its advantages extend to the use of large numbers of solvents and electrolytes for a wide temperature range, analysis in seconds,

determination of reaction kinetic and mechanistic predictions, ability to develop a theory and the ease generation of different potential wave form leading to different techniques.

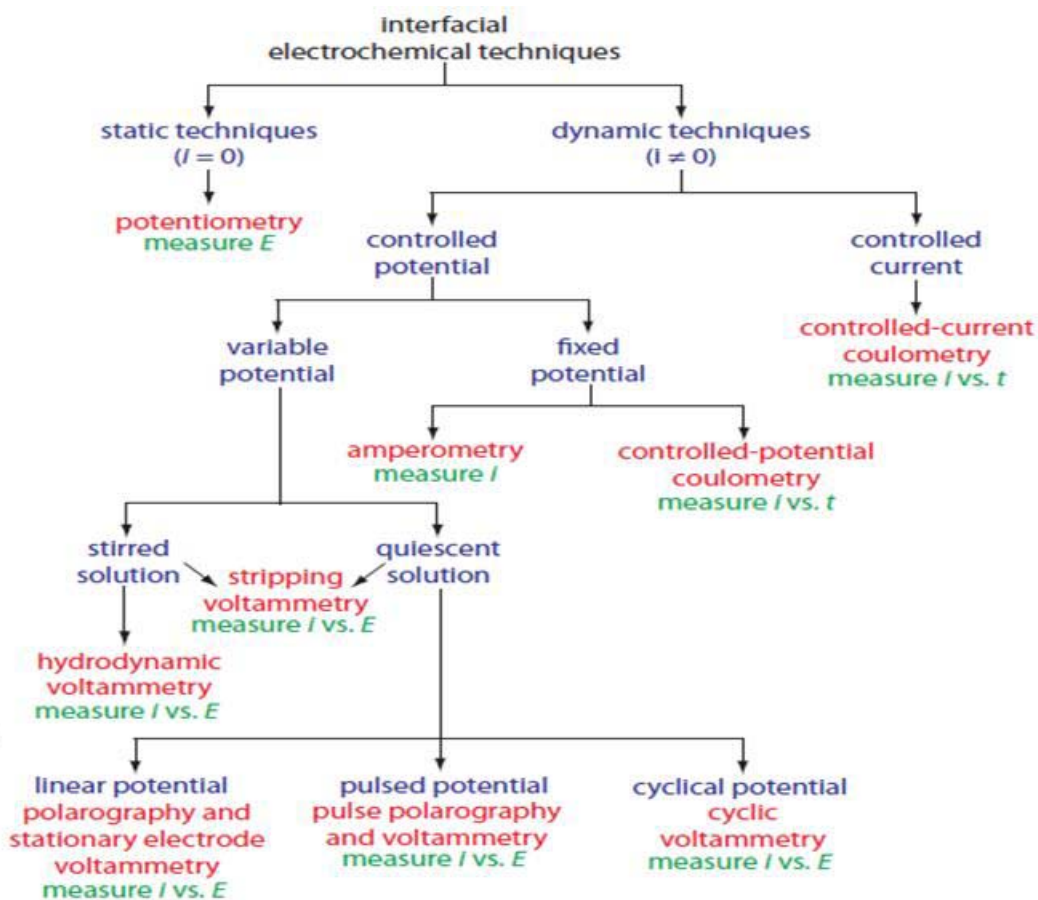


**Figure 1.2:** Classifications of interfacial electrochemical methods (4).



### **1.2.1 Polarography**

Polarography is any form of voltammetry technique in which the working electrode is dropping mercury electrode. Mercury as a working electrode has some special properties particularly its renewable surface. Although, it has a wide cathodic potential range of applications but limited by its toxicity and low anodic applications (3).

### **1.2.2 Voltammetry**

Most voltammetric techniques are aimed to increase the ratio between faradaic and non - faradaic current by lowering the background current, thus improving the detection limit to about  $10^{-8}$ M concentrations (5). There are different types of voltammetry based on the excitation waveform and current sampling regime.

#### **1.2.2.1 Normal Pulse Voltammetry**

Normal pulse voltammetry excitation signal (Figure 1.3) consist of a series of pulses of increasing amplitude applied to successive drop at a preselected time near the end of each drop lifetime (3).

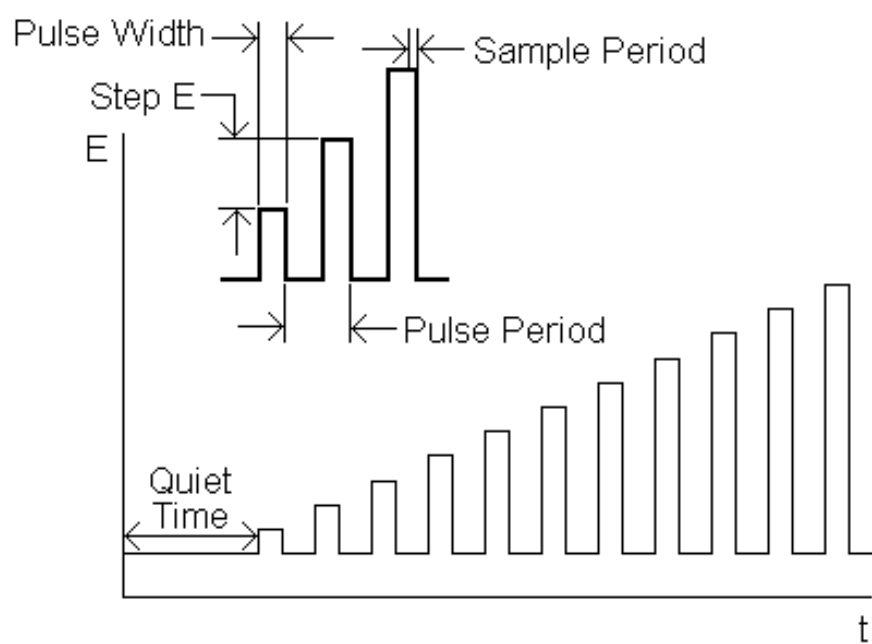


**Figure 1.3:** Excitation signal for normal pulse voltammetry (3).

### **1.2.2.2 Differential Pulse Voltammetry**

Differential pulse voltammetry consist of a fixed magnitude pulses superimposed on a linear potential ramp which are applied to the working electrode at a time just before the end of the drop (3). The current is sampled twice just before and after the application of the pulse as shown in Figure 1.4.

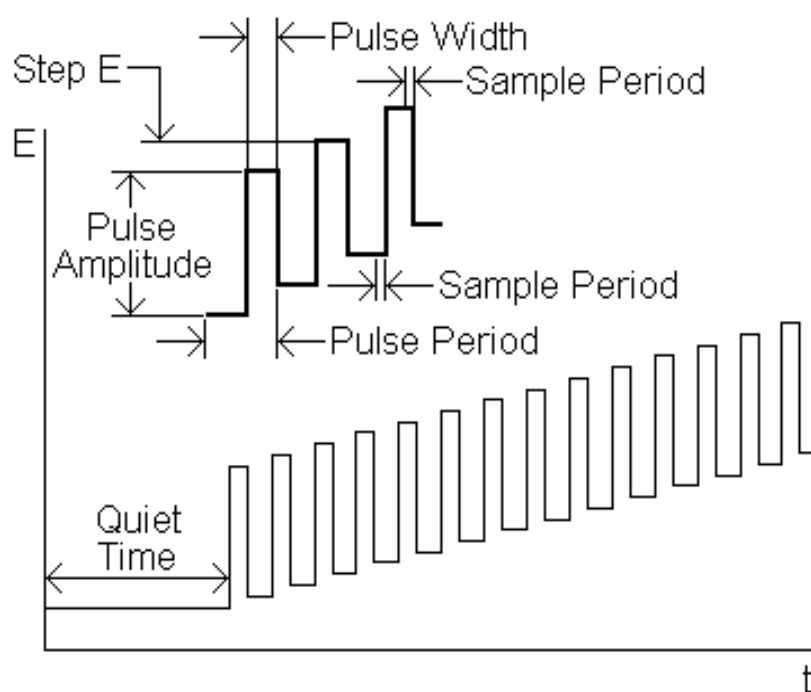


**Figure 1.4:** Excitation signal for differential pulse voltammetry (3).

### 1.2.2.3 Square Wave Stripping Voltammetry

Square wave stripping voltammetry consist symmetrical square wave pulse of large amplitude superimposed on a staircase waveform of step height where the forward pulse of the square wave coincides with the stair case step (6) (Figure 1.5). The current is sampled twice during each square wave cycle, once at the end of the forward pulse and once at the end of reverse pulse. The net current is taking by the difference between the forward and the reverse current (Figure 1.6) (6).

It has many advantages over differential pulse voltammetry technique in terms of its speed and a very low detection limit of about  $1 \times 10^{-8} \text{M}$ . The reverse nature of the wave and it rapid scanning capability make possible for kinetic studies. A comparison study shows that the reversible and irreversible responses from square wave voltammetry are 3.3 and 4 times respectively higher the current response from differential pulse voltammetry (7).

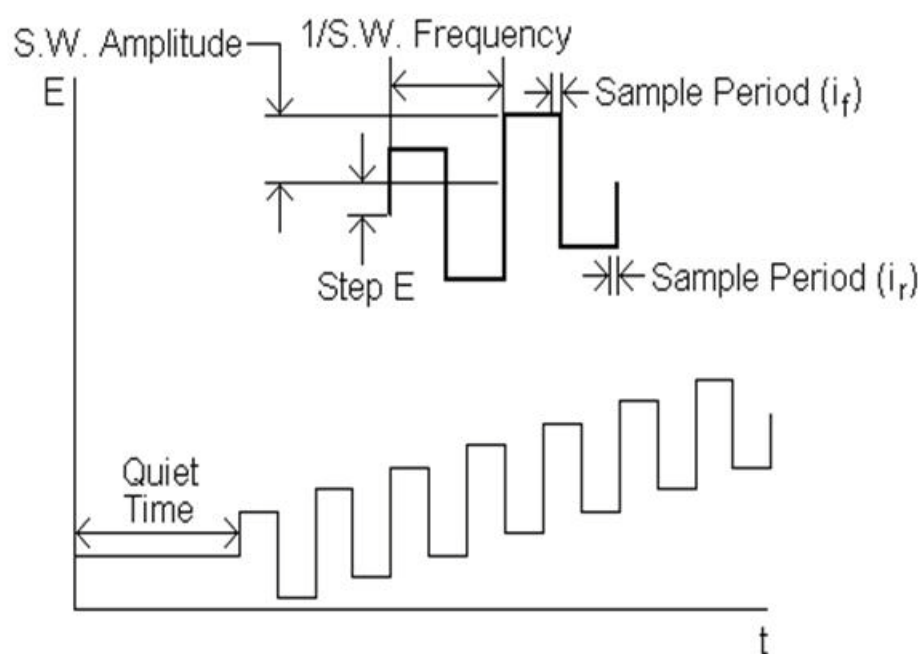


**Figure 1.5:** Square wave voltammetry waveform (6).

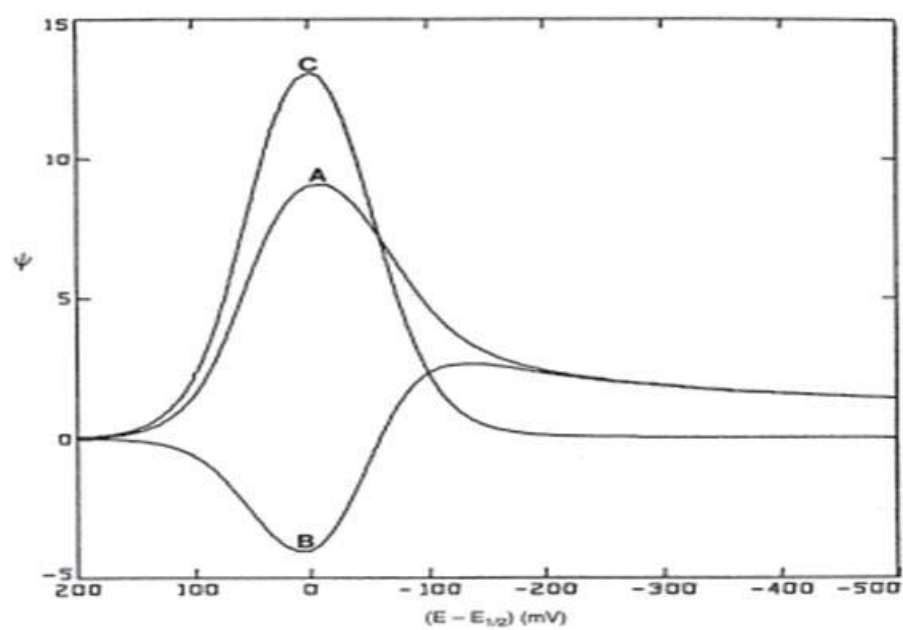


**Figure 1.6:** Square wave stripping voltammograms for  $i_f$  (C),  $i_r$  (B) and net current (A)

(6).

#### **1.2.2.4 Cyclic Voltammetry**

Cyclic voltammetry is a very important voltammetric technique due to its use in a vast range of investigations apart from the general quantitative and qualitative analysis from its voltammogram. It uses to investigate a reversible and irreversible species, provides information thermodynamics and kinetic of redox processes, adsorption processes and so on for any electro active species (3).

Cyclic voltammetry makes use of a triangular wave (Figure 1.7) by scanning linearly the potential of the working electrode. During the potential sweep (minimum of 2 sweeps for a cycle), the potentiostat measures the resulting current positively or negatively base on choice. Single or multiple cycles can also be investigated depending on the information sought. The characteristic peaks in the cyclic voltammograms are caused by the formation of the diffusion layer near the electrode surface (8). The voltammograms obtained can be classified into three; reversible (Figure 1.8), quasi reversible, and irreversible.



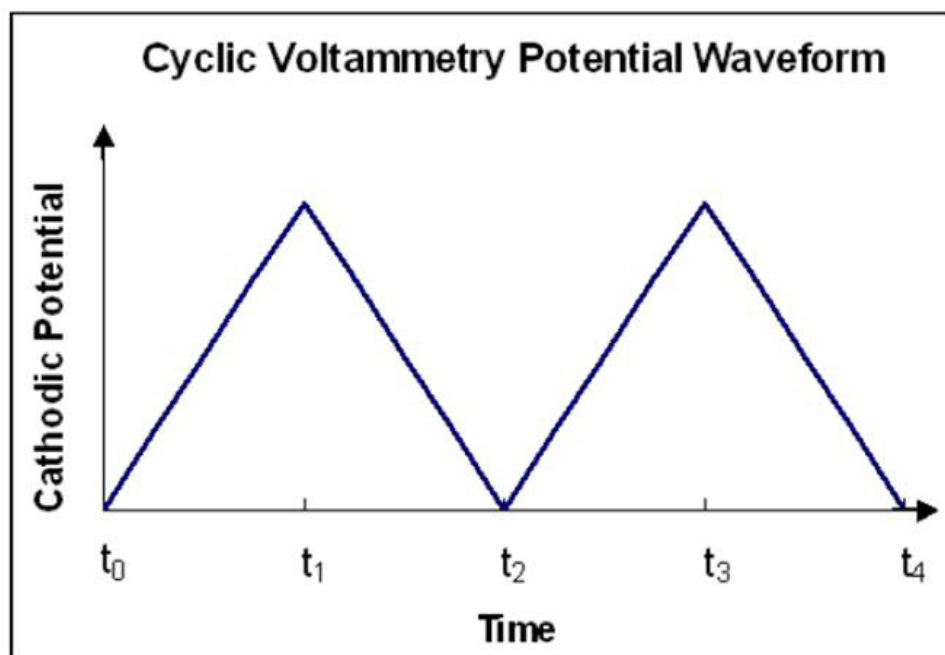


**Figure 1.7:** Potential-time excitation signals in cyclic voltammetric experiment (8).

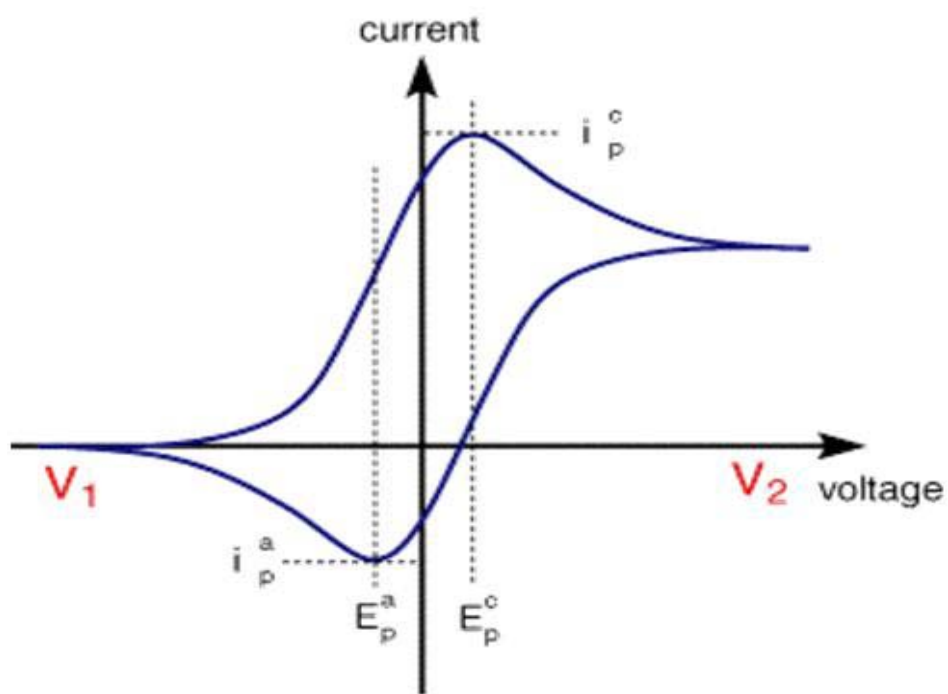


**Figure 1.8:** Typical cyclic voltammogram, where  $i_p^c$  and  $i_p^a$  show the peak cathodic and anodic current respectively for a reversible reaction (8).

### **1.3 ELECTROANALYTICAL CELL IN VOLTAMMETRY**

Potentiometry is a static technique that does not require flow of current and involves two-electrode system. Voltammetry technique is three-electrode system and involves applying current, and often referred to as a dynamic technique (Figure 1.2). The electrodes are; reference electrode, counter or auxiliary electrode and working electrode (4).

#### **1.3.1 Reference Electrodes**

Reference electrode must provide a stable potential in any sample composition. Its potential is measured against the working electrode. The common reference electrodes are silver-silver chloride and saturated calomel reference electrodes (4).

#### **1.3.2 Counter or Auxiliary Electrodes**

Counter electrode is responsible for the measurement of current between itself and the working electrode and prevents current getting to the reference electrode. The commonly used counter electrode is platinum wire (4).

#### **1.3.3 Working Electrodes**

Working electrodes are the electrodes that influence the performance of voltammetric procedures by providing high signal to noise ratio and high reproducible response. The choice of the electrode depend on the redox behavior of the target analyte, background current over potential region, potential window, surface reproducibility, toxicity and so

on (3). The most popular are the noble metals (platinum, gold, copper), mercury and carbons related electrodes.

#### **1.3.3.1 Mercury Electrodes**

Mercury electrodes have high hydrogen over-voltage and a wide cathodic potential window compared to other solid electrode materials and possesses a highly reproducible, new and smooth surface. But the oxidation of mercury at low anodic potential and its toxicity limited its applications.

There are several types of mercury electrodes such as dropping mercury electrode (DME), mercury film electrode (MFE), static mercury drop electrode (SMDE) and hanging mercury drop electrode (HMDE) (3).

#### **1.3.3.2 Carbon Electrodes**

There are many solid electrodes such as the noble metals (platinum and gold) and non-metal solids electrodes based on carbon materials that have a widespread application in electrochemistry due to their broad potential window, low cost, low background current, chemical inertness and their suitability for many sensing applications (3).

##### **1.3.3.2.1 Glassy or Virteous Carbon Electrodes (GCE)**

Glassy carbon (GC) is a non-graphitized carbon electrode. It has excellent mechanical and electrical properties, chemical inertness, stability, impermeability to gas and liquid, wide potential window and relatively high reproducible performance (9). They can be fabricated as different shapes, sizes and sections.

#### **1.3.3.2.2 Carbon Paste Electrodes (CPE)**

A carbon paste is a composite prepared by mixing graphite powder and mineral oil in the right proportion to form a paste (Figure 1.9 A). These electrodes are widely used in voltammetric measurements because they are easily obtainable at low cost and at the same time suitable for making an electrode material modified with admixture of other compounds for different applications in sensors and biosensors (10).

#### **1.3.3.2.3 Glassy Carbon Paste Electrodes (GCPE)**

Glassy carbon paste is a carbon composite electrode material prepared by the mixing of a glassy carbon micro particle powder and a mineral oil in a proportion that will form a suitable paste for analytical determination purposes. It has a composite advantage along with the glassy carbon properties ranging from excellent mechanical and electrical properties, chemical inertness, and impermeability to gas and liquid, wide potential window compared with the convectional carbon paste electrode. Significant differences between the structure carbon paste and glassy carbon paste can be observed in Figure 1.10 by scanning electron microscopy (SEM) images (11).

#### **1.3.3.2.4 Graphite Pencil Electrodes (GPE)**

Pencil leads that are renewable have been in use for many years as a writing device. However, the leads have been explored as an electrode material few years ago in

electroanalytical determinations of analytes. A good example is its use as electrode in the anodic stripping voltammetric determinations of trace metals (12)

Moreover, in contrast to other carbon electrode, it can be extruded to different lengths to obtain different surface areas. This makes graphite pencil suitable for many applications. Pentel pencil (Japan) is usually used and its fabrication can be achieved by soldering a metallic wire to the metallic part that holds the lead in place in the pencil (Figure 1.9B).

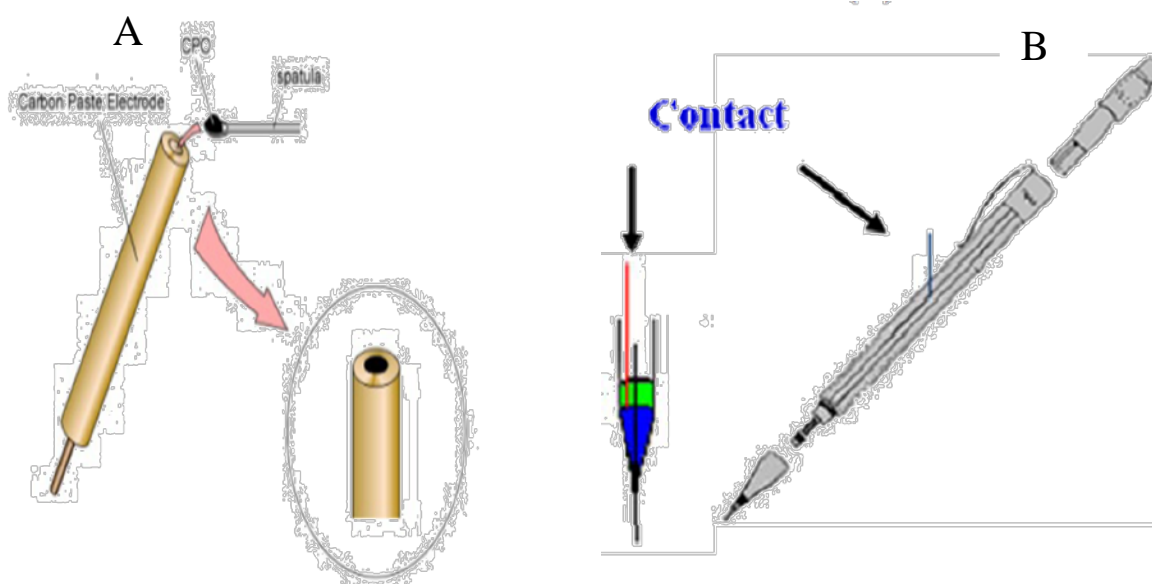


**Figure 1.9:** Schematic diagrams of (A) carbon paste electrode (CPE) and graphite pencil electrode (GPE) (12).

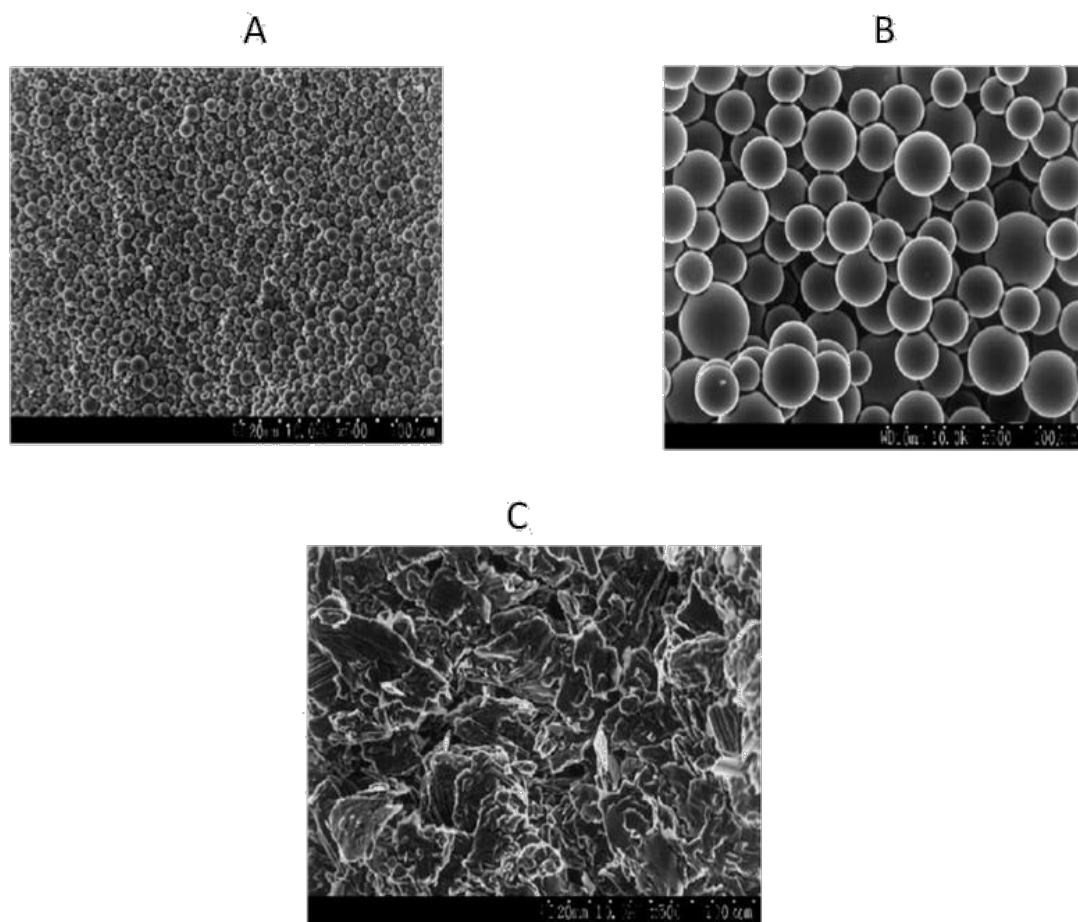


**Figure 1.10:** SEM images of (A) 0.4 – 12  $\mu\text{m}$  GCP particle size (B) 20 – 50  $\mu\text{m}$  GCP particle size and (C) CP (11).



### **1.3.3.3 Modified Electrodes (MEs)**

Chemically modified electrodes are representative of a modern approach to deliberately alter the surface of solids electrodes in order to alleviate some problems related to selectivity, sensitivity and stability of solid electrodes materials. Applications that lead to the improvements of these electrodes with chemicals such as the carbon nanotubes, different metals nanoparticles and so on are extensively discussed (13 ,14).

## **1.4 PHENOLS**

Phenol and considerable numbers of its derivative are extensively useful in the chemical industries due to their toxicity. They are widely used in the manufactures of pesticides, disinfectants, fumigants and so on (15). Organophosphorous and chlorinated phenoxyacids which are popular environmental pollutant active ingredients also yield Chloro and nitro phenol as major degradation products and most of these phenolic compounds has toxic effects on plants and animals (16).

### **1.4.1 Significance of Chlorophenols**

There are five basic types of chlorophenols which are classified based on the numbers of chlorine atoms on the benzene ring. In addition to phenol, Figure 1.11 shows the five basic types of chlorophenols. However, these types of chlorophenols can be permuted to give nineteen chlorophenols products that are commercially available (17).

All these compounds are solid except 2-chlorophenol that is liquid at room temperature. Chlorophenols have strong medicinal taste and odor; small amount in part per billion (ppb) to part per trillion (ppt) can be tasted in water when water are treated with chlorine that can lead to mono or di- chlorophenols if certain contaminant are present and bad taste in fish due to its accumulation. Chlorophenols with at least 2 chlorine atoms either used as pesticides or converted pesticides, some are produced during bleaching of wood pulp in paper production, some especially 4-chlorophenol are used as antiseptics (18, 19). Fungicides, bactericides, herbicides, preservatives and so on that are being released in into the environment go into the water with very few escape to the air are all product of chlorophenols.

However, chlorophenols are highly toxic, low biodegradable and their extent of environmental pollution call for proper investigation which will give a comprehensive understanding of the appropriate methods for determinations of phenolic compounds.

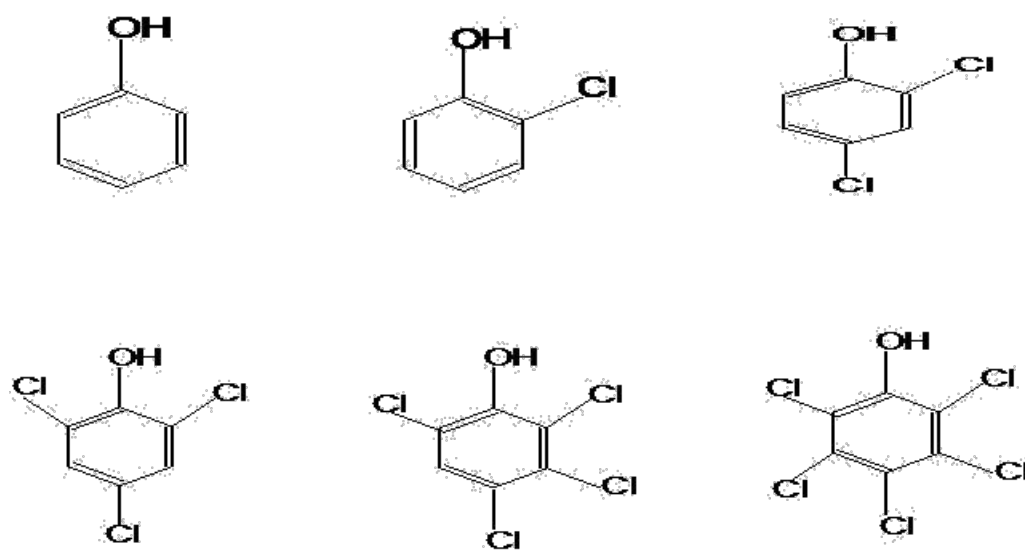


**Figure 1.11:** Chemical structures of phenol and the five basic types of chlorophenols.

## 1.5 OBJECTIVES

The objectives of the proposed research are to;

- Investigate the oxidation pathways of phenol and chlorophenol derivatives at low concentration via cyclic voltammetry (CV) and square wave voltammetry (SWV).
- Obtain and improve the fouling signals at a single scan for possible analytical determinations.

## **CHAPTER 2**

### **2.0 LITERATURE REVIEW**

#### **2.1 ANALYTICAL DETERMINATION OF PHENOLIC COMPOUNDS**

Detection of phenolic compounds especially the chlorophenols is of great importance owing to their presence in a broad range of chemical manufacturing products that are available for several human uses and some human consumptions that riches in these pollutants and their toxicity (15). Chlorophenols pollution is considered to be a major problem in the world due to its toxicity at low concentration level. It has been studied and found to represent a major public health concerns because they are ubiquitous and affect several organs in human (16). For these reasons, a lot of analytical techniques for the determination of phenols have been reported.

A lot of methods through analytical techniques for the determination of phenols have been reported. These methods include capillary gas chromatography (GC-FID) (20), GC-MS (21, 22), reverse phase high pressured liquid chromatography (HPLC) followed by GC-MS (23, 24), HPLC-UV (25) HPLC-MS (26) liquid phase micro extraction HPLC-GC (LPME-HPLC-GC-MS) (27), colorimetric methods (28 - 30), spectrophotometric (31 - 40) biosensor-based methods (41 - 46) and several electroanalytical techniques (48 - 54).

A simultaneous determination of phenol, cresol, xylenol isomers and naphthol in urine by capillary gas chromatography (GC) was reported by Grazyna B. 1996 (20), where all the ten substances were separated by gas chromatographically using a capillary column (ultra 2) of cross-linked 5% phenyl methyl silicone.

A quantification of phenolic antioxidant in rat cerebrospinal fluid after oral administration of compound containing 21 phenolic compounds where just three (ferulic acid, tyrosol and hydroxytyrosol) were detected via GC-MS by Zafra-Gomez A. et al. 2010 (21) and pre-concentration with determination of eight phenolic compounds in water samples by in situ derivitization with a liquid-liquid micro extraction was reported to be achieved by GC-MS by Faraji H. et al. 2009 (22).

Trace determination of phenol in natural water extraction by a new graphitized carbon black cartridge (carbograph 4) followed by liquid chromatography (LC) and re- analysis after phenol derivitization had been reported by Di Corcia A. et al. 1996 (24). This method is a solid-phase extraction that is highly sensitive and selective with a robust liquid chromatography for the determination of the USEPA (United State Environmental Protection Agency) eleven priority pollutant phenols.

Angelino S and Gennaro M. C. 1997 (25) reported an ion-interaction RP-HPLC with UV detection for simultaneous separation and determination of eleven EPA priority phenol pollutants based on the capability of the phenolic compounds to form ion pairs with alkyl ammonium ion, while an ordinary HPLC-UV was developed for the simultaneous quantification ketoprofen and naproxen sodium along with phenol red as a non-absorbable marker for in situ permeability studies by Zakeri-Milani P. et al. 2005 (26).

Besides, Proestos C. et al. 2006 (23), utilized RP-HPLC coupled with GC-MS for the determination of aromatic plant.

A two steps liquid phase micro extraction coupled with HPLC for the determination of environmental water sample was introduced by Zhang P. et al. 2011 (28), with a high enrichment factor. This LPME-HPLC was a plus to the series of HPLC technique because it avoids a derivatization step that is always necessary in GC analysis.

The synthesis of simple, extensively conjugated chromophores as substitutes for 4-aminoantipyrine (4-AAP) capable of causing hyperchromic shift when coupled with phenol have been described by Alonso M.V. et al. 2004 (30). The 4-aminopyrazolone derivative synthesized was subsequently applied for the spectrophotometric assay of phenolic compounds and its advantages and disadvantages were highlighted.

A lot of spectrophotometric techniques relating to phenols had been reported. Such techniques include determination of phenols in sweet potato root by Vieira I. C. and Fatibello-Filho O. 1998 (33). Tea infusion, tomato and apple juice by fluorescence according to Shaghghi M. et al. 2008 (36), water by Kang C. et al. 2000 (37), nifedipine by Rahman N. and Hoda M. 2002 (39), quantification of a enzymes activity to produced 4-substituted phenol by Nolan L. C. and O'Connor K. E. 2005 (34). Kinetic spectrophotometric with the aid of artificial neural network by Ni Y. et al. 2011 (35), study of reaction via liquid chromatography LC with diode and MS detection by Fiamegos Y. C. et al. 2002 (38) and comparative study for principal component regression (PCR) partial least square (PLS) reported by Hemmateenejad B. et al. 2007 (40).

The hydrodynamics and oxygen transfer characteristics of a fluidized bed reactor (FBR) and the performance in the continuous biodegradations of phenol and 4-chlorophenol containing influent when the FBR was loaded with *Candida Tropicalis* yeast immobilized on a granular activated carbon (GAC) particles was reported by Galindez-Mayer J. et al. 2008 (41). The removal efficiency of both phenol and a 4-chlorophenol in the bioreactor challenge at increasing volumetric loading rate of pollutants was study and determined by HPLC. Immobilized biomass on GAC was estimated from their nitrogen content.

Among these techniques, conventional colorimetry and spectrometry are easily disturbed by the color of detected components, gas chromatography usually spent a long time for separation before detections; while High Pressured Liquid Chromatography (HPLC) needs preparation of an efficient compatible mobile phase with the stationary phase which will unquestionably consume a lot of reagent (organic and inorganic solvents) and may even leads to environmental pollution when these reagents are discharged.

## **2.2 ELECTROANALYTICAL DETERMINATION OF PHENOLIC COMPOUNDS**

Electroanalytical technique has attracted considerable interest due its simplicity, fastness, convenience and low cost. Glassy Carbon Electrode (GCE) is the most common working electrode utilized in the study of phenols determinations due to its high stability and precise detection as reported by Adams R. N. 1996 (48). It is a common knowledge that most phenols can be easily oxidized at various types of solid anodes leading to the



formation of phenoxy radicals in the first scan and further polymerization of these primary oxidation products result in the formation of polymeric film as comprehensively discussed by Adams R. N. 1996, page 363 (48).

This fouling effect associated to the solid electrode whose scanning electron microscope (SEM) is shown in Figure 2.1 on GCE surface is a great challenge to phenols sensitivity and limitation in practice.

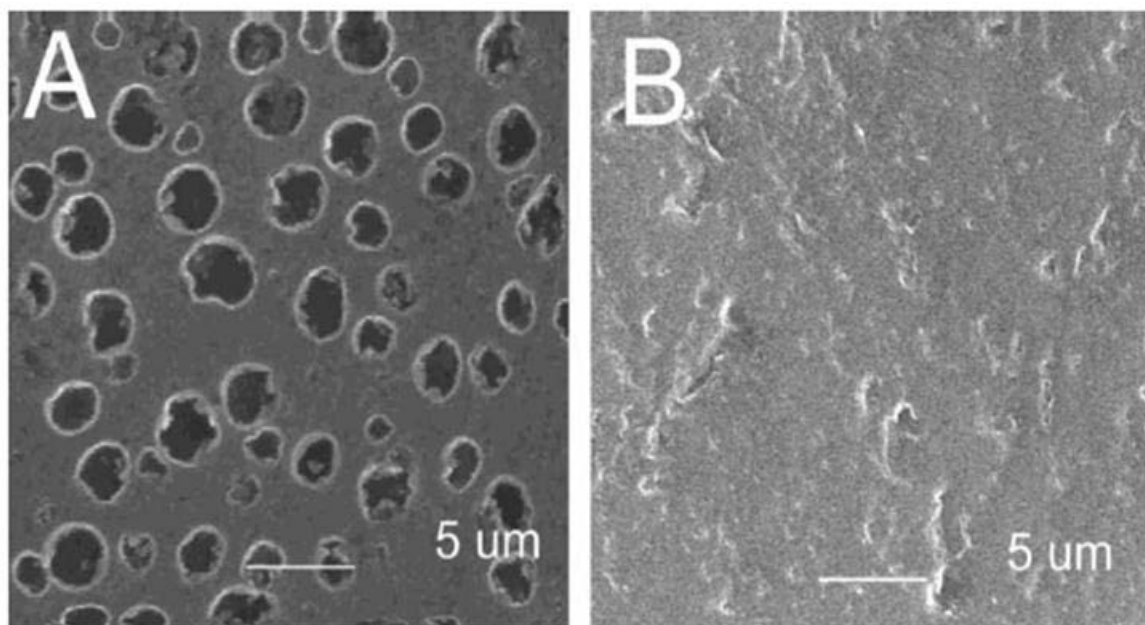


**Figure 2.1:** SEM micrographs of: (A) polyphenol-covered GC electrode; (B) GC substrate (57).

### **2.2.1 Attempts to Alleviate Fouling Effect on Solid Electrodes**

Some procedures have been described in an attempt to alleviate the problem of the film on electrodes surfaces.

Voltammetric detection of phenol at platinum-polytyramine composite electrodes in acidic media was described by Spataru T. and Spataru N. 2010 (49). The composite was obtained by depositing platinum nanoparticles in a polytyramine matrix, electrochemically formed on graphite substrate was used as electrode material for the investigation of phenol oxidation by use of anodic voltammetry. According to the result obtained in acidic media, it was proven to be a simple and rapid method for the determination of phenol with much resistant to fouling compared with the bare smooth platinum electrode.

Modification of montmorillonite with cationic surfactant cetyltrimethylammonium bromide to form CTAB-montmorillonite calcium (CTAB-MMT) on a glassy carbon paste electrode (GCPE) reported by Yang H. et al. 2008 (50) shows a higher accumulation efficiency to 4-chlorophenol compared with the unmodified electrode.

A couple of biosensors had been reported for the determination of phenolic compounds. Biosensors for the determination of phenols based on cross-linked enzymes crystals (CLEC) by Roy J. J. et al. 2005 (42), amperometric biosensor based on multiple wall carbon nanotubes poly (pyrrole)-horseradish peroxidase nano composite (MWCNTs-poly-pyrrole) film on a gold surface by Korkut S. et al. 2008 (43), tyrosinase biosensor based on pH-sensitive field effect transistor by Anh T. M. et al. 2002 (44), amperometric

phenol biosensor based on polyaniline by Wang P. et al. 2009 (45), determination of phenols in water based on enzymes tyrosinase by Adamski J. et al. 2010 (46), an immobilization of tyrosinase on single wall carbon nanotubes (SWCNTs) modified GCE covers with nafion films was successfully constructed by Zhao Q et al. 2005 (53) for the determinations of phenolic compounds based on the tyrosinase-single walled Carbon Nanotubes (SWCNTs) sensor (53).

Enhancements of the glassy carbon electrode with surfactants in the electrochemical determination of phenol and mechanism research have also been reported by Wang X et al. 2008 (54). The surfactants includes cetyl trimethyl ammonium chloride and cetyl pyridinium chloride, on trinitrophenol, 2,4-dinitrophenol, 2,5-dinitrophenol, Ortho-dihydroxybenzenes, Para-dihydroxybenzenes, 1-Naphthol and 2-Naphthol.

Acetylene black film modified glassy carbon electrode had also been used by Sun D. and Zhang H. 2006 (51) for 2-chlorophenol determination in water sample. This was achieved by dispersing acetylene black (AB) in the presence of dihexadecyl hydrogen phosphate (DHP) to form a homogenous and stable AB-DHP suspension and was coated on GCE by coating technology for the determinations of 2-chlorophenol with a better sensitivity when compared with a bared GCE.

Stable and sensitive electrochemical detection of phenolic compounds at multiple wall carbon nanotubes (MWCNTs) modified glassy carbon electrode was also reported by Wang J. et al. 2003 (52), which leads to the enhancement of stability and sensitivity of voltammetric and amperometric measurement of phenolic compounds. The cyclic

voltammetric experiments indicate that the redox process of surface confined layer that promote the phenol oxidation and enhanced current signals in both techniques.

### 2.2.2 Electro-oxidation of Chlorophenols

Several advanced oxidation processes (AOPs) for treatment of waste water due to low biodegradability of Chlorophenols had been reviewed by Pera-Titus M. et al. 2004 (55). The techniques for studies includes hydrogen peroxides based ( $\text{H}_2\text{O}_2 + \text{UV}$ , Fenton, photo-Fenton and Fenton like processes), photolysis, photo catalysis, and ozone based processes ( $\text{O}_3$ ,  $\text{O}_3 + \text{UV}$ ,  $\text{O}_3 + \text{catalyst}$ ).

Oxidation of Chlorophenols (CPs) in alkaline solution on platinum electrode was also reported by Ezerskis Z and Jusys Z. 2001 (56). The potentiodynamic studies were carried out by cyclic voltammetry, galvanostatic electrolysis and GC-MS for ten hours. These studies reveal the relative rate of oxidation reactions of phenols that Phenols > mono-CPs > di-CPs > tri-CPs > tetra-CPs > penta-CPs and the effect of chlorine atom interactions with the hydroxyl functional group. Besides, stability of chlorophenols depends on degree of chlorination and isomerization, proximity of chlorine atoms to hydroxyl group leads to weakness in the hydrogen dissociation constant ( $\text{pK}_a$ ) of phenol. Monochlorophenols [ 2-chlorophenol (8.45) > 3-chlorophenol (9.1) > 4-chlorophenol (9.38)], also dichlorophenols [2,6 -dichlorophenol (6.8) > 2,3-dichlorophenol (7.45) > 2,4-dichlorophenol (7.85) > 3,4-dichlorophenol (8.39)].

Electro-oxidations investigations at pH 2.2 reveal a dual pathway routes for 2,4-dichlorophenol and other poly chlorinated phenols had also been reported by Ureta-Zanartu M. S et al. 2002 (57). It was reported that the reactions commence with the formation of phenoxy radical, then one path leads to polymerization of the phenoxy radical at high concentrations while the other leads to a quinonic like product at lower concentration of the chlorophenols where the ortho isomers is oxidized at lower potential than the para isomer. It was further reported that soluble quinone-like product may give a shoulder peak and that similar result was obtained in oxygen saturated solution but nitrogen bubbling give a small increase in anodic peak and decrease in cathodic peak.

However, the fouling effect that was considered as the problem of the GCE was utilized for the study of the oxidation pathway of phenols and para- substituted phenols by Enache T. A. and Oliveira-Brett A.M. 2011 (58). It was discovered that the oxidation of phenol is pH dependent and irreversible in one step, and followed by hydrolyses in ortho and para position leading to two oxidation products and that of para substituted possess a similar characteristic with a single oxidation product at the ortho position.

A mechanism of oxidation reaction pathway that leads to dimerization of pentachlorophenol to 2,3,4,5,6-pentachloro-4-pentachlorophenoxy-2,5 -cyclohexadienone had been proposed by Codognoto L. et al. 2005 (59). This was achieved on the boron doped diamond (BDD) electrode surface with square wave stripping voltammetry.

## CHAPTER 3

### 3.0 RESEARCH METHODOLOGY

The ultimate aim of this research is to use electrochemical techniques to study the oxidation and reduction pathways of phenol and chlorophenol derivatives for proper understanding of its oxidation reactions. The Knowledge obtained will afford us to predict the possible product for phenol redox reaction with the consideration of its ortho, meta and para positions substituent.

To achieve this goal our research will first address several important questions:

1. Why do the signals obtained for phenolic compounds on glassy carbon electrode (GCE) always reduced after the first scan?
2. What is responsible for this behavior?
3. What is obtainable from this behavior?
4. Is it possible to obtain other peaks than the irreversible first oxidize anodic peak in a single scan? If yes
5. Can they be improved for possible electroanalytical determinations?

The answer to all of these questions will have a significant impact towards understanding the phenols electrochemical redox reactions.

### **3.1 CHEMICALS AND REAGENTS PREPARATIONS**

#### **3.1.1 Chemicals**

2-chlorophenol (2CP), 2,4-dichlorophenol (2,4DCP), 2,6-dichlorophenol (2,6DCP), 2,4,6-trichlorophenol (2,4,6TCP), pentachlorophenol sodium salt (PCPNa salt), and 0.05 microns gamma alumina powder were purchased from Sigma–Aldrich. Monosodium dihydrogen phosphate ( $\text{NaH}_2\text{PO}_4$ ) was obtained from Fisher Scientific. Phenol, hydroquinone and disodium hydrogen phosphate ( $\text{Na}_2\text{HPO}_4$ ) were supplied by Fluka.

However, Table 3.1 shows the properties of the chemicals involves in our investigation.



**Table 3.1: Properties of Phenol and Chlorophenols Derivatives.**

Compounds	Mol.Wt	Appearance	MP ( ° C )	BP( °C )	Sp. Gr.	pK <sub>a</sub>
Phenol	94.11	Transparent cryst. solid	40.50	181.7	1.07	10.00/9.71
2-Chlorophenol	128.56	Light amber liquid	8.00– 9.00	175-176	1.24	8.29/8.22
2,4-dichlorophenol	163.00	White-off-white cryst.	42.00- 44.00	209-210	1.38	8.09/7.40
2,6-dichlorophenol	163.00	White-light brown cryst.	65.00- 68.00	218-220	1.27	6.79/6.30
2,4,6-trichlorophenol	197.45	White tan flakes	65.00- 66.00	246	1.49	6.21/6.30
Pentachlorophenol	288.32	White flakes	NA	≥300	1.10	NA

### **3.1.2 Reagents Preparations**

All solutions were prepared with ultrapure water of resistivity  $18.2 \text{ M}\Omega\text{cm}^{-1}$ , which was obtained direct from an ultrapure water system (Figure 3.1).

#### **3.1.2.1 Supporting Electrolyte Solutions**

The supporting electrolytes were 0.1 M phosphate buffer solutions (PBS) with different pH's between pH 5.00 and 9.00, and were prepared by dissolving appropriate quantity of mono and disodium hydrogen phosphate salts in ultrapure water.

Moreover, extreme conditions such as alkaline medium (56) and acidic medium (57) had been reported for the electro oxidations of chlorophenols with no justification for their optimum pH. So we have carried out our investigation with a standard phosphate buffer solution without any pH adjustment in order to retain the buffer capacity as shown in Table 3.2 bearing in mind that the lowest pH that is obtainable in a phosphate buffer solution is 4.50 and the highest is 9.00.

**Table 3.2: Compositions for Various pHs of 0.1M Phosphate Buffer Solutions for 100ml Solution.**

<b>pH</b>	<b>0.20 M NaH<sub>2</sub>PO<sub>4</sub> (ml)</b>	<b>0.20M Na<sub>2</sub>HPO<sub>4</sub> (ml)</b>
5.00	49.32	0.68
6.00	43.12	6.88
7.00	16.73	33.27
8.00	2.18	47.82
9.00	0.04	49.96



**Figure 3.1:** Single distilled, double distilled and ultrapure water systems.

### 3.1.2.2 Preparations of Standard Solutions

1. **Phenol stock solutions:** 0.028 g was dissolved in deionized water in 10 ml flask to make 30 mM solution to minimized error and diluted by 10 factors in another 10 ml flask to yield 3 mM solution.
2. **2-Chlorophenol stock solutions:** 31.4  $\mu\text{L}$  was mixed with deionized water in 10ml flask to make 30 mM solution to minimized error and diluted by 10 factors in another 10 ml flask to yield 3 mM solution. 0.3 mM was also prepared from this by dilution.
3. **2,4-dichlorophenol stock solutions:** 0.048 g was dissolved in 10% 0.1 M NaOH deionized water in 10ml flask to make 30 mM solution and diluted by 10 factors in another 10 ml flask to yield 3 mM solution.
4. **2,6-dichlorophenol stock solutions:** 0.048 g was dissolved in 10% 0.1 M NaOH deionized water in 10ml flask to make 30 mM solution to minimized error and diluted by 10 factors in another 10 ml flask to yield 3 mM solution.
5. **2,4,6-trichlorophenol stock solution:** 0.059 g was dissolved in 10% 0.1 M NaOH deionized water in 10 ml flask to make 30 mM solution and dilute by 10 factors in another 10 ml flask to yield 3 mM solution.
6. **Penta-Chloro sodium salt stock solution:** 0.086 g was dissolved in deionized water in 10 ml flask to make 30 mM solution to minimized error and dilute by 10 factors in another 10 ml flask to yield 3 mM solution.

7. **Hydroquinone stock solution:** 0.033 g was dissolved in deionized water in 10 ml flask to make 30 mM solution to minimized error and dilute by 10 factors in another 10 ml flask to yield 3 mM solution.

## **3.2 EXPERIMENTAL SET-UP**

### **3.2.1 Electrode Materials**

Glassy carbon electrode is the working electrode of choice due to its high stability and precision compared with other solid electrodes according to Adams R. N. 1969 (48). Silver/Silver chloride (Ag/AgCl) in potassium chloride solution is the reference electrode while platinum wire serves as the counter electrode.

The glassy carbon electrode (GCE) due to the expected fouling from the first oxidized product was polished with 0.05 microns gamma alumina powder after rinse with deionized water for every scanning.

### **3.2.2 Potentiostat /galvanostat Units**

Voltammetry measurements were performed with an electrochemical workstation (CHI1140A, CH Instruments Inc, Austin, TX, USA). GCE (polished with 0.05 microns gamma alumina powder prior every experiment) as a working electrode, Ag/AgCl reference electrode (in 3M KCl, CHI111, CH Instruments Inc) and platinum wire counter

electrode (CHI115, CH Instruments Inc) were inserted into the 3.0 ml glass cell through holes in its Teflon cover as shown in Figure 3.2B.

However, the experimental set-up (Figure 3.2A) consists of the potentiostat/ galvanostat unit, electrochemical cells and the solution cell that are all integrated with a computer system.

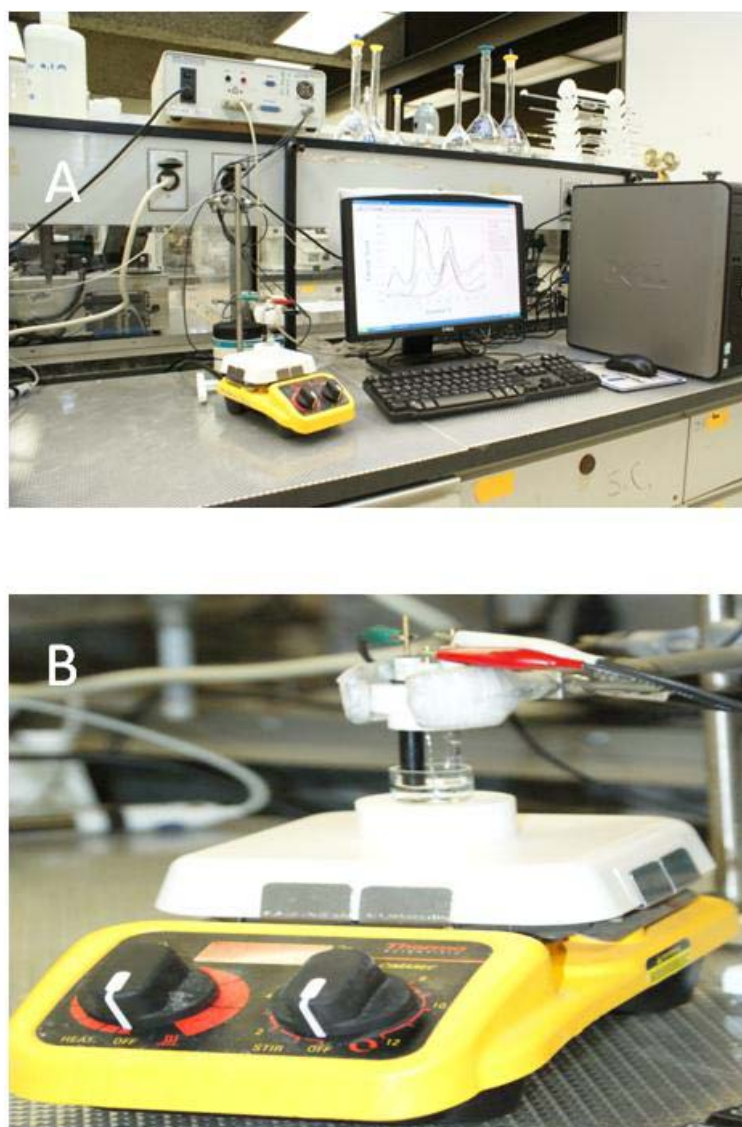


**Figure 3.2:** (A) Experimental set-up and (B) Electrochemical cell.



### 3.3 PROCEDURES AND STRATEGIES

To control the oxidation reaction of isomerization of the electrochemically produced phenoxy radical at a relatively low concentration ( $25\ \mu\text{M} - 30\ \mu\text{M}$ ) of phenol and its chloro-derivatives at their corresponding optimum pH value and accumulation potential of +0.40V was confirmed as reported by Ureta-Zanartu M. S et al. 2002 (57). The effect of the accumulation potential on the first oxidized peak was also studied and exploited for possible analytical application. The fouling effect on the electrode through various scanning without polishing the GCE at the presence of the analyte and in the blank solution was investigated, too.

However, in order to ascertain our techniques, we have investigated the electro-decomposition potentials of the phenol and chlorophenol derivatives under the same square wave adsorptive voltammetry parameters relates the possible shifts of their potential to their dissociation constant ( $\text{pK}_a$ ) and thus confirm the fouling effect on the electrode through several scanning without electrode polishing.

These will serve as a proof to justify the potency of our technique.

### 3.3.1 Electrochemical Optimization

The potential window to be adopted was based on the electro-decomposition potentials of the phenols detected on the glassy carbon electrode. It is expected that the  $pK_a$  values for the phenol and its chloroderivatives are different and this will not allow us to investigate all the analyte on the same pH to yield an efficient result.

Based on this, we have investigated the anodic peak of the phenols with different concentration of phosphate buffer solution (PBS) and later used the optimized concentration of the PBS to study the best pH for each analyte to carry out our research.

Moreover, with the optimized pH, we have adopted the scanning of the studied analytes without polishing the glassy carbon electrode surface right after previous scan in the presence of the analyte to investigate the isomers that result to fouling of the electrode and then tested using the same technique on a solution containing the analyte to obtain the anodic peak and immediately transfer the electrode to a blank solution to confirm the disappearance of the anodic peak while retaining the isomerizes peaks.

These procedures were utilized on square wave adsorptive stripping voltammetry and also validated with cyclic voltammetry.

We have also used cyclic voltammetry to identify the reversible and irreversible peaks for each analyte and for electro-analytical investigation of the dependency of chlorophenols oxidation products on the concentration of the analyte and the possible pathways oxidation routes.

We have introduced a procedure that will lead to the generations of the phenoxy radical and at the same time the expected isomerizes peaks at a single anodic scan which will definitely eliminate the use of multiple scanning for the investigation of products of the oxidation of phenol and chlorophenol derivatives. We then moved to improve the peak signals for possible analytical determinations.

### **3.3.2 Analytical Performance**

Following the optimization of the preparation conditions and analytical protocol, we have assessed the overall analytical performance of the technique by its reproducibility of seven consecutive measurements of the same concentration and conditions.

## **CHAPTER 4**

### **4.0 RESULTS AND DISCUSSIONS**

#### **4.1 ELECTROCHEMICAL INVESTIGATION OF PHENOL AND CHLOROPHENOL DERIVATIVES**

Electroanalytical determinations of phenols are always carried out at a very low accumulation potential preferably about 200 mV lower than their electro-decomposition potentials. On the other hand, the information on the accumulation potential of phenols is rarely reported in literature due to the undesirable peaks obtained from most phenols at a potential above their electro-decomposition potentials. In order to avoid complex reactions on the surface of glassy carbon electrode during oxidation of phenol and chlorophenol derivatives, we decided to operate at a mild accumulation potential (+400 mV) which is lower than all of the analyte potentials. Besides, to avoid polymerization reactions of phenols and according to the findings of Ureta-Zanartu M. S. et al. 2002 (57), we have decided to work at 30  $\mu$ M concentration of each analyte for our investigations.

#### **4.1.1 Proof of Concept Using Square Wave Stripping Adsorptive Voltammetry (SWSV) Technique for Electrochemical Investigation of Phenol and Chlorophenol Derivatives**

In order to ascertain the potency of our techniques, we have investigated the electro-decomposition potentials of phenol and chlorophenol derivatives under the same parameters of square wave stripping voltammetry and then related the shifts of their corresponding dissociation constants ( $\text{pK}_a$ ). The peak potentials and the corresponding shift of all the phenols as shown in Table 4.1 and Figure 4.1a respectively. Both experimental and calculated hydrogen dissociation constants ( $\text{pK}_a$ ) are shown also in Table 4.1 as well as the corresponding plot (Figure 4.1b).

**Table 4.1: Electro-decomposition Potentials, Experimental and Calculated  $pK_a$  Values of Phenol and Chlorophenol Derivatives.**

Compounds	$E_p$ (V)	Exp. $pK_a$	Cal. $pK_a$
Phenol	0.730	10.00	9.71
2-chlorophenol	0.704	8.29	8.22
2,4-dichlorophenol	0.688	8.09	7.40
2,6-dichlorophenol	0.608	6.79	7.03
2,4,6-trichlorophenol	0.584	6.21	6.30
Pentachlorophenol	0.696	4.90	5.55

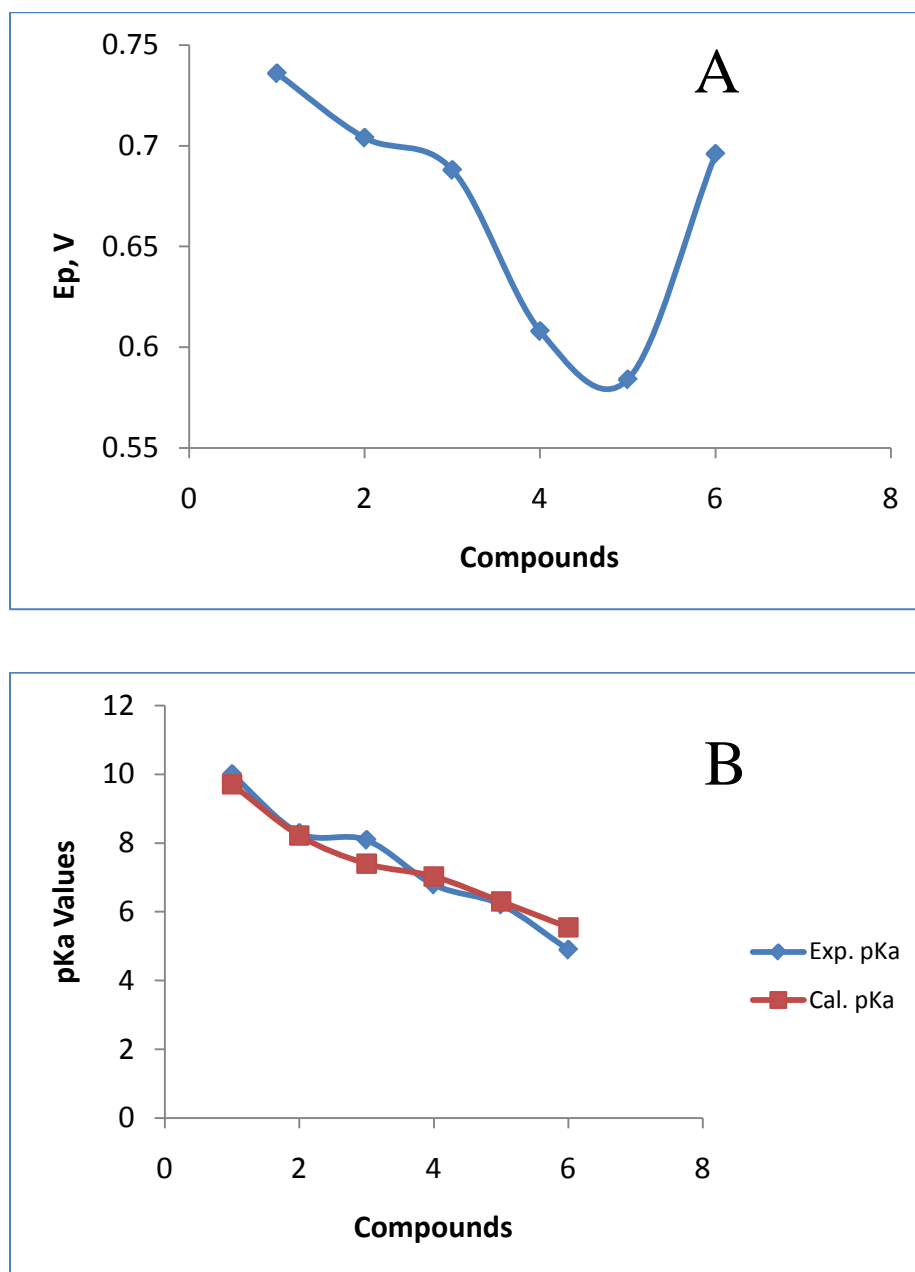


**Figure 4.1:** (A) Plot of phenols and their corresponding oxidation peak potentials (B) Plot of phenols and their corresponding experimental and calculated  $pK_a$  values.

#### **4.1.2 Electrochemical Investigation at Different pHs Using Cyclic Voltammetry and Square Wave Stripping Voltammetry**

The optimization of the electrolyte solution is a major contribution to the efficiency of any technique in electrochemical investigation. In order to carry out our investigation at the pH with the best electrochemical signal for each analyte, the effect of pH must be investigated.

However, extreme conditions such as alkaline medium by Ezerskis Z. and Jusys Z. 2001 (56) and acidic medium by Ureta-Zanartu et al. 2002 (57) had been reported for the electro-oxidations of chlorophenols with no justification for their optimum pH.

##### **4.1.2.1 Investigation Using Cyclic Voltammetry (CV)**

The pH dependence of the phenol and chlorophenol derivatives was studied systematically by CV at the accumulation potential of +0.40 V in the pH range of 5.00 to 9.00 of 0.1 M phosphate buffer solutions (Figure 4.2 to Figure 4.7). As the pH increases, the electro-decomposition potential shifted towards less positive potential (except in Figure 4.7) due to the hindrance of the oxidation at low concentrations of protons. This is in agreement with the work of Enache T. A. and Oliveira-Brett A.M, 2011 (58) for a successive differential pulse (DP) voltammograms for 25  $\mu$ M phenol in pHs between 1.0 and 12.0 of the same phosphate buffer solution. However, there is no shift observed for pentachlorophenol due to the fact that there is no hydrogen atom to be dissociated in the



compound as shown in Figure 4.7. Figure 4.8 shows the oxidation peaks signals of the studied phenols at +0.40V for various pHs by CV. The behavior of these oxidation peaks can be simply explained by the anion concentration  $[A^-]$  of the phenols in the oxidation reaction.

As shown in Figures 4.2 and 4.8, the oxidation peak of phenol increases as the  $[A^-]$  increases which at the same time proportional to the increase in the pH value from 5.0 to 9.0. The pentachlorophenol behaves in opposite direction as shown in Figure 4.7. These implies that the  $[A^-]$  of phenol is moving towards the optimum value while that of pentachlorophenol moves away from the optimum value considering their corresponding  $pK_a$  value as shown in Table 4.1. However, as the  $[A^-]$  of 2-chlorophenol, 2,4-dichlorophenol, 2,6-dichlorophenol, 2,4,6-trichlorophenol increases, the oxidation peak increases until the equilibrium point is reached where any further increase in the  $[A^-]$  will no longer favors the oxidation peak as explained by the Le Chatelier's principle on the effect of change in condition of a chemical equilibrium. The corresponding optimum  $[A^-]$  shown in Table 4.2 for each phenol and chlorophenol derivative is calculated through the equilibrium constant ( $K_a$ ) expression. The  $K_a$  and the hydrogen ion concentration  $[H^+]$  values were calculated from the experimental  $pK_a$  value shown in Table 4.1 of analyte and their optimum pH values.

The effect of pH of phenol (Figure 4.2), 2-chlorophenol (Figure 4.3), 2,4-dichlorophenol (Figure 4.4), 2,6-dichlorophenol (Figure 4.5), 2,4,6-trichlorophenol (Figure 4.6) and pentachlorophenol (Figure 4.7) with their corresponding plot are shown in the corresponding Figures mentioned above. Besides, the optimum pHs of all phenol and

chlorophenol derivative according to their corresponding voltammograms are shown in Table 4.2 as well as their corresponding charts in Figure 4.8.

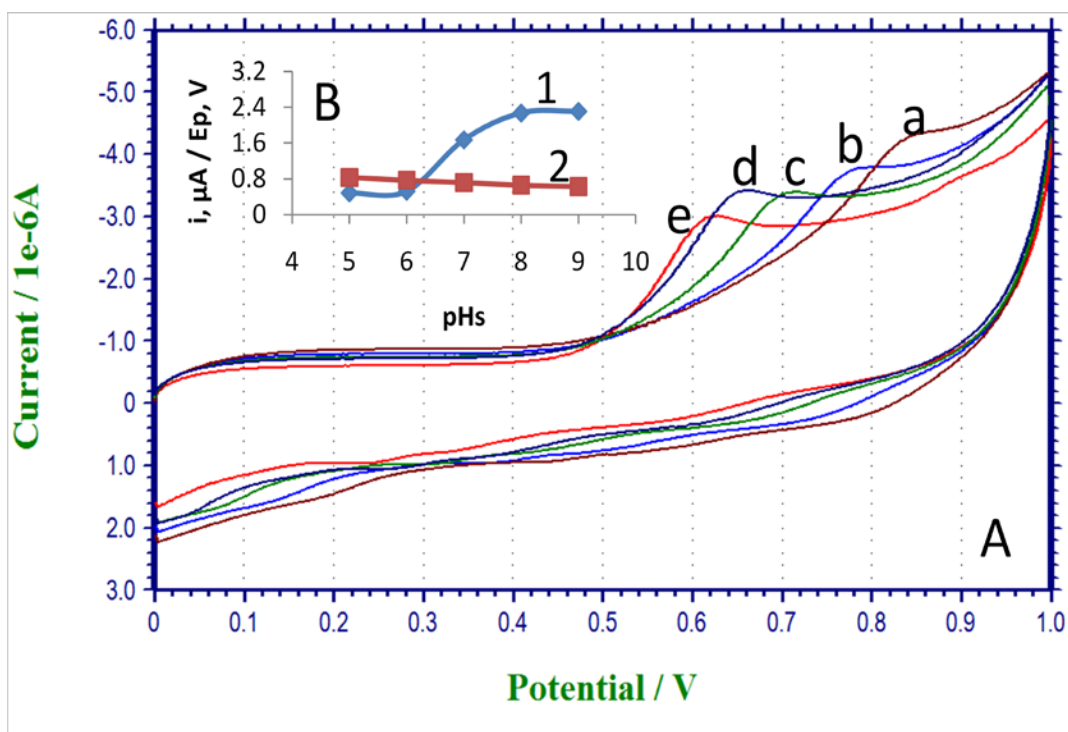


**Figure 4.2:** (A) Cyclic voltammograms of 30  $\mu$ M phenol at +0.40 V accumulation potential, 60s accumulation time in 0.1 M PBS at different pHs. (a) 5.00, (b) 6.00, (c) 7.00, (d) 8.00 and (e) 9.00. (B) Corresponding plots showing the peak heights (1) and the peak shift (2) in the electro-decomposition potentials.

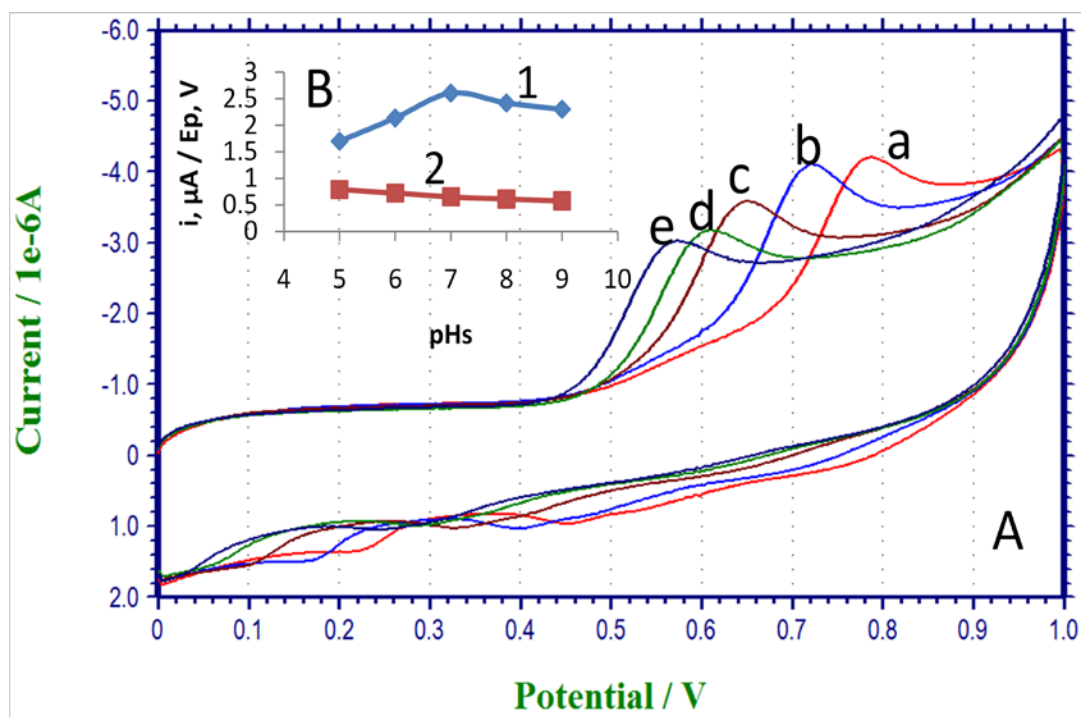


**Figure 4.3:** (A) Cyclic voltammograms of 30  $\mu\text{M}$  2-chlorophenol at +0.40 V accumulation potential, 60s accumulation time in 0.1 M PBS at different pHs. (a) 5.00, (b) 6.00, (c) 7.00, (d) 8.00 and (e) 9.00. (B) Corresponding plots showing the peak heights (1) and the peak shift (2) in the electro-decomposition potentials.

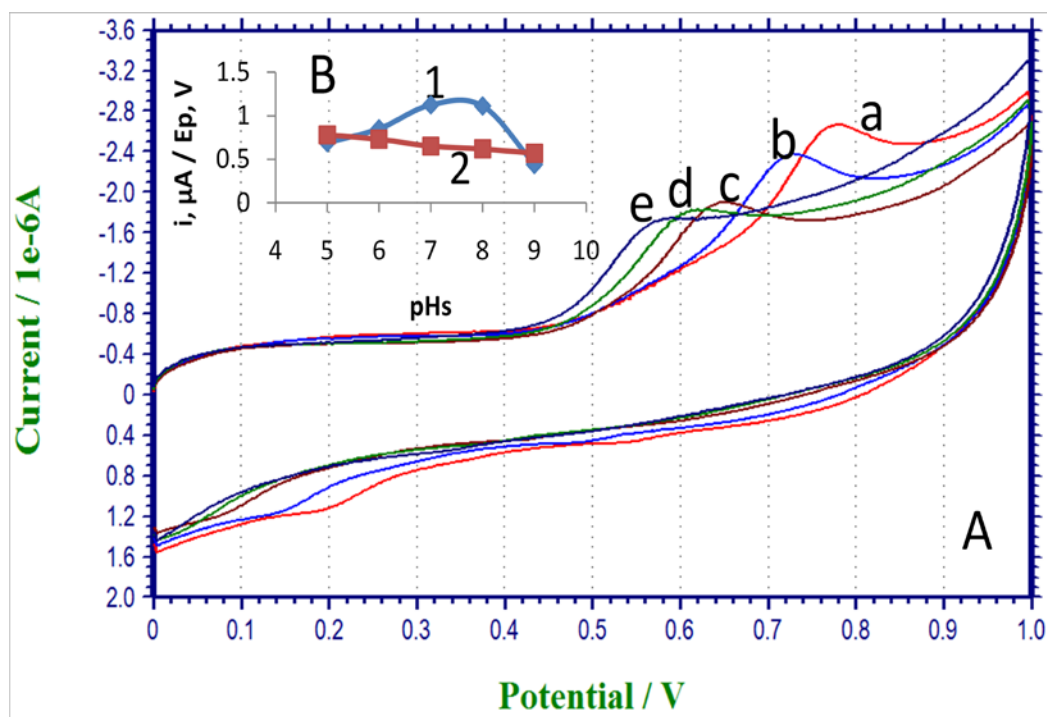


**Figure 4.4:** (A) Cyclic voltammograms of 30  $\mu\text{M}$  2,4-dichlorophenols at +0.40 V accumulation potential, 60s accumulation time in 0.1 M PBS at different pHs. (b) 5.00, (b) 6.00, (c) 7.00, (d) 8.00 and (e) 9.00. (B) Corresponding plots showing the peak heights (2) and the peak shift (2) in the electro-decomposition potentials.

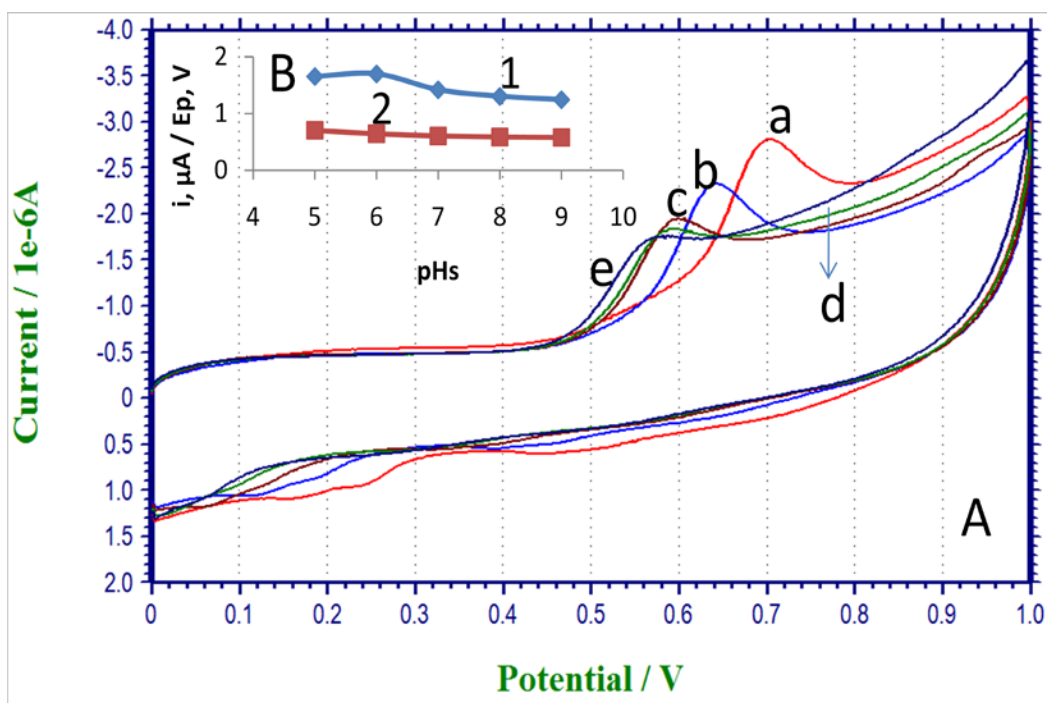


**Figure 4.5:** (A) Cyclic voltammograms of 30  $\mu\text{M}$  2,6-dichlorophenols at +0.40 V accumulation potential, 60s accumulation time in 0.1 M PBS at different pHs. (a) 5.00, (b) 6.00, (c) 7.00, (d) 8.00 and (e) 9.00. (B) Corresponding plots showing the peak heights (1) and the peak shift (2) in the electro-decomposition potentials.

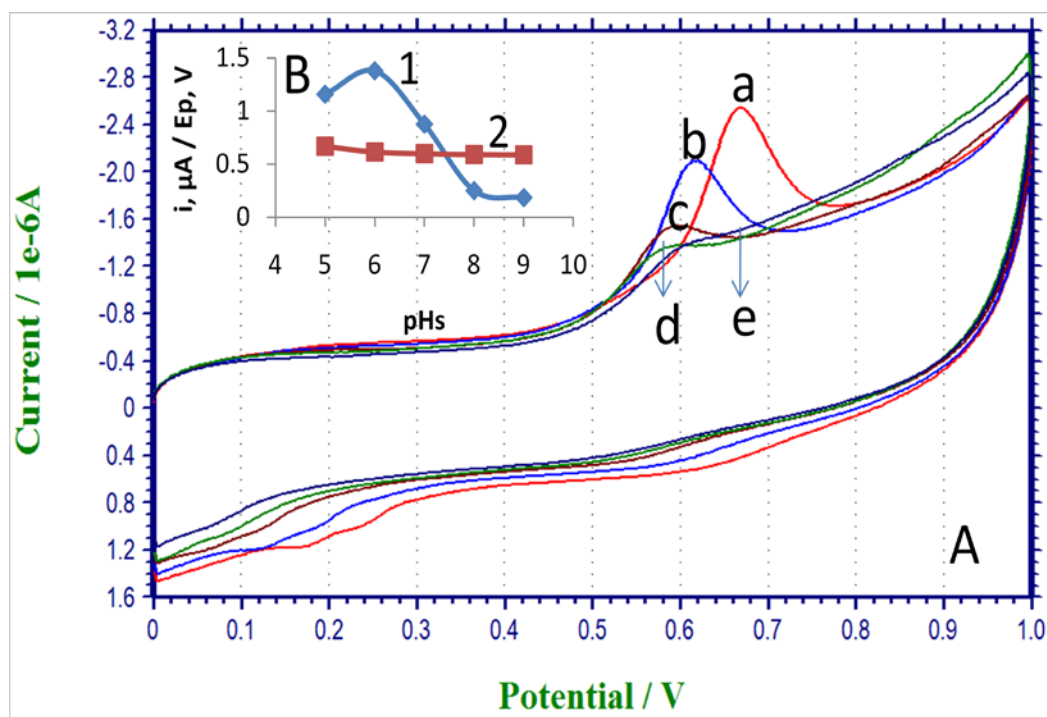


**Figure 4.6:** (A) Cyclic voltammograms of 30  $\mu\text{M}$  2,4,6-trichlorophenol at +0.40 V accumulation potential, 60s accumulation time in 0.1 M PBS at different pHs. (a) 5.00, (b) 6.00, (c) 7.00, (e) 8.00 and (e) 9.00. (B) Corresponding plots showing the peak heights (1) and the peak shift (2) in the electro-decomposition potentials.

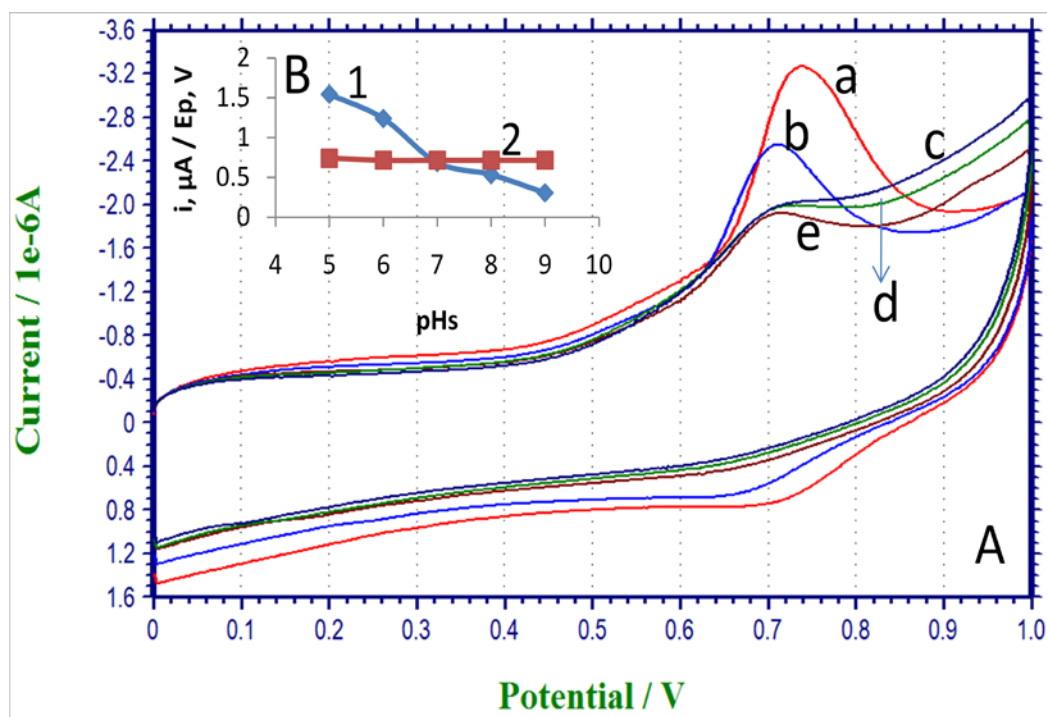


**Figure 4.7:** (A) Cyclic voltammograms of 30  $\mu\text{M}$  Pentachlorophenol at +0.40 V accumulation potential, 60s accumulation time in 0.1 M PBS at different pHs. (a) 5.00, (b) 6.00, (c) 7.00, (d) 8.00 and (e) 9.00. (B) Corresponding plots showing the peak heights (1) and the peak shift (2) in the electro-decomposition potentials.



**Table 4.2: Optimum pH,  $[A^-]$  and Their Corresponding  $E_p$  of Cyclic Voltammetry Technique for Phenol and Chlorophenol Derivatives.**

Compounds	Opt. pH	$E_p$ (V)	Exp. $pK_a$	$[A^-]$ M
Phenol	9.00	0.626	10.00	$3.00 \times 10^{-6}$
2-chlorophenol	7.00	0.652	8.29	$1.54 \times 10^{-6}$
2,4-dichlorophenol	7.00	0.652	8.09	$2.44 \times 10^{-6}$
2,6-dichlorophenol	6.00	0.644	6.79	$4.87 \times 10^{-6}$
2,4,6-trichlorophenol	6.00	0.614	6.29	$1.54 \times 10^{-5}$
Pentachlorophenol	5.00	0.740	NA	$3.00 \times 10^{-5}$

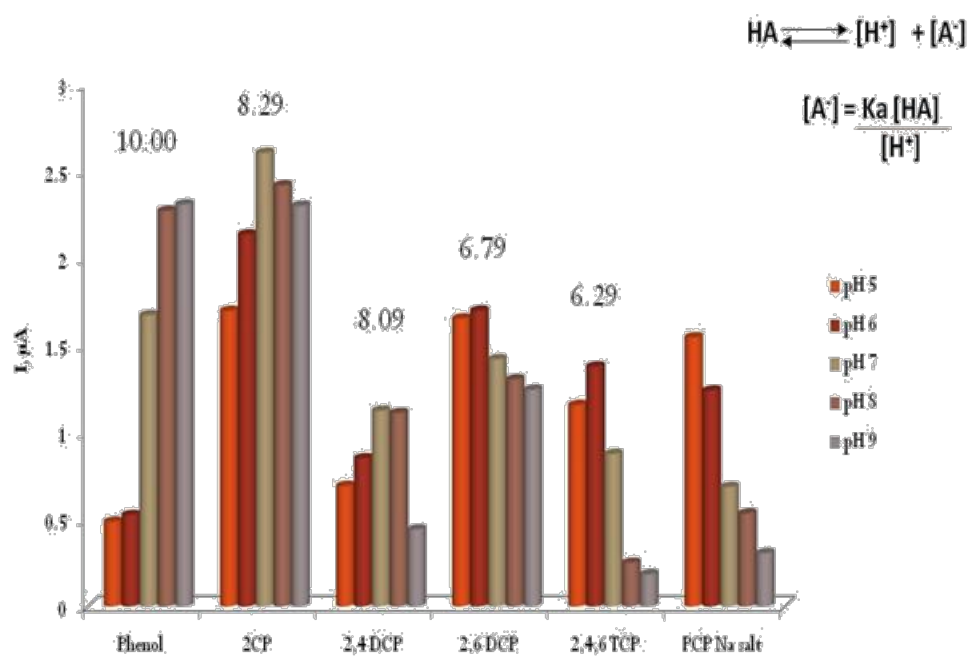


**Figure 4.8:** Chart of the pH effect and the corresponding pK<sub>a</sub> by Cyclic Voltammetry.

#### 4.1.2.2 Investigation Using Square Wave Stripping Voltammetry (SWSV)

The pH dependence of the phenol and chlorophenol derivatives was also studied systematically by SWV at +0.40 V accumulation potential in the pH range of 5.00 to 9.00 of 0.1 M Phosphate buffer solutions (Figures 4.9 to Figure 4.14). As the pH increases, the electro-decomposition potential shifted towards less positive potentials due to the hindrance of the oxidation at low concentrations of protons. This was in agreement with the CV investigation (4.1.2.1). As obtained in the CV investigation, there was no shift observed for pentachlorophenol due to the fact that there is no hydrogen atom to be dissociated in the compound as shown in Figure 4.14. Figure 4.15 shows the oxidation peak signals of the studied phenols at +0.40V for various pHs by SWV with optimum pH of 6.00 for 2,4-dichlorophenol in contrast with optimum pH 7.00 for the CV Studies. The behavior of these oxidation peaks can be simply explained by the anion concentrations  $[A^-]$  of the phenols in the oxidation reaction.

As shown in Figures 4.9 and 4.15, the oxidation peaks of phenol increases as the  $[A^-]$  increases which is proportional to increase in pH from 5.00 to 9.00 while that of pentachlorophenol behaves in opposite direction as shown in Figure 4.14. These implies that the phenol  $[A^-]$  was also moving towards the optimum value while that of pentachlorophenol moves away from the optimum value considering their corresponding pKa value as shown in Table 4.1. However, as the  $[A^-]$  of 2-chlorophenol, 2,4-dichlorophenol, 2,6-dichlorophenol, 2,4,6-trichlorophenol increases, the oxidation peak increase until the equilibrium point is reached where any further increase in the  $[A^-]$  will

no longer favors the oxidation peak as explain by the le chatelier's principle to explain the effect of change in condition of a chemical equilibrium. The corresponding optimum  $[A^-]$  shown in Table 4.2 for each phenol are calculated through the equilibrium constant ( $K_a$ ) expression. The  $K_a$  and the hydrogen ion concentration  $[H^+]$  values were calculated from the experimental  $pK_a$  shown in Table 4.1 of analyte and their optimum pH.

The effects of pH of phenol (Figure 4.9), 2-chlorophenol (Figure 4.10), 2,4-dichlorophenol (Figure 4.11), 2,6-dichlorophenol (Figure 4.12), 2,4,6-trichlorophenol (Figure 4.13) and pentachlorophenol sodium salt (Figure 4.14) with their corresponding plot are shown in the corresponding Figures mentioned above. Besides, the optimum pH of all phenols according to the voltammograms is shown in Table 4.3 and their corresponding chart in Figure 4.15.

The effects of pH of phenol (Figure 4.9), 2-chlorophenol (Figure 4.10), 2,4-dichlorophenol (Figure 4.11), 2,6-dichlorophenol (Figure 4.12), 2,4,6-trichlorophenol (Figure 4.13) and pentachlorophenol sodium salt (Figure 4.14) with their corresponding plot are shown in the corresponding Figures mentioned above. Besides, the optimum pH of all phenols according to the voltammograms is shown in Table 4.3 and their corresponding chart in Figure 4.15.

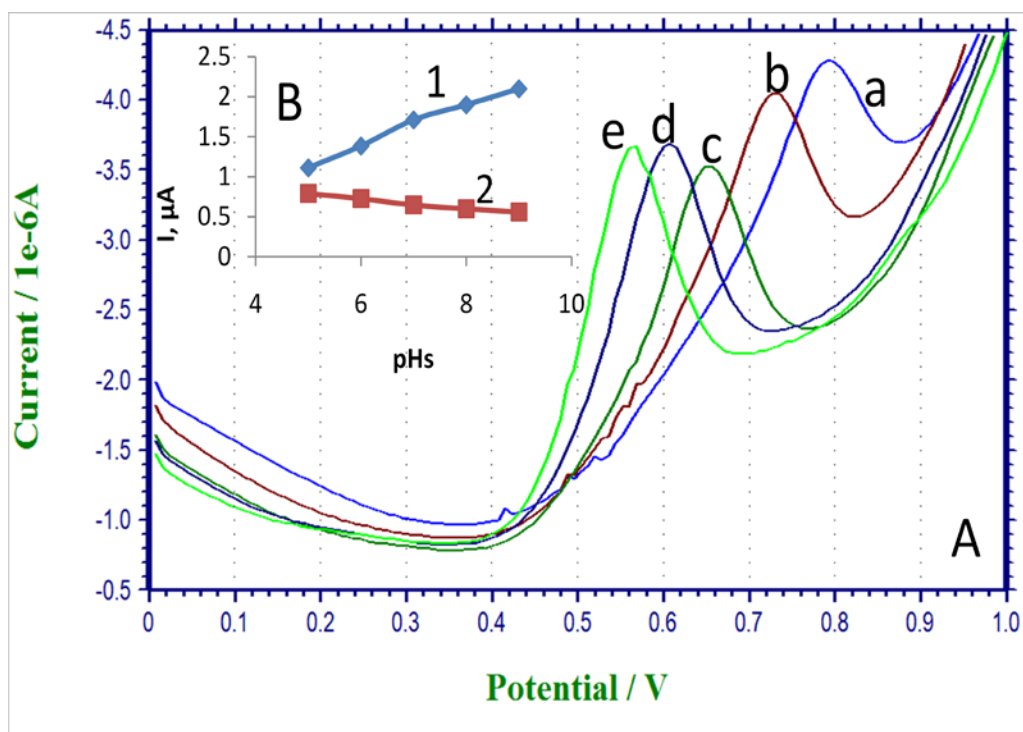


**Figure 4.9:** (A) Square wave stripping voltammograms of 30  $\mu$ M phenol at +0.40 V accumulation potential, 60s accumulation time in 0.1 M PBS at different pHs. (a) 5.00, (b) 6.00, (c) 7.00, (d) 8.00 and (e) 9.00. (B) Corresponding plots showing the peak area (1) and the peak shift (2) in the electro-decomposition potentials.

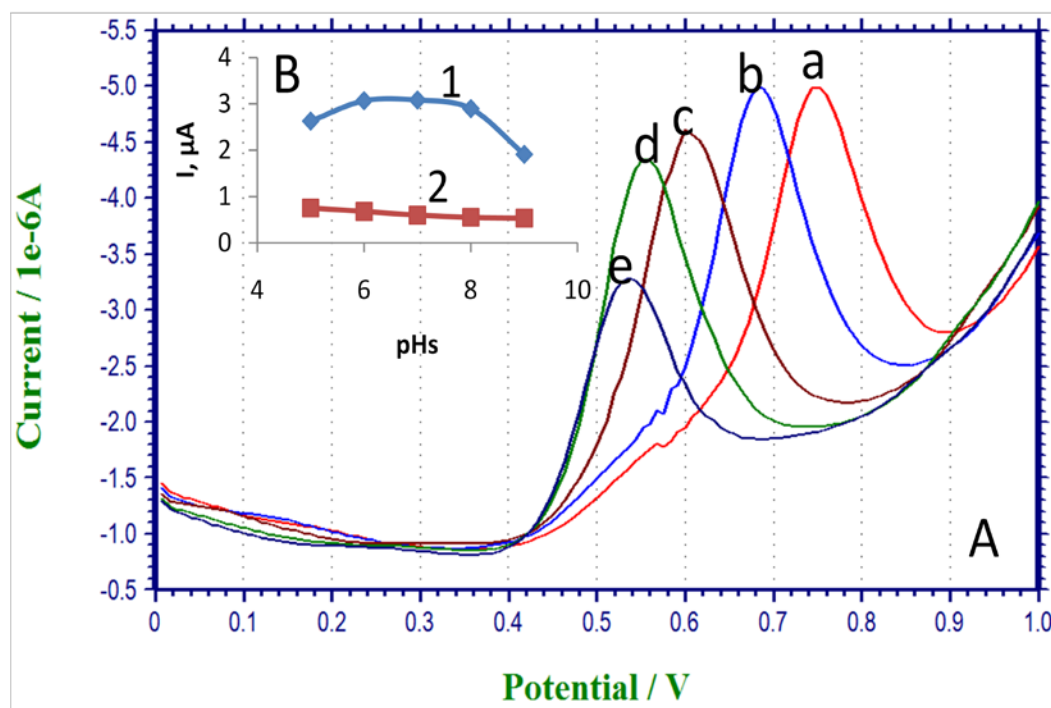


**Figure 4.10:** (A) Square wave stripping voltammograms of 30  $\mu\text{M}$  2-chlorophenol at +0.40 V accumulation potential, 60s accumulation time in 0.1 M PBS at different pHs. (a) 5.00, (b) 6.00, (c) 7.00, (d) 8.00 and (e) 9.00. (B) Corresponding plots showing the peak area (1) and the peak shift (2) in the electro-decomposition potentials.

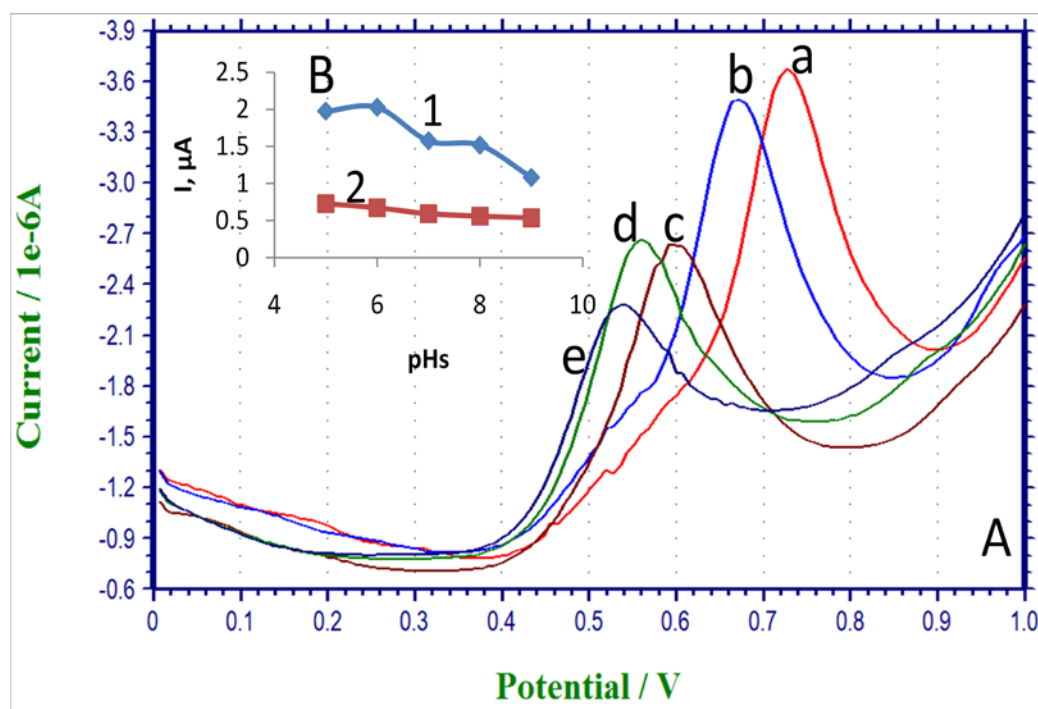


**Figure 4.11:** (A) Square wave stripping voltammograms of 30  $\mu\text{M}$  2,4-dichlorophenol at +0.40 V accumulation potential, 60s accumulation time in 0.1 M PBS at different pHs. (a) 5.00, (b) 6.00, (c) 7.00, (e) 8.00 and (e) 9.00. (B) Corresponding plots showing the peak area (1) and the peak shift (2) in the electro-decomposition potentials.

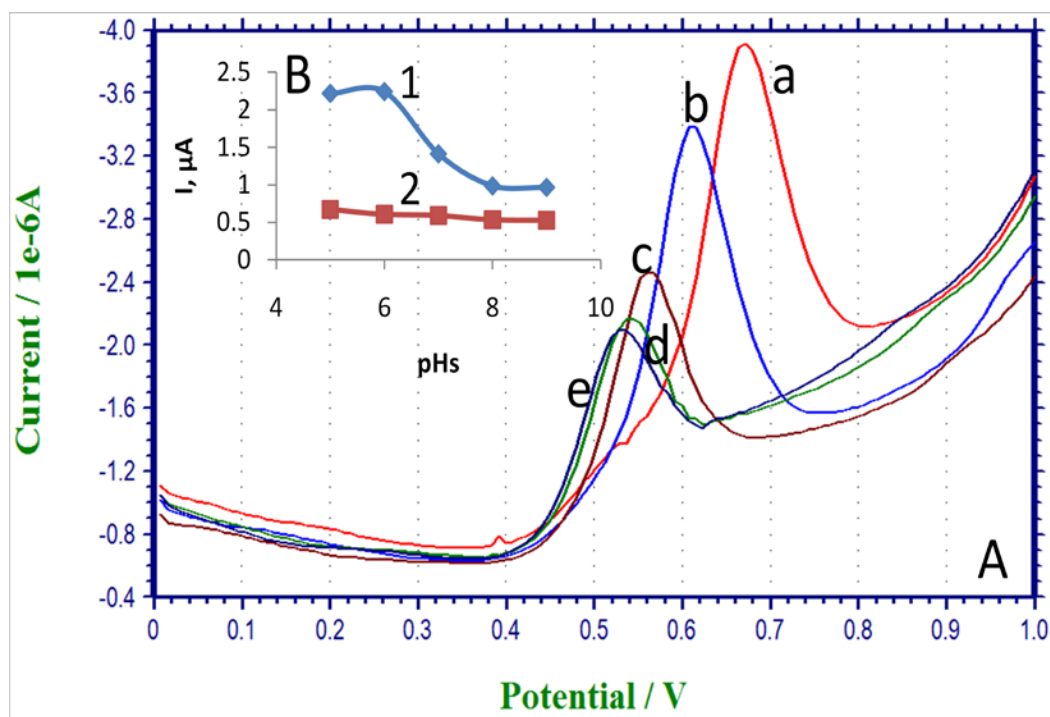


**Figure 4.12:** (A) Square wave stripping voltammograms of 30 $\mu$ M 2,6-dichlorophenol at +0.40 V accumulation potential, 60s accumulation time in 0.1 M PBS at different pHs. (a) 5.00, (b) 6.00, (c) 7.00, (d) 8.00 and (e) 9.00. (B) Corresponding plots showing the peak area (1) and the peak shift (2) in the electro-decomposition potentials.



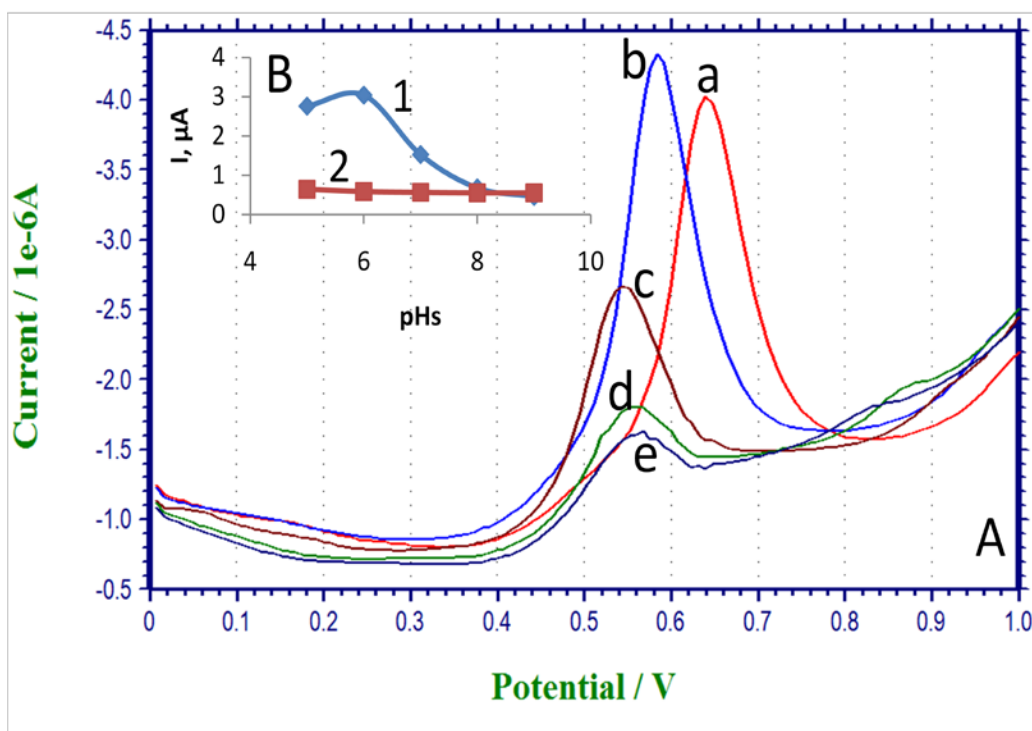


**Figure 4.13:** (A) Square wave stripping voltammograms of 30  $\mu\text{M}$  2,4,6-trichlorophenol at +0.40 V accumulation potential, 60s accumulation time in 0.1 M PBS at different pHs. (a) 5.00, (b) 6.00, (c) 7.00, (d) 8.00 and (e) 9.00. (B) Corresponding plots showing the peak area (1) and the peak shift (2) in the electro-decomposition potentials.

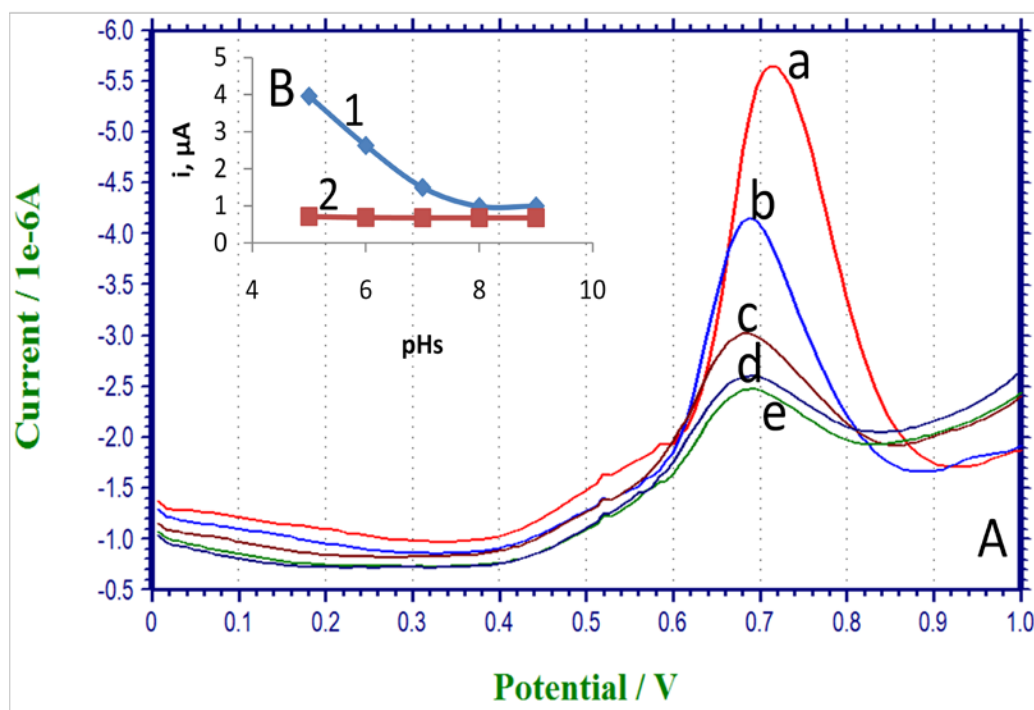


**Figure 4.14:** (A) Square wave stripping voltammograms of 30  $\mu\text{M}$  Pentachlorophenol sodium salt at +0.40 V accumulation potential, 60s accumulation time in 0.1 M PBS at different pHs. (a) 5.00, (b) 6.00, (c) 7.00, (d) 8.00 and (e) 9.00. (B) Corresponding plots showing the peak area (1) and the peak shift (2) in electro-decomposition potentials.

**Table 4.3: Optimum pH,  $[A^-]$  and Their Corresponding  $E_p$  of Square Wave Stripping Voltammetry Technique for Phenol and Chlorophenol Derivatives.**

Compounds	Opt. pH	$E_p$ (V)	Exp. $pK_a$	$[A^-]$ M
Phenol	9.00	0.626	10.00	$3.00 \times 10^{-6}$
2-chlorophenol	7.00	0.652	8.29	$1.54 \times 10^{-6}$
2,4-dichlorophenol	6.00	0.652	8.09	$2.44 \times 10^{-7}$
2,6-dichlorophenol	6.00	0.644	6.79	$4.87 \times 10^{-6}$
2,4,6-trichlorophenol	6.00	0.614	6.29	$1.54 \times 10^{-5}$
Pentachlorophenol	5.00	0.740	NA	$3.00 \times 10^{-5}$

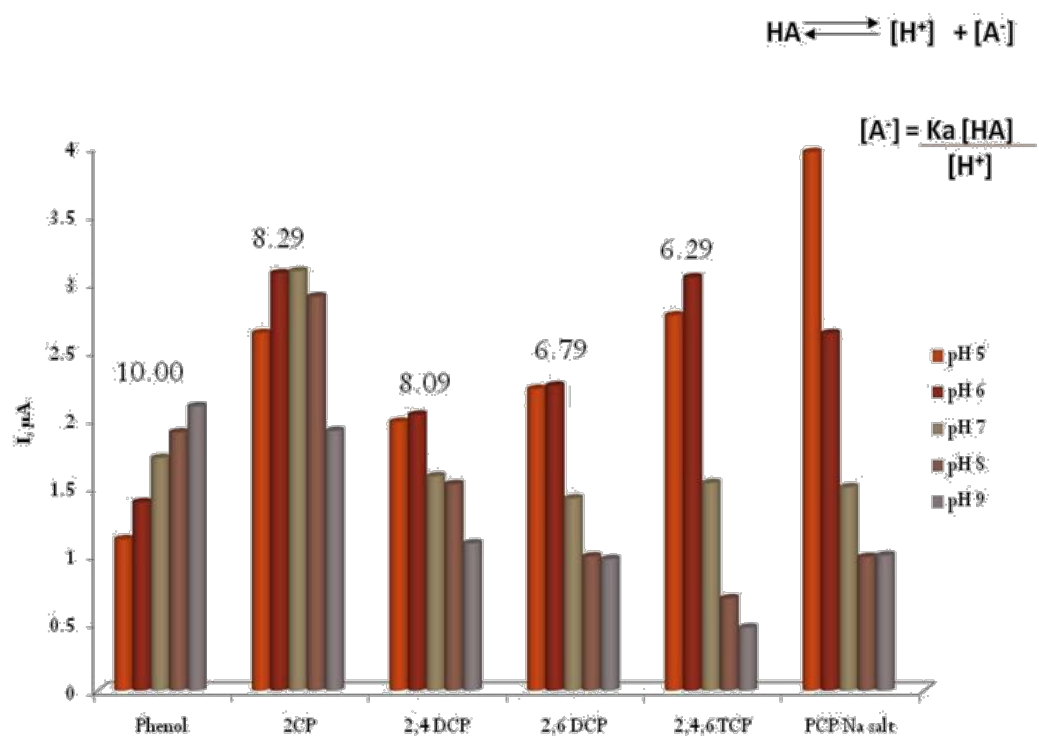


**Figure 4.15:** Chart of the pH effect and the corresponding  $\text{pK}_a$  by Square Wave Stripping Voltammetry.

#### **4.1.3 Confirmation of Fouling on Glassy Carbon Electrode (GCE) by Cyclic Voltammetry and Square Wave Stripping Voltammetry**

Passivation of the solid electrodes especially the glassy carbon is a major problem affecting the sensitivity of phenolic compounds in electro-analytical determinations. However, for the confirmations of fouling effects of phenol and chlorophenol derivatives, we have adopted the procedure reported by Enache T. A and Oleveira-Brett A. M. et al. 2011 (58). The strategy of scanning and rescanning without polishing the electrode was used to investigate the fouling effect of phenol and para substituted phenols by cyclic voltammetry and differential pulse voltammetry techniques in 0.1 M phosphate buffer solution of pH 7.00. However, we have moved a step further in our procedure by having a third scan in a blank solution without polishing the electrode to show the disappearance of the first oxidized peak and retaining the isomerized product peaks.

The results obtained for phenol in both techniques in Figure 4.16 is similar to what is reported by Enache T. A and Oleveira-Brett A. M. et al. 2011 (58). However, comparing the voltammograms of phenol (Figure 4.16) and 2-chlorophenol (Figure 4.17) was surprisingly to be almost the same. This was in agreement with the conclusion of Ezerskis Z. and Jusys Z. 2001 (56) in their potentiodynamic investigations of chlorophenols at platinum electrode in alkaline solution, that phenol and 2-chlorophenol exhibits a similar oxidation reaction.

Besides, due to a very weak signals of the fouling effects of all the phenol and chlorophenol derivatives compared with the first oxidized signal in both techniques

makes it difficult to analyze as shown in the 2,4-dichlorophenol (Figure 4.18), 2,6-dichlorophenol (Figure 4.19) and 2,4,6-trichlorophenol (Figure 4.20). However, pentachlorophenol seems not to foul the surface of the electrode by what Figure 4.21 reveals. These might lead to the conclusion that all chlorophenols except the pentachlorophenol possess fouling effects which is in conformity with the conclusion of Ureta-Zanartu M. S. et al. 2002 (57), that all chlorophenols apart from pentachlorophenol leads to the passivation of solid electrodes.

The multiple cycles of cyclic voltammograms for 2-chlorophenol and pentachlorophenol sodium salt at the surface in the same solution shown in Figure 4.22 is a representative of all chlorophenols confirming their fouling effects. Besides the fouling effect on the oxidation peaks (other peaks in Figure 4.22A) confirming the isomerized product which are reversible for phenol and chlorophenols while the absence of these peaks in Figure 4.22B further confirmed that there is no isomerized product in pentachlorophenol which is a representative of pentachlorophenol.

These results clear the misconception that is reported by Ureta-Zanartu M. S. et al. 2002 (57) that all chlorophenols except pentachlorophenol exhibit fouling effect. It was reported that all chlorophenols undergo diffusion controlled electrode processes except pentachlorophenol that undergoes only adsorption controlled electrode process. However, pentachlorophenol does not possess diffusion controlled electrode process because there is no way it can leads to an isomerized product, yet other chlorophenols including phenol can exhibit some adsorption and desorption due to the possibility of a reversible isomerized product as shown in Figure 4.22A.

The misconception can be further cleared by Figure 4.22C showing the multiple cycles of cyclic voltammograms of hydroquinone which possess a reversible oxidation peaks with almost no fouling compared with Figure 4.22A and 4.22B. Comparative studies of Figure 4.22 proved that all chlorophenols with no exception exhibit fouling on the surface of GCE as a result of the irreversible oxidation peaks products.

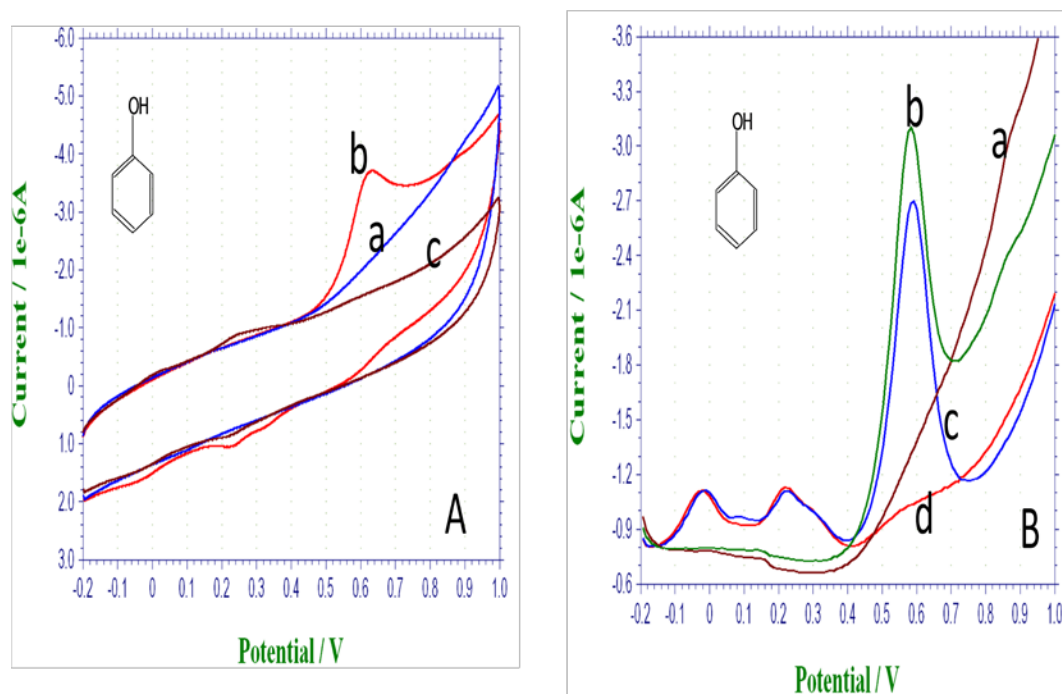


**Figure 4.16:** (A) Cyclic voltammograms (B) Square wave stripping voltammograms for 30  $\mu\text{M}$  phenol at +0.40V accumulation potential, 60s accumulation time in 0.1M PBS pH 9.00 (a) blank, (b) first scan, (c) second scan without polishing and (d) rescan in the blank solution without polishing right after scanning in 30  $\mu\text{M}$  phenol. (Note, c in A is same as d in B)



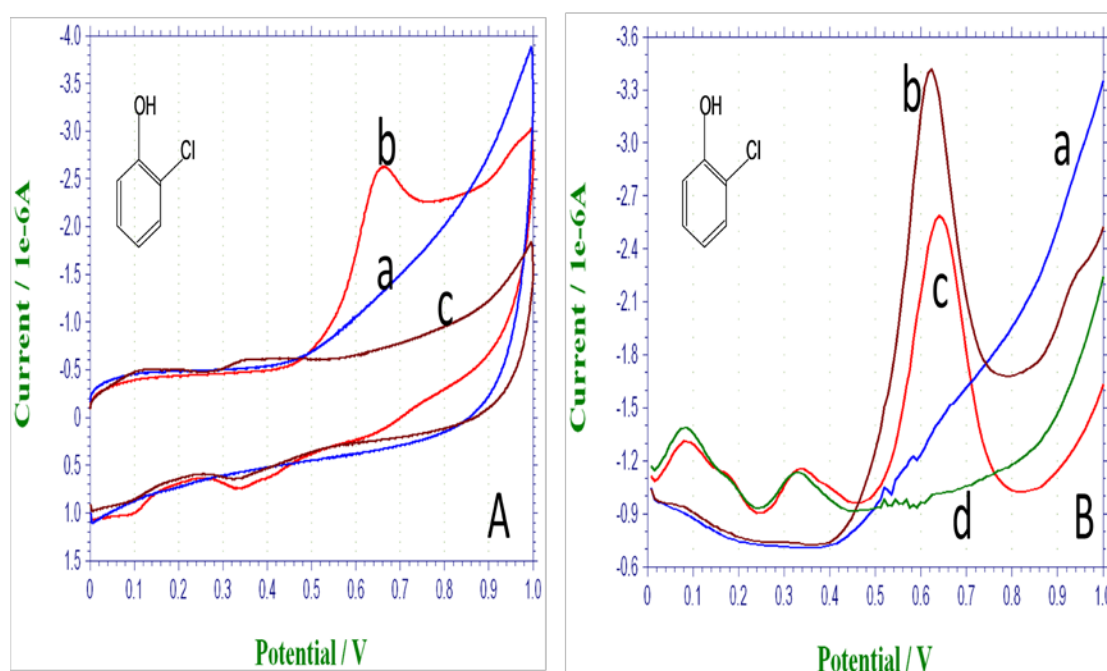


**Figure 4.17:** (A) Cyclic voltammograms (B) Square wave stripping voltammograms for 30  $\mu\text{M}$  2-chlorophenol at +0.40V accumulation potential, 60s accumulation time in 0.1M PBS pH 7.00 (a) blank, (b) first scan, (c) second scan without polishing and (d) rescan in the blank solution without polishing right after scanning in 30 $\mu\text{M}$  2-chlorophenol. (Note, C in A is same as d in B)

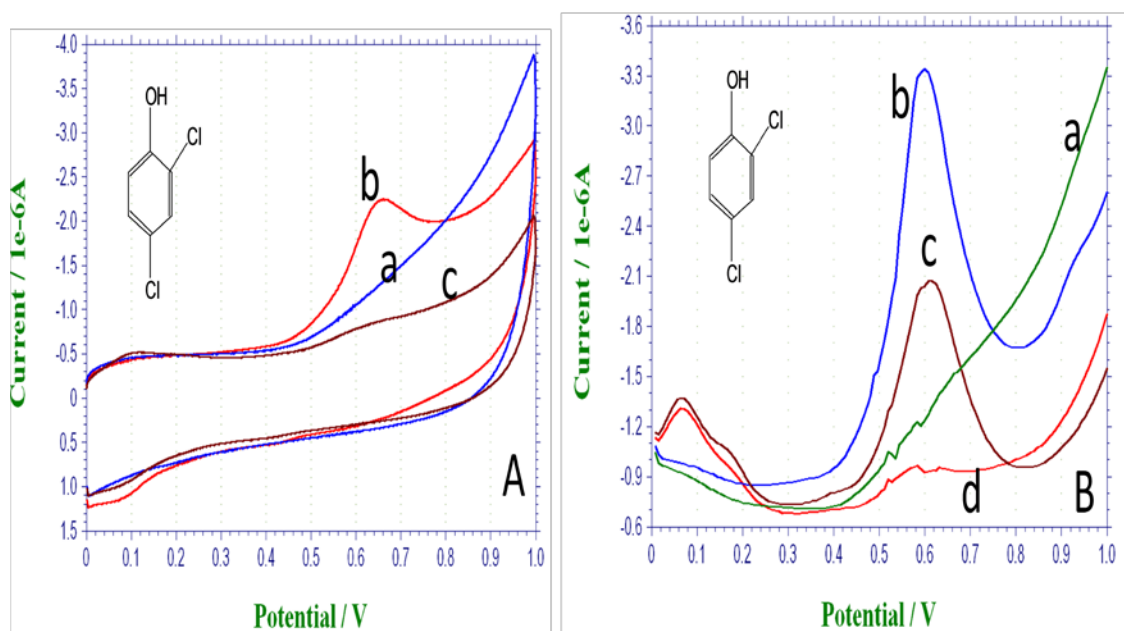


**Figure 4.18:** (A) Cyclic voltammograms (B) Square wave stripping voltammograms for 30  $\mu\text{M}$  2,4-dichlorophenol at +0.40 V accumulation potential, 60s accumulation time in 0.1M PBS pH 7.00 (a) blank, (b) first scan, (c) second scan without polishing and (d) rescan in the blank solution without polishing right after scanning in 30  $\mu\text{M}$  2,4-dichlorophenol. (Note, c in A is same as d in B)

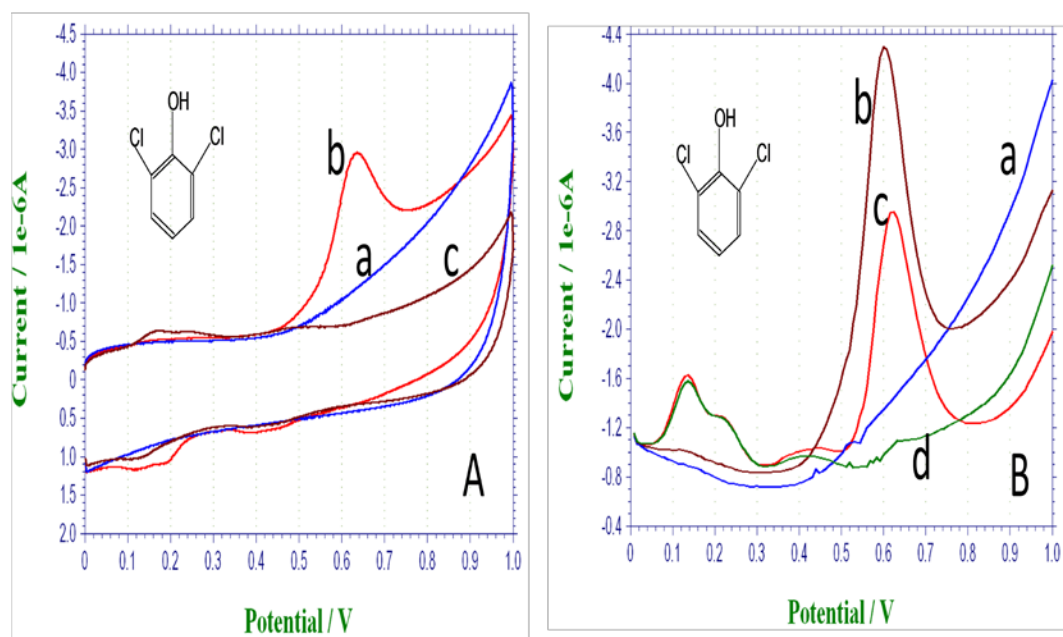


**Figure 4.19:** (A) Cyclic voltammograms (B) Square wave stripping voltammograms for 30  $\mu\text{M}$  2,6-dichlorophenol at +0.40 V accumulation potential, 60s accumulation time in 0.1 M PBS pH 6.00 (a) blank, (b) first scan, (c) second scan without polishing and (d) rescan in the blank solution without polishing after scanning with 30  $\mu\text{M}$  2,6-dichlorophenol. (Note, c in A is same as d in B)

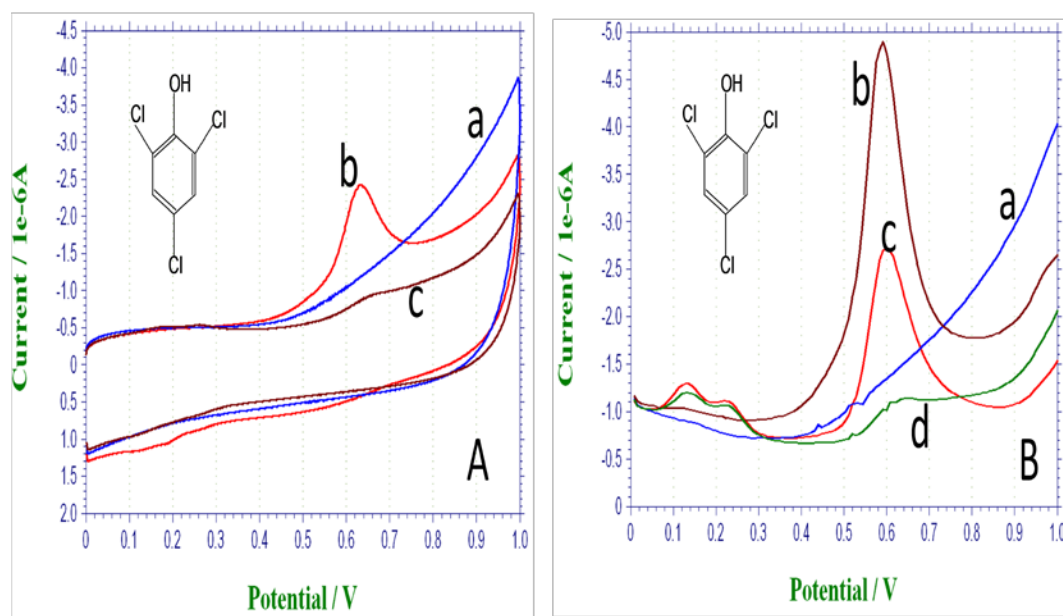


**Figure 4.20:** (A) Cyclic voltammograms (B) Square wave stripping voltammograms for 30  $\mu\text{M}$  2,4,6-trichlorophenol at +0.40 V accumulation potential, 60s accumulation time in 0.1 M PBS pH 6.00 (a) blank, (b) first scan, (c) second scan without polishing and (d) rescan in the blank solution without polishing right after scanning with 30 $\mu\text{M}$  2,4,6- trichlorophenol. (Note, c in A is same as d in B)

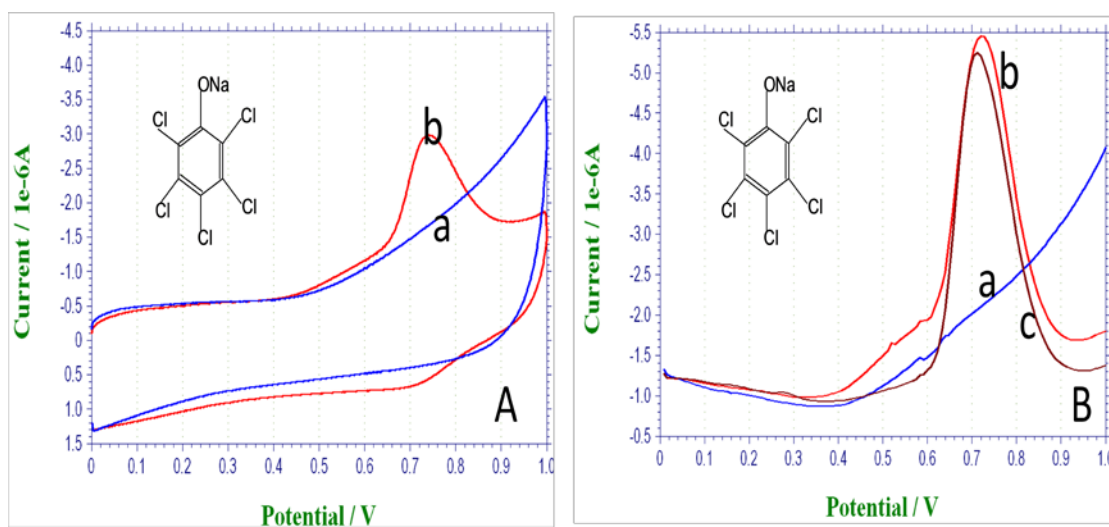


**Figure 4.21:** (A) Cyclic voltammograms (B) Square wave stripping voltammograms for 30  $\mu\text{M}$  pentachlorophenol at +0.40 V accumulations potential, 60s accumulation time in 0.1 M PBS pH 5.00 (a) blank, (b) first scan (c) second scan without polishing.

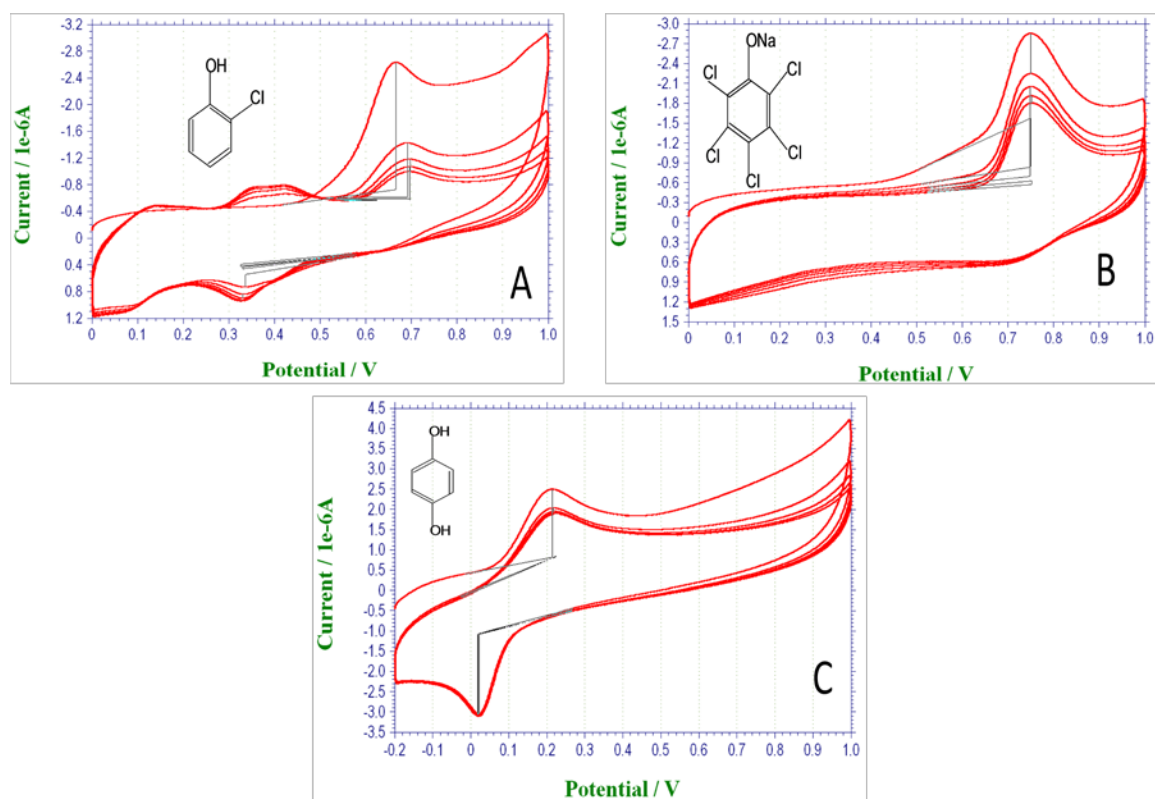


**Figure 4.22:** Cyclic voltammograms for 5 cycles at +0.40 V accumulation potential, 60s accumulation time in 0.1 M PBS at corresponding optimized pH for (A) 2-chlorophenol, pH 7.00, (B) Pentachlorophenol sodium salt, pH 5.00 and (C) Hydroquinone, pH 7.00.

#### **4.1.4 Electrochemical Investigation at Different Accumulation Potentials Using Cyclic Voltammetry and Square Wave Stripping Voltammetry**

The mode of controlling reaction in electrochemical analysis can either be by controlling current or by controlling potential. However, cyclic voltammetry and square wave stripping voltammetry are both potential control voltammetric techniques. This afford us the opportunity to control the rate of oxidation and reduction (redox) reactions of phenol and chlorophenol derivatives by varying the accumulation potential between 400 mV and 1000 mV.

##### **4.1.4.1 Investigation Using Cyclic Voltammetry**

The first oxidized anodic peak signal was found to be reducing in magnitude from +400 mV to +1000 mV while some peaks emerge at lower potentials. These peaks appearing at lower potentials representing the ortho and para product as proven by Enache T. A. and Oliveira-Brett A.M 2011 (58) were increasing as the accumulation potential increases. Besides, they were the same as those observed from our procedure of confirming fouling on the GCE surface with a weaker signal. The effect of potential on the phenol and chlorophenol derivative makes it possible to obtain the isomerized product peaks at a single scan with increasing as the potential increases.

However, the isomerized products peak are relatively weak compared to the first oxidized peak, and also difficult to visually identify the number of the isomerized product peaks.

The closeness of these peaks will make further investigation to be very tedious using cyclic voltammetry due to the overlapping of the peaks as shown in Figure 4.23 and 4.24 for phenol and 2-chlorophenol respectively.

The voltammograms obtained for 2,4-dichlorophenol, 2,6-dichlorophenol and 2,4,6-trichlorophenol as shown in Figures 4.25, 4.26 and 4.27 respectively were similar to the previous voltammograms in our formal procedure, yet with a stronger signals. They were also very close apart from that of 2,4-dichlorophenol that has a single isomerized product peak (Figure 4.26). Moreover, no isomerized product was observed in the voltammograms of pentachlorophenol sodium salt for all the potentials between +400 mV and +1000 mV as shown in Figure 4.28.



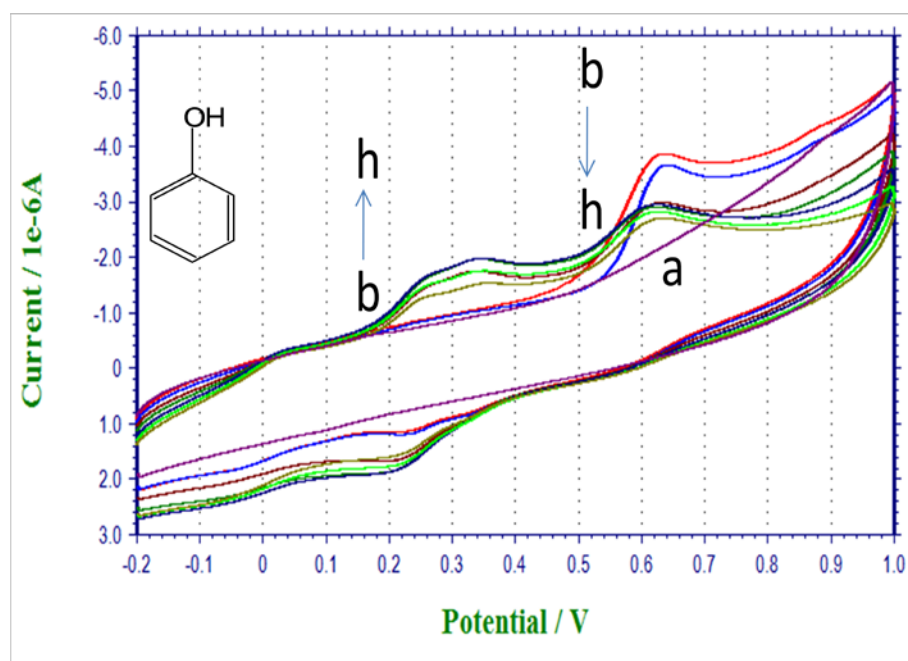


**Figure 4.23:** Cyclic voltammograms for 30 μM phenol showing the signal behavior at different accumulation potentials (a) blank at 400 mV, (b) 400mV, (c) 500 mV, (d) 600 mV, (e) 700 mV, (f) 800 mV, (g) 900 mV (h) 1000 mV. Working conditions: scan rate, 100 mV/s; sample interval, 2 mV and accumulation time, 60 s in 0.1 M PBS at pH 9.00.

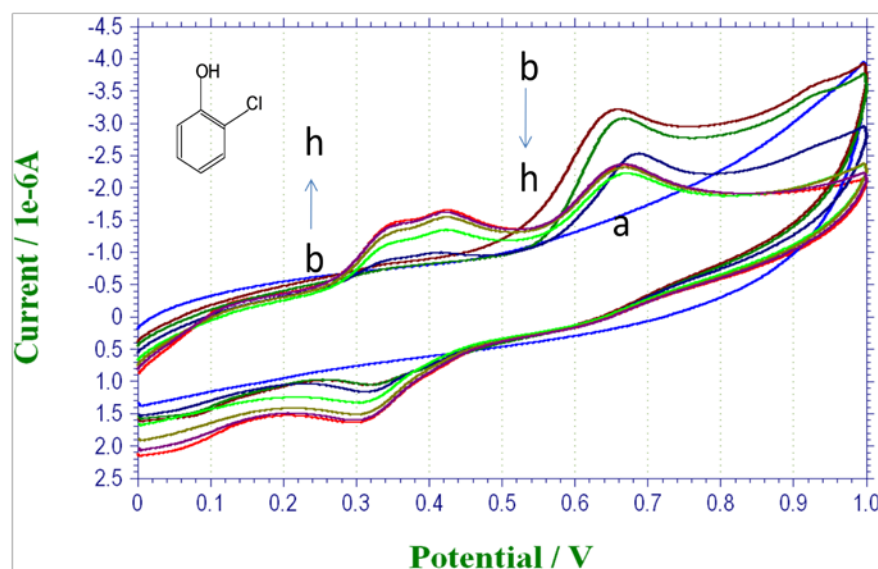


**Figure 4.24:** Cyclic voltammograms of 30  $\mu\text{M}$  2-chlorophenol showing the signal behavior at different accumulation potentials (a) blank at 400 mV, (b) 400mV, (c) 500 mV, (d) 600 mV, (e) 700 mV, (f) 800 mV, (g) 900 mV (h) 1000 mV. Working conditions: scan rate, 100 mV/s; sample interval, 2 mV and accumulation time, 60 s in 0.1 M PBS at pH 7.00.

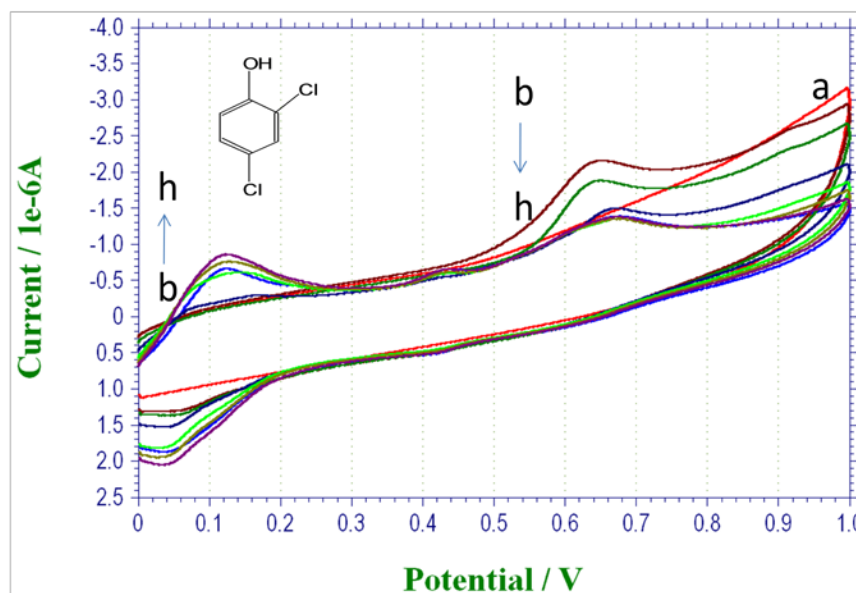


**Figure 4.25:** Cyclic voltammograms of 30  $\mu\text{M}$  2,4-dichlorophenols showing the signal behavior at different accumulation potentials (a) blank at 400 mV, (b) 400mV, (c) 500 mV, (d) 600 mV, (e) 700 mV, (f) 800 mV, (g) 900 mV (h) 1000 mV. Working conditions: scan rate, 100 mV/s; sample interval, 2 mV and accumulation time, 60 s in 0.1 M PBS at pH 7.00.

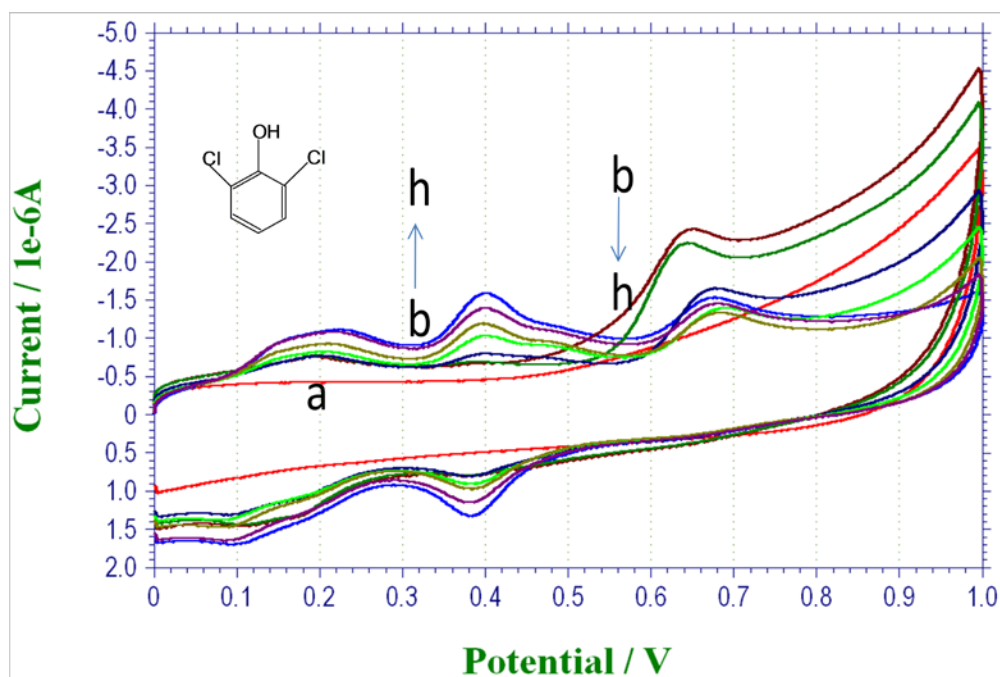


**Figure 4.26:** Cyclic voltammograms of 30  $\mu\text{M}$  2,6-dichlorophenols showing the signal behavior at different accumulation potentials (a) blank at 400 mV, (b) 400mV, (c) 500 mV, (d) 600 mV, (e) 700 mV, (f) 800 mV, (g) 900 mV (h) 1000 mV. Working conditions: scan rate, 100 mV/s; sample interval, 2 mV and accumulation time, 60 s in 0.1 M PBS at pH 6.00.

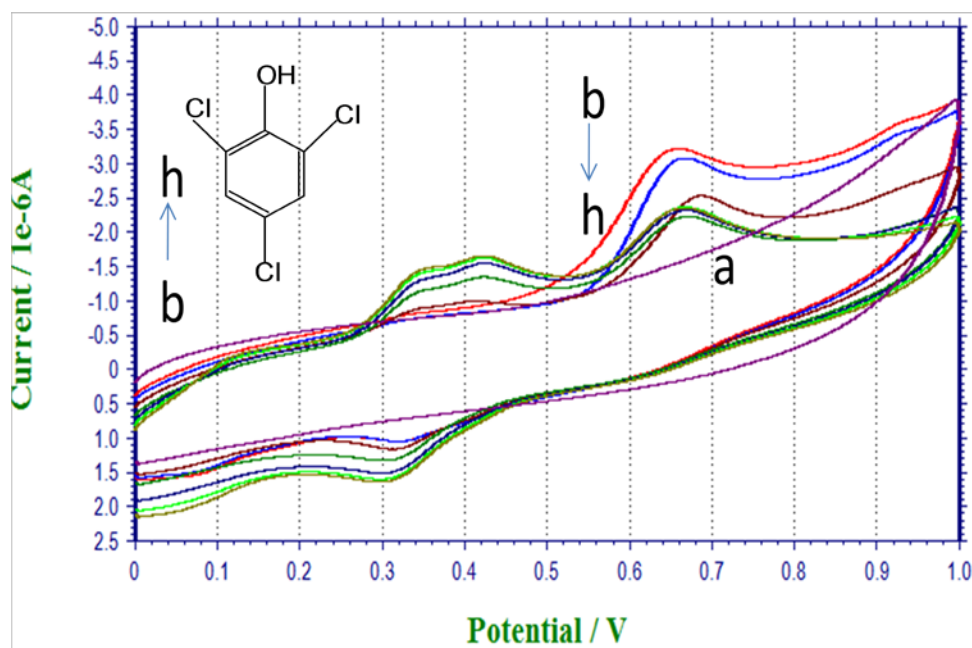


**Figure 4.27:** Cyclic voltammograms of 30μM 2,4,6-trichlorophenols showing the signal behavior at different accumulation potentials (a) blank at 400 mV, (b) 400mV, (c) 500 mV, (d) 600 mV, (e) 700 mV, (f) 800 mV, (g) 900 mV (h) 1000 mV. Working conditions: scan rate, 100 mV/s; sample interval, 2 mV and accumulation time, 60 s in 0.1 M PBS at pH 6.00.

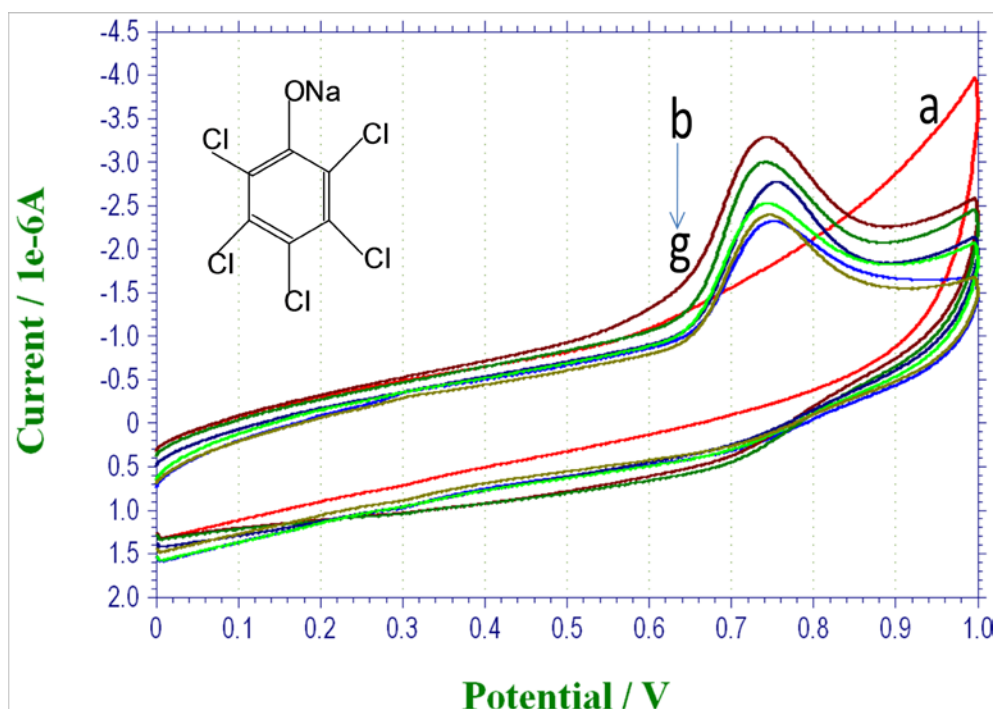


**Figure 4.28:** Cyclic voltammograms of 30  $\mu$ M pentachlorophenol sodium salt showing the signal behavior at different accumulation potentials (a) blank at 500 mV, (b) 500mV, (c) 600 mV, (d) 700 mV, (e) 800 mV, (f) 900 mV, (g) 1000 mV. Working conditions: scan rate, 100 mV/s; sample interval, 2 mV and accumulation time, 60 s in 0.1 M PBS at pH 5.00.

#### 4.1.4.2 Investigation Using Square Wave Stripping Voltammetry

The same effect observed using cyclic voltammetry where the first oxidized anodic peak signal was found to be reducing in magnitude between +400 mV and +1000 mV while new peaks emerged at lower potential were confirmed with the square wave stripping voltammetry. These peaks at a lower potential representing the ortho and the para product were increasing as the accumulation potential increases.

In contrast with the relatively weaker peaks of the isomerized product observed using cyclic voltammetry, the peaks were very huge to the extent of overcoming the first oxidized peak at higher potentials. Apart from this, the peaks are well separated which makes it easy to identify the number of expected isomerized product as shown in Figure 4.29 and 4.30 for phenol and 2-chlorophenol respectively with both having similar isomerized products. The separation of these peaks will make it easy and afford us the opportunity to investigate further with square wave stripping voltammetry rather than cyclic voltammetry.

The voltammograms obtained for 2,6-dichlorophenol and 2,4,6-trichlorophenol as shown in Figures 4.32 and 4.33 respectively were similar to the voltammograms obtained for the same compounds (Figure 4.26 and 4.27) in cyclic voltammetry technique with stronger signals.

However, there were additional peaks observed in the square wave stripping voltammograms of 2,4-dichlorophenol in Figure 4.31 and pentachlorophenol sodium salt in Figure 4.34 due to the higher sensitivity of the square wave stripping voltammetry

technique compare with the cyclic voltammetry technique. The new peak (at about  $E_p = +0.3$  V) that starts to appear when the accumulation potential reaches +600 mV for the pentachlorophenol (PCP) sodium salt voltammograms is in agreement with what was reported by Codognoto et al. 2005 (59) as a dimerized product peak of PCP using same SWV technique. A similar reason can be used to explain the peak (at about  $E_p = +0.4$  V  $E_p$ ) for the 2,4-dichlorophenol voltammograms. The additional peak is likely to be as a result of a polymerization reaction which cannot be found in Figure 4.25 and 4.28 for 2,4-dichlorophenol and pentachlorophenol sodium salt respectively, due to lower sensitivity in cyclic voltammetry compared with square wave stripping voltammetry.

Moreover, we can assume that the first oxidation peak at about  $E_p = +0.40$  V is a radical (phenoxy radical), which can be further isomerize to ortho and para products as predicted by Ureta-Zanartu M. S. et al. 2002 (57) and Enache T. A. and Oliveira-Brett A.M 2011 (58). The results of the investigation and their agreement with what had been earlier reported can also be used to propose schemes for phenol and chlorophenol derivatives redox reactions.

The effect of accumulation potential of all the investigated compounds can be simplified by representing its effect at both +0.40 V and +1.00 V accumulation potentials as shown in Figure 4.35 for the square wave stripping voltammetry. The summarized accumulation potential effect was used to propose schemes I-VI as shown in Figures 4.36 and 4.37 for the oxidation and reduction pathways for phenol and chlorophenol derivatives.



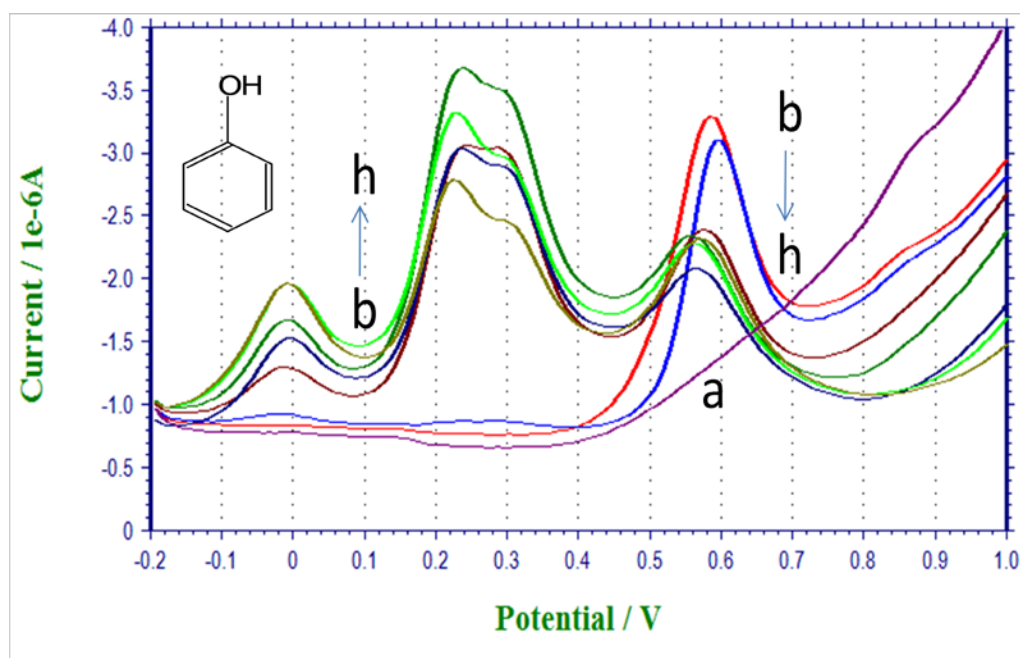


**Figure 4.29:** Square wave stripping voltammograms for 30  $\mu\text{M}$  phenol showing the signal behavior at different accumulation potentials (a) blank at 400 mV, (b) 400mV, (c) 500 mV, (d) 600 mV, (e) 700 mV, (f) 800 mV, (g) 900 mV (h) 1000 mV. Working conditions: amplitude, 25 mV; frequency 15 Hz; increment, 8 mV and accumulation time, 60 s in 0.1M PBS at pH 9.00.

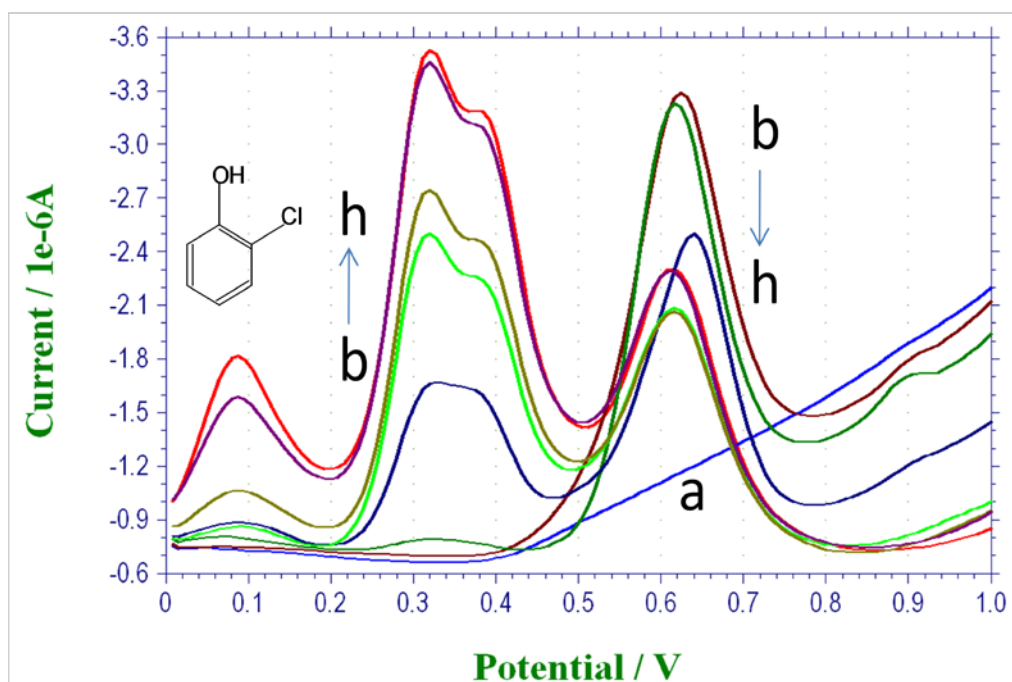


**Figure 4.30:** Square wave stripping voltammograms of 30  $\mu\text{M}$  2-chlorophenol showing the signal behavior at different accumulation potentials (a) blank at 400 mV, (b) 400mV, (c) 500 mV, (d) 600 mV, (e) 700 mV, (f) 800 mV, (g) 900 mV (h) 1000 mV. Working conditions: amplitude, 25 mV; frequency 15 Hz; increment, 8 mV and accumulation time, 60 s in 0.1M PBS at pH 7.00.

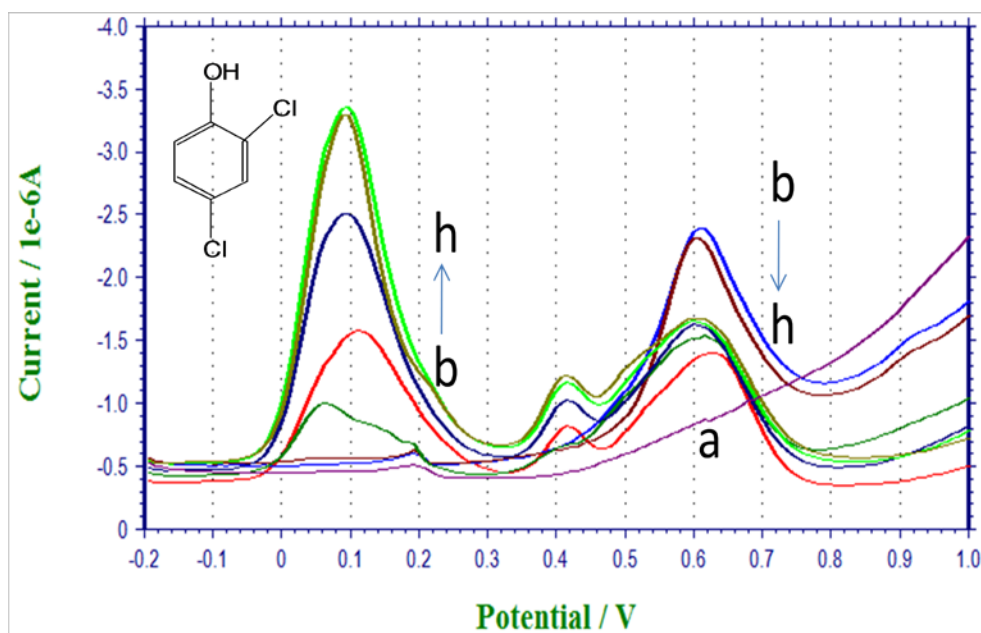


**Figure 4.31:** Square wave stripping voltammograms of 30  $\mu\text{M}$  2,4-dichlorophenols showing the signal behavior at different accumulation potentials (a) blank at 400 mV, (b) 400mV, (c) 500 mV, (d) 600 mV, (e) 700 mV, (f) 800 mV, (g) 900 mV (h) 1000 mV. Working conditions: amplitude, 25 mV; frequency 15 Hz; increment, 8 mV and accumulation time, 60 s in 0.1M PBS at pH 7.00.

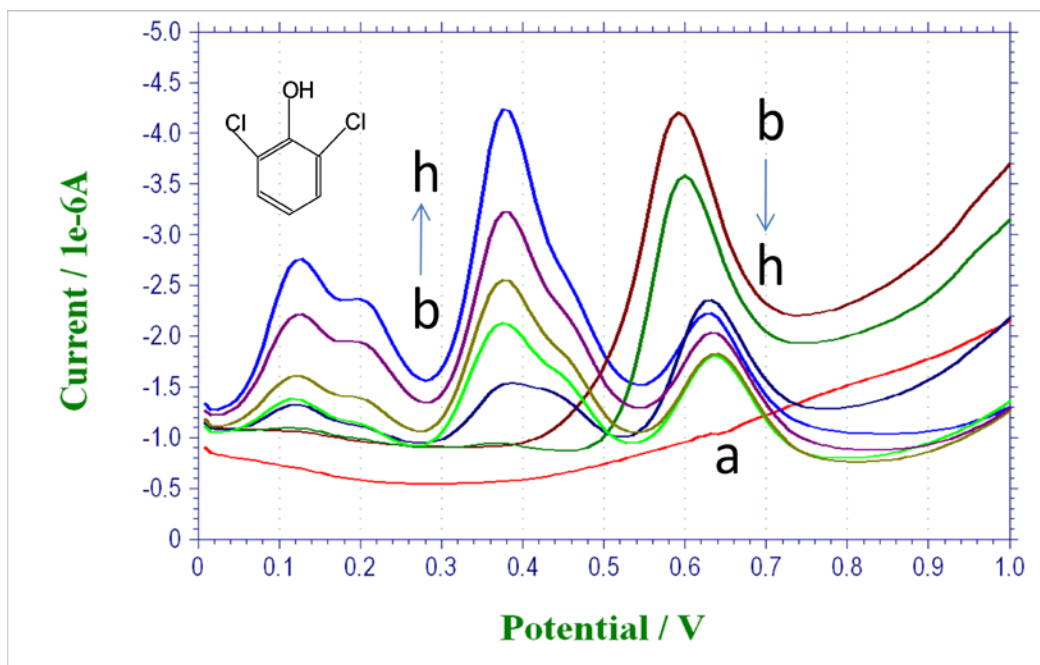


**Figure 4.32:** Square wave stripping voltammograms of 30  $\mu\text{M}$  2,6-dichlorophenols showing the signal behavior at different accumulation potentials (a) blank at 400 mV, (b) 400mV, (c) 500 mV, (d) 600 mV, (e) 700 mV, (f) 800 mV, (g) 900 mV (h) 1000 mV. Working conditions: amplitude, 25 mV; frequency 15 Hz; increment, 8 mV and accumulation time, 60 s in 0.1M PBS at pH 6.00.

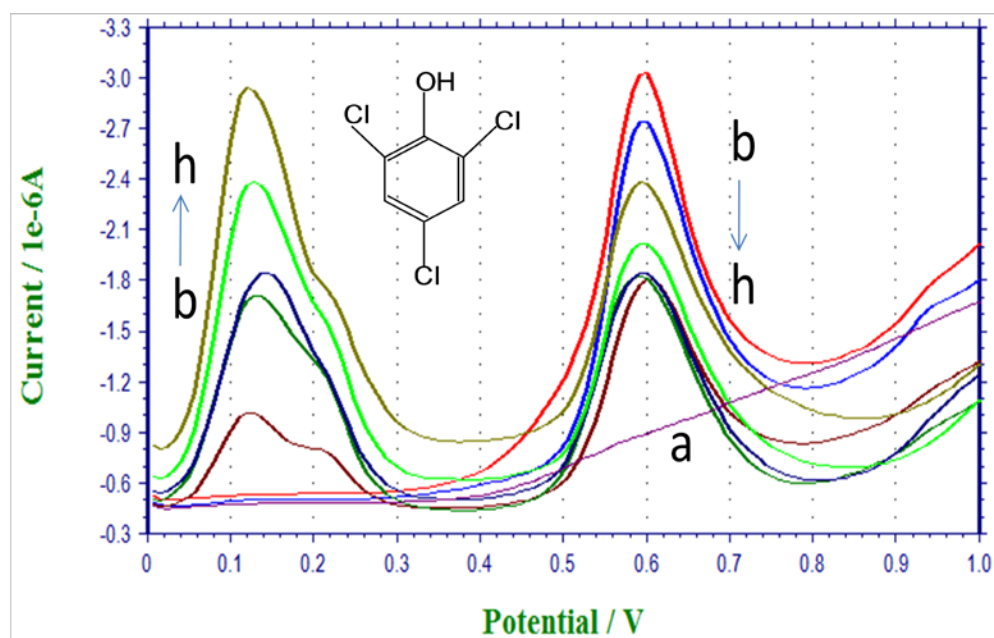


**Figure 4.33:** Square wave stripping voltammograms of 30 μM 2,4,6-trichlorophenol showing the signal behavior at different accumulation potentials (a) blank at 400 mV, (b) 400 mV, (c) 500 mV, (d) 600 mV, (e) 700 mV, (f) 800 mV, (g) 900 mV (h) 1000 mV. Working conditions: amplitude, 25 mV; frequency 15 Hz; increment, 8 mV and accumulation time, 60 s in 0.1M PBS at pH 6.00.

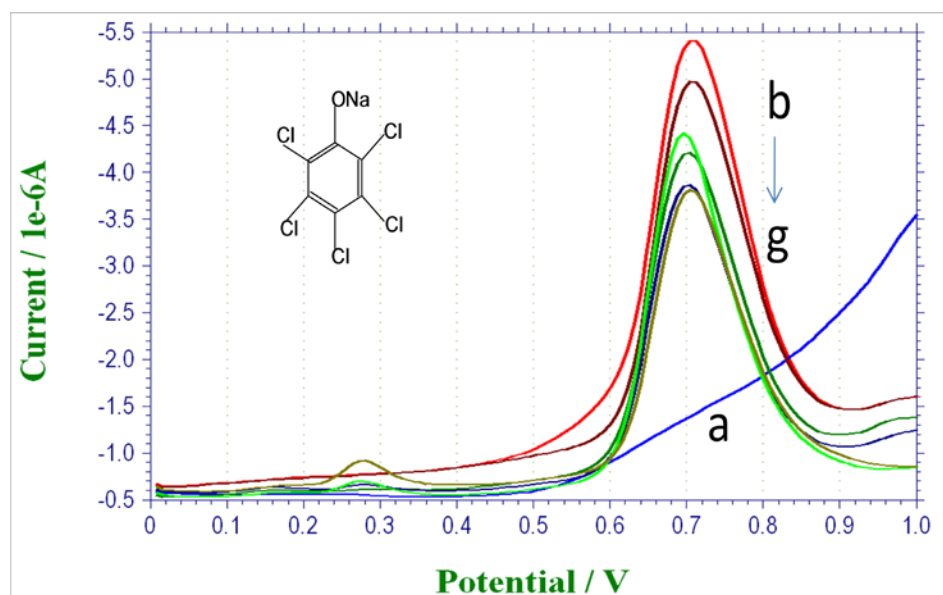


**Figure 4.34:** Square wave stripping voltammograms of 30  $\mu\text{M}$  pentachlorophenol sodium salt showing the signal behavior at different accumulation potentials (a) blank at 500 mV, (b) 500mV, (c) 600 mV, (d) 700 mV, (e) 800 mV, (f) 900 mV, (g) 1000 mV. Working conditions: amplitude, 25 mV; frequency 15 Hz; increment, 8 mV and accumulation time, 60 s in 0.1M PBS at pH 5.00.

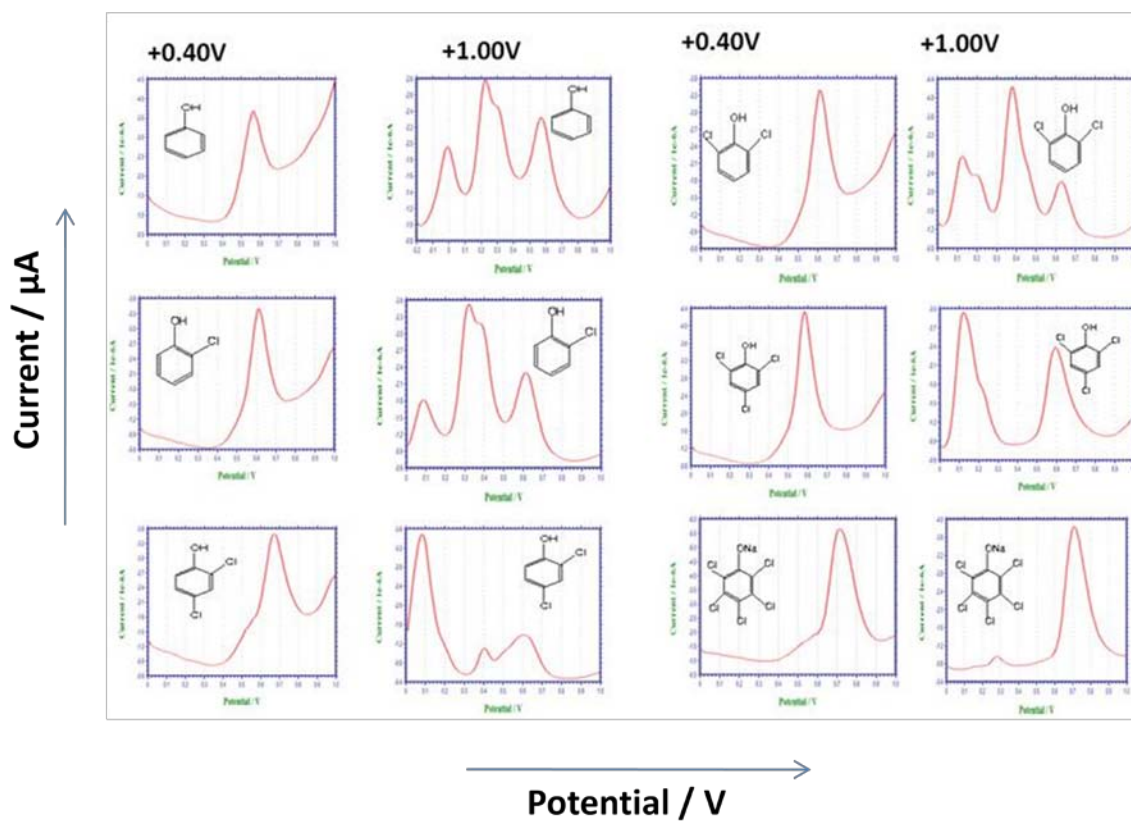


**Figure 4.35:** Effect of accumulation potential on the studied phenol and chlorophenol derivatives using square wave stripping voltammetry at +0.40 V and +1.00 V.

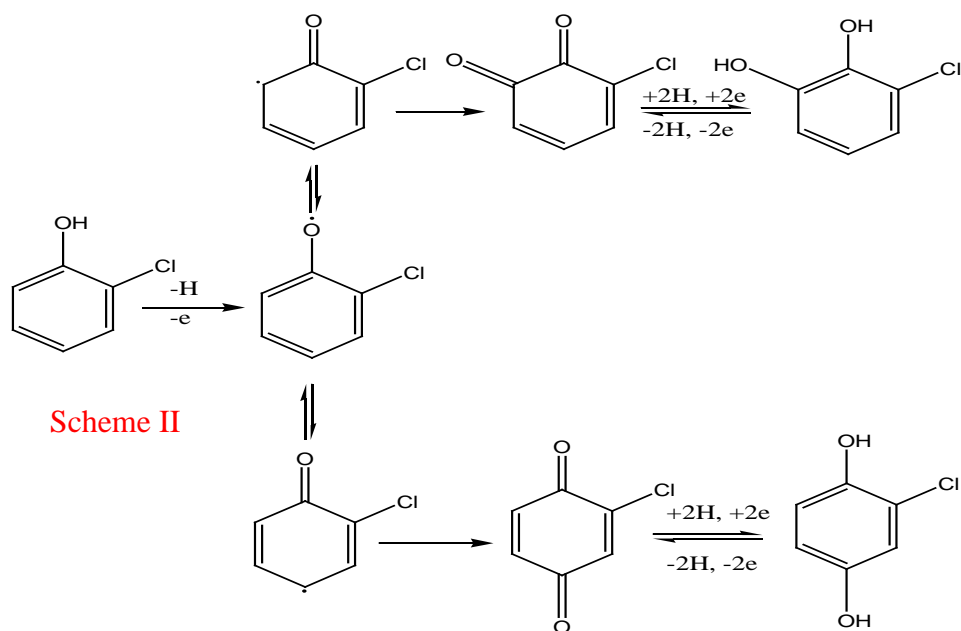
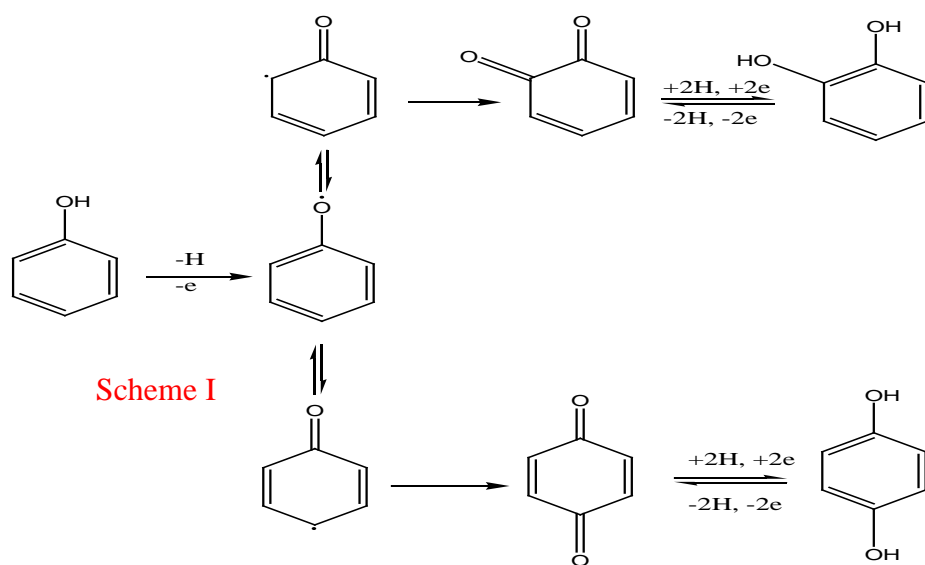
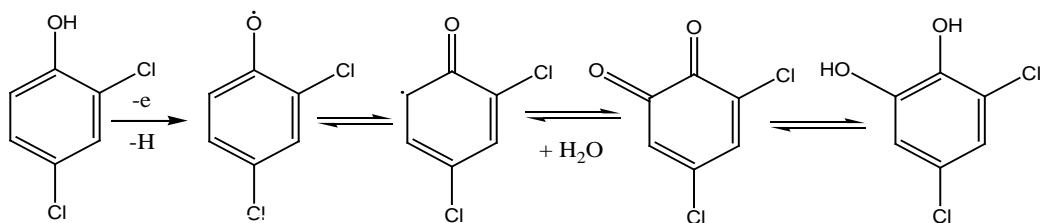
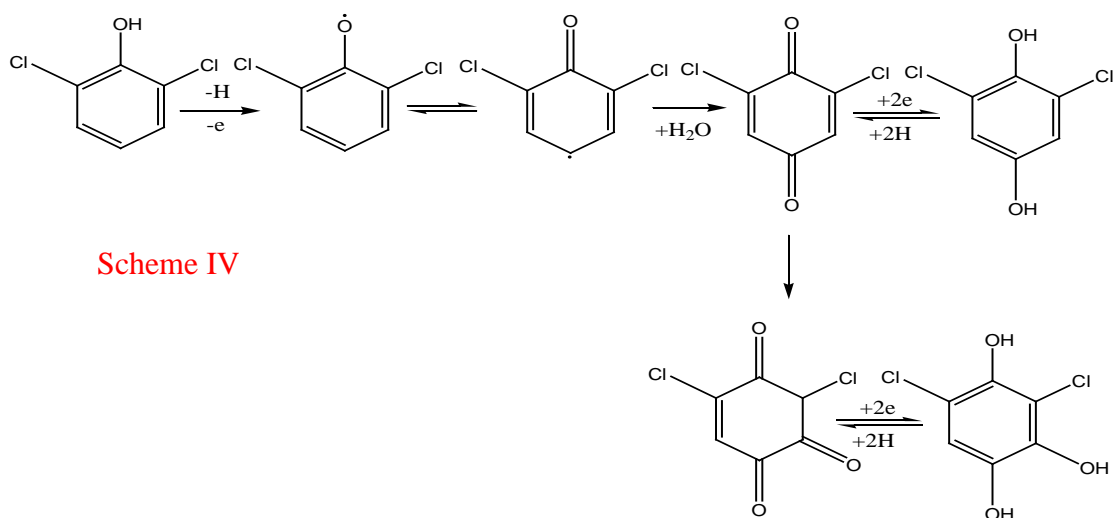


**Figure 4.36:** Scheme I and II showing the oxidation and reduction pathways of phenol and 2-chlorophenol.

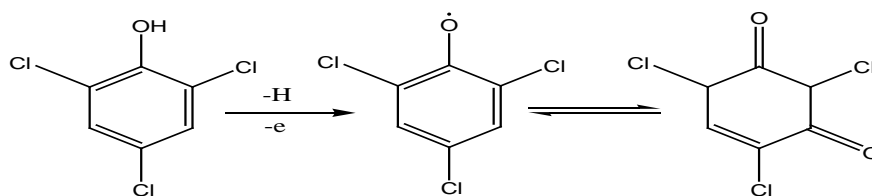




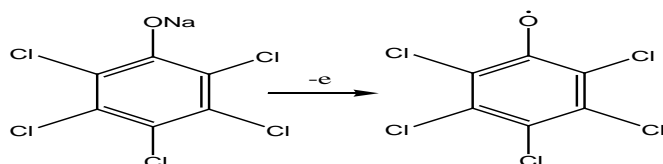
Scheme III



Scheme IV



Scheme V



Scheme VI

**Figure 4.37:** Scheme III, IV, V and VI showing the oxidation and reduction pathways of 2,4-dichlorophenol, 2,6-dichphenol, 2,4,6-trichlorophenol and pentachlorophenol sodium salt.

## 4.2 ANALYTICAL DETERMINATION OF 2-CHLOROPHENOL

There is a need to highlight the peaks resulted from the accumulation potential effect of 2-chlorophenol for proper understanding and possible utilization in analytical determination.

The first oxidized peak obtained at a mild potential (maximum potential of +0.40 V) which had been the only peak ever used in electrochemical investigation and analytical determination of 2-chlorophenol will be indicated as peak one (P1). The other peaks (along with P1 obtained between +0.50 V and +1.20V) that resulted from the fouling effect of the phenol which are at the same time the product of isomerization of 2-chlorophenol are labeled as peak two (P2) and peak three (P3) as shown in Figure 4.38. These peaks had been considered as problem to the sensitivity of phenolic compounds and here are being utilized for possible analytical determination.

The behavior of the peaks in relation to their effect of accumulation potential was illustrated by plotting their height against the accumulation potential as shown in Figure 4.39.

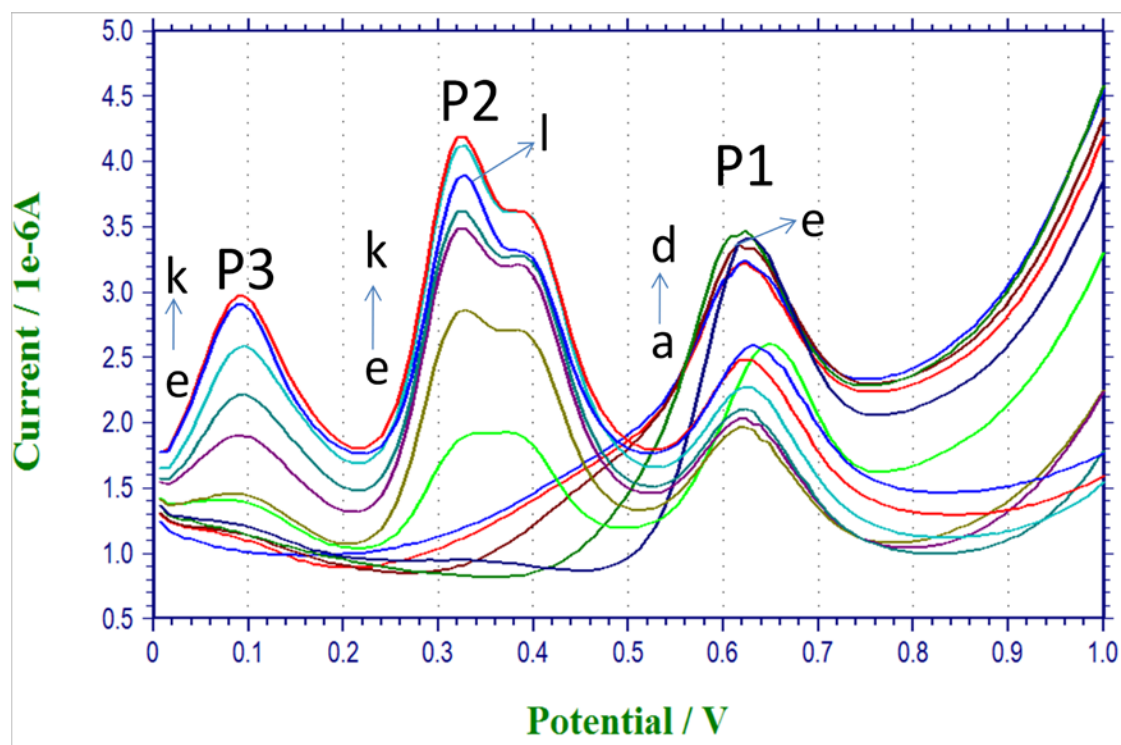


**Figure 4.38:** Square wave stripping voltammograms of 30  $\mu\text{M}$  2-chlorophenol showing the signal behavior at different accumulation potentials: (a) 100 mV, (b) 200 mV, (c) 300 mV, (d) 400 mV, (e) 500 mV, (f) 600 mV, (g) 700 mV, (h) 800 mV, (i) 900 mV, (j) 1000 mV, (k) 1100 mV and (l) 1200 mV for 60s accumulation time in 0.1 M PBS at pH 7.00. Other working conditions, as in Figure 4.30.

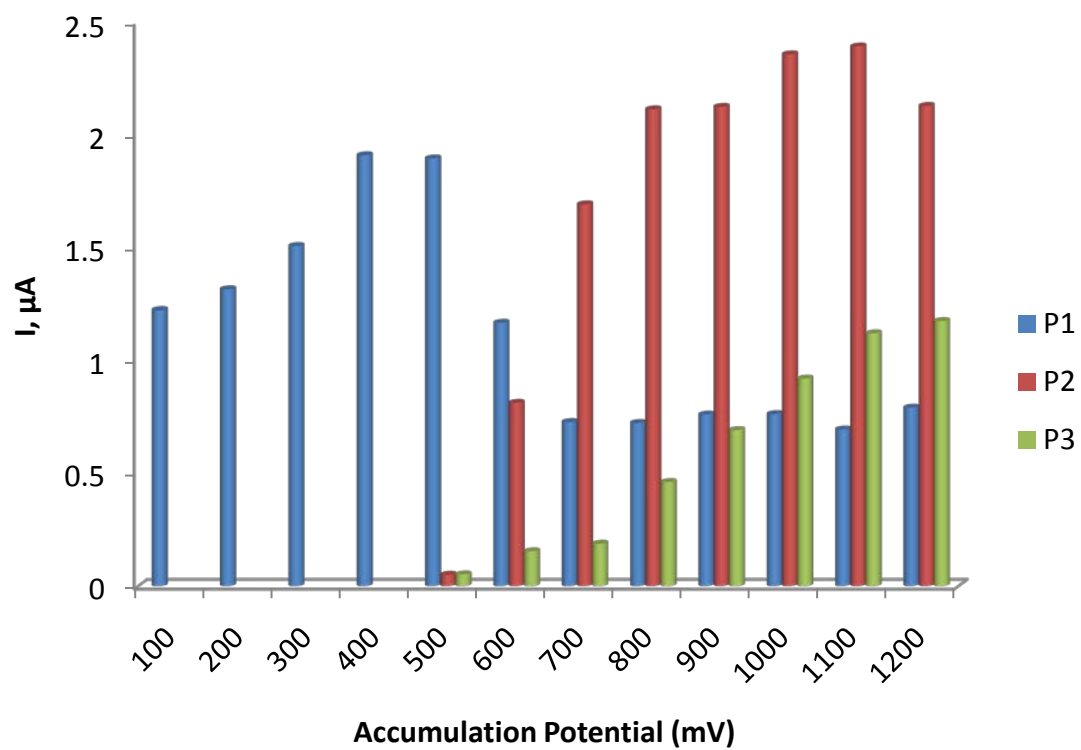


**Figure 4.39:** Corresponding plot showing the peak heights and accumulation potentials of 2-chlorophenol.

#### 4.2.1 Electrochemical Optimization of Peak One (P1) of 2-Chlorophenol

The optimization of peak one (P1 at +0.40V) was carried out in 0.1 M phosphate buffer solution of pH 7.00 according to the optimum pH condition in Table 4.3. The voltammograms and the corresponding plots for the optimum amplitude as shown in Figure 4.40 shows that the peak height was increasing linearly from 15 mV to 50 mV and that any further increase in amplitude leads to a lower peak height.

The effect of frequency at 50 mV amplitude (Figure 4.41) shows a similar behavior with an increase in the peak height between 15 Hz and 100 Hz with a relatively lower peak height at 125 Hz. This means that 100 Hz is the optimum frequency. Similarly, the increment optimum value at 100 Hz was found to be 8 mV when it was studied between 2 mV and 10 mV as shown in Figure 4.42.

The accumulation time was studied with both 30  $\mu$ M and 20  $\mu$ M 2-chlorophenol between 15 s and 120 s. However, the optimum accumulation time for both concentrations was found to be 60 s as shown in Figure 4.43 and 4.44 for 30  $\mu$ M and 20  $\mu$ M, respectively. An attempt to investigate at a lower concentration (10  $\mu$ M) gives a signal that is similar to the blank (solution without 2-chlorophenol).

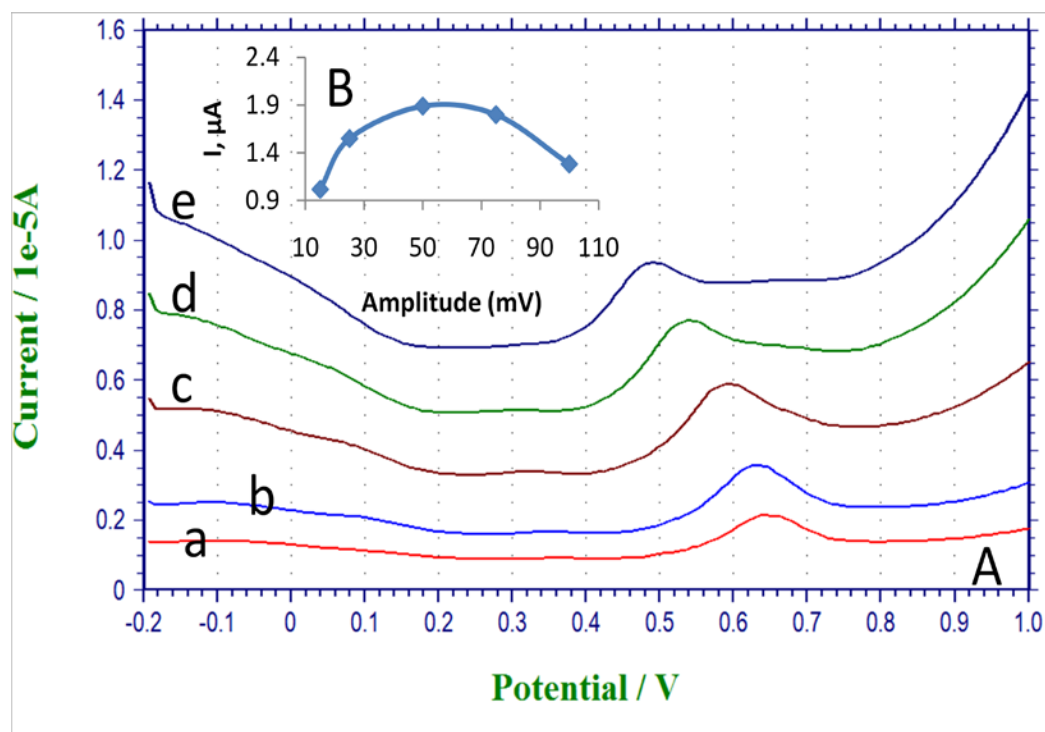


**Figure 4.40:** (A) Square wave stripping voltammograms for 30  $\mu\text{M}$  2-chlorophenol in 0.1 M of pH 7.00 PBS at different amplitudes: (a) 15 mV, (b) 25 mV, (c) 50 mV, (d) 75 mV and (e) 100 mV. Working conditions: accumulation time 60s; accumulation potential, +0.40 V; pulse width, 8 mV and frequency, 15 Hz. (B) Corresponding plots of Current ( $\mu\text{A}$ ) vs. Amplitude (mV).

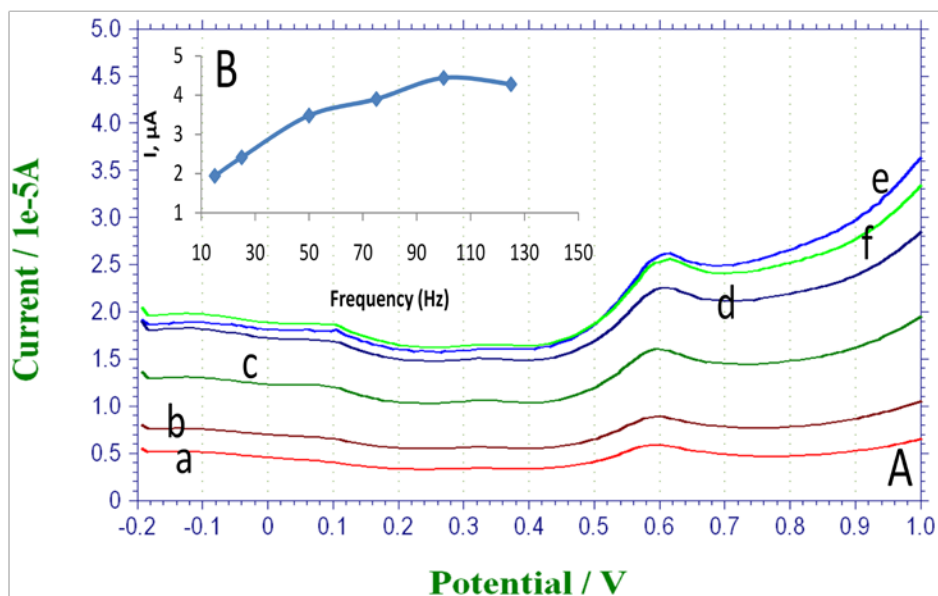


**Figure 4.41:** (A) Square wave stripping voltammograms for 30  $\mu\text{M}$  2-chlorophenol in 0.1 M PBS of pH 7.00 at 50 mV amplitude for different frequencies: (a) 15 Hz, (b) 25 Hz, (c) 50 Hz, (d) 75 Hz, (e) 100 Hz and (f) 125 Hz. Other working conditions as in Figure 4.40. (B) Corresponding plots of Current ( $\mu\text{A}$ ) vs. Frequency (Hz).

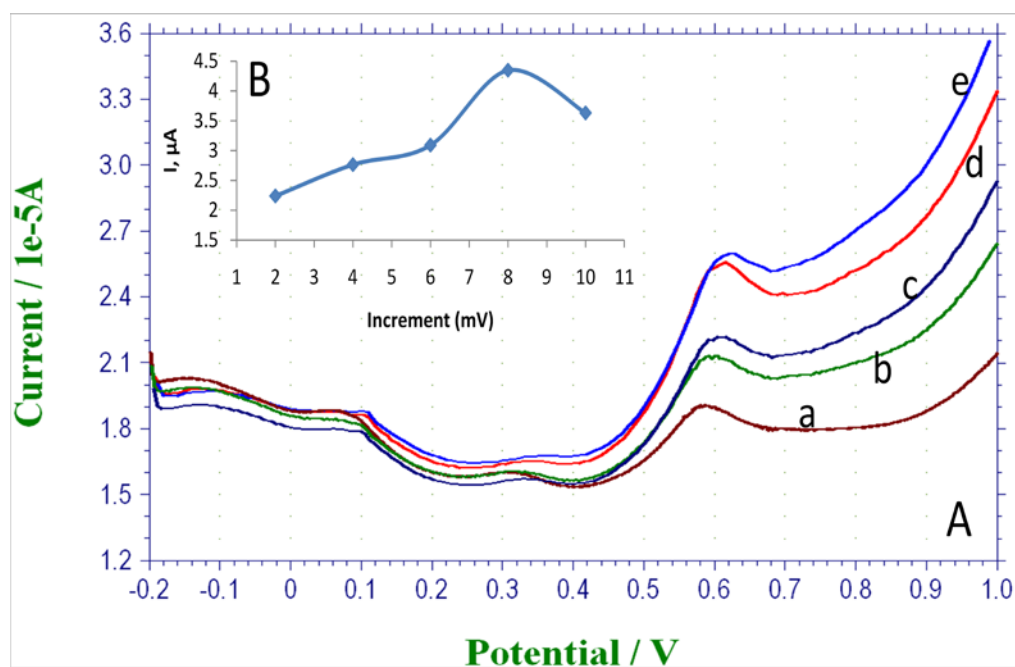


**Figure 4.42:** (A) Square wave stripping voltammograms for 30  $\mu\text{M}$  2-chlorophenol in 0.1 M PBS of pH 7.00 at 100 Hz frequency for different pulse widths: (a) 2 mV, (b) 4 mV, (c) 6 mV, (d) 8 mV and (e) 10 mV. Other working conditions as in Figure 4.40. (B) Corresponding plots of Current ( $\mu\text{A}$ ) vs. Increment, pulse width (mV).



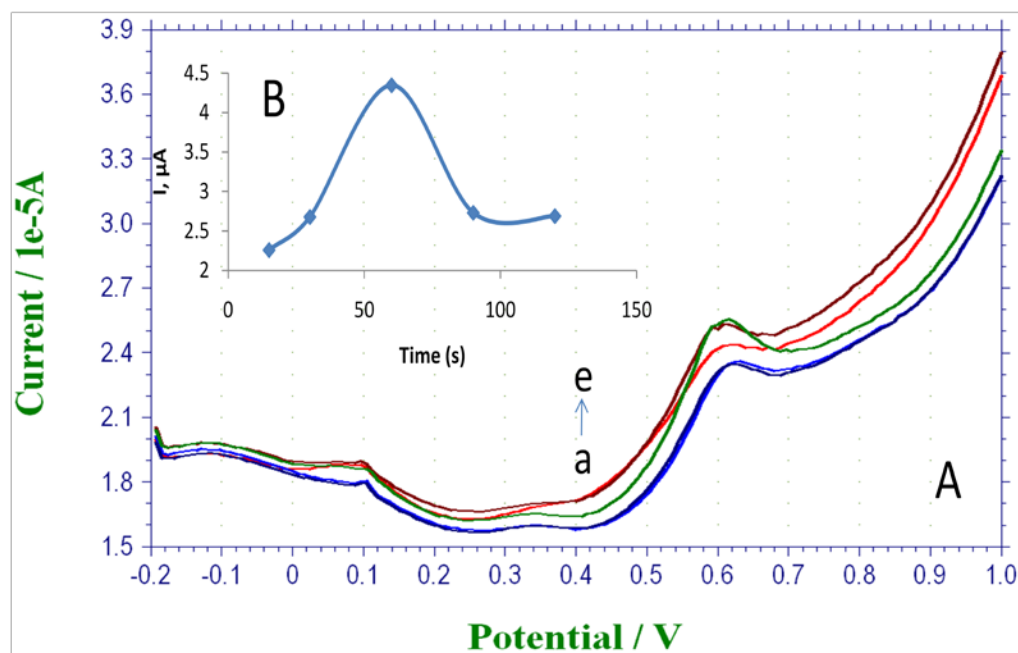


**Figure 4.43:** (A) Square wave stripping voltammograms for 30  $\mu$ M 2-chlorophenol in 0.1 M PBS of pH 7.00 at 8 mV pulse width for different accumulation times: (a) 15 s, (b) 30 s, (c) 60 s, (d) 90 s and (e) 120 s. Other working conditions as in Figure 4.40. (B) Corresponding plots of Current ( $\mu$ A) vs. Accumulation time (s).

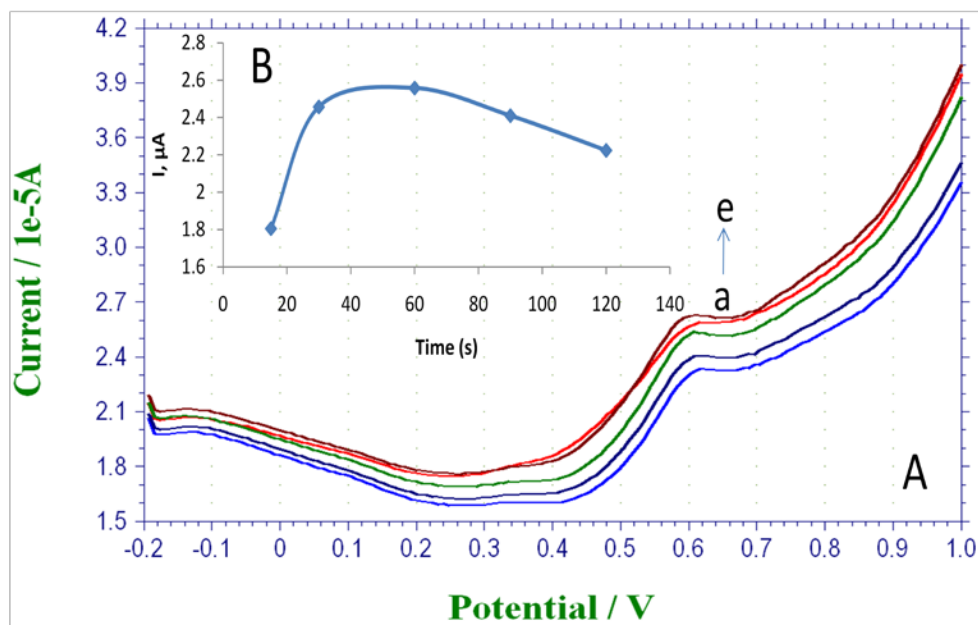


**Figure 4.44:** (A) Square wave stripping voltammograms for 20  $\mu$ M 2-chlorophenol in 0.1 M PBS of pH 7.00 at 8mV pulse width for different accumulation times: (a) 15 s, (b) 30 s, (c) 60 s, (d) 90 s and (e) 120 s. Other working conditions as in Figure 4.40. (B) Corresponding plot of Current ( $\mu$ A) vs. Accumulation time (s).

#### 4.2.2 Electrochemical Optimization of Peak Two (P2) of 2-Chlorophenol

The signal obtained for peak two (P2) compare with peak one (P1) as shown in Figure 4.39 showed that it is a more promising peak for future analytical determination than the peak one. Yet peak three (P3) is not in any way to compete with the other two peaks (P1 and P2). So, more investigation is required for the utilization of peak two (P2).

However, the investigation in Figure 4.39 was carried out at pH 7.00 which is the optimum pH for peak one and that cannot be assumed as the optimum pH for peak two.

In respect to this, the optimization of peak two (P2 at +1.10 V) will be considered from its pH effect as shown in Figure 4.45 while other electrochemical parameters are optimized in 0.1M phosphate buffer solution pH 5.00.

The effect of frequency was studied between 15 Hz and 125 Hz (Figure 4.46) with an increase in peak height up to 100 Hz with a relatively lower peak at 125 Hz.

Besides, amplitude effect at 100 Hz (Figure 4.47) between 15 mV and 150 mV was accompanied by the disappearance of peak three (peak at  $E_p$  about +0.80 V) with an optimum value of 100 mV. A similar behavior was observed with increment (pulse width) at 100 mV amplitude where an increase in peak height between 2 mV and 8 mV was observed as shown in Figure 4.48 with a relatively lower peak height at 10 mV.

The accumulation time was studied also with 30  $\mu$ M and 10  $\mu$ M 2-chlorophenol between 15 s and 120 s. The optimum accumulation time for both concentrations was found to be 60 s as shown in Figure 4.49 and 4.50 for 30 $\mu$ M and 10 $\mu$ M, respectively. The obtained

results are a clear indication of a better sensitivity of peak two (P2) compared with peak one (P1).

Moreover, the optimization parameters for both peak 1 (at +0.40 V) and peak 2 (at +1.10 V) are tabulated in Table 4.4.

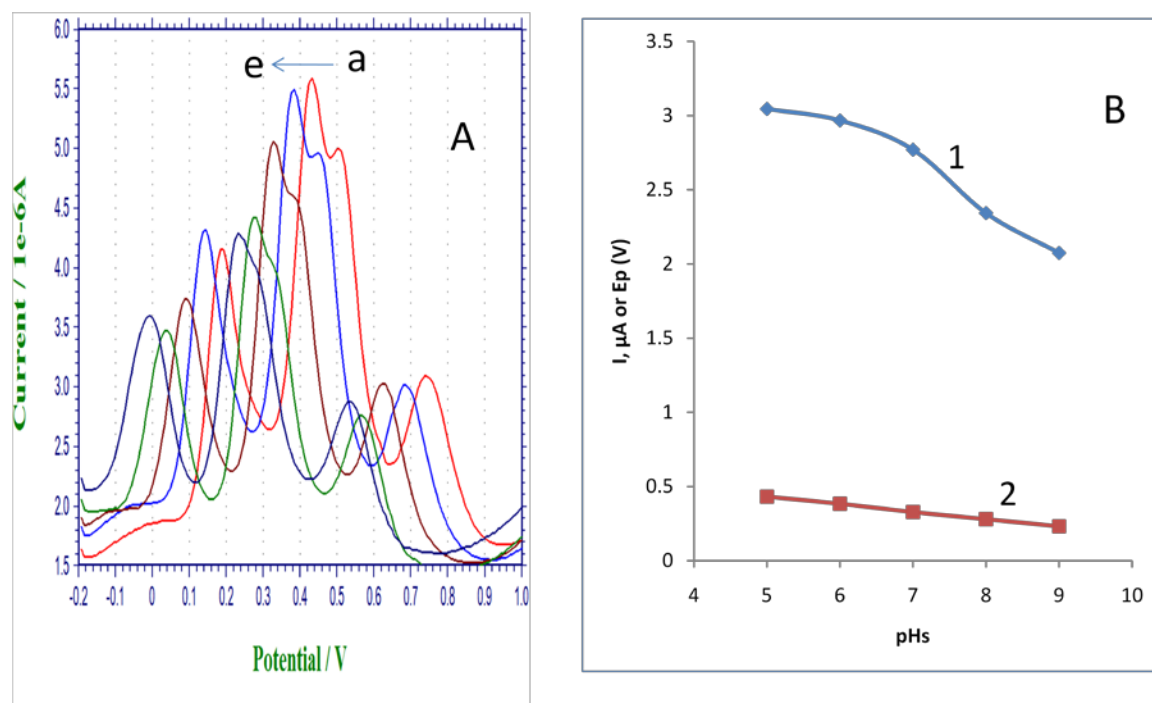


**Figure 4.45:** (A) Square wave stripping voltammograms of 30  $\mu\text{M}$  2-chlorophenol at +1.10 V accumulation potential 0.1 M PBS at different pHs. (a) 5.00, (b) 6.00, (c) 7.00, (d) 8.00 and (e) 9.00. Working conditions: accumulation time, 60 s; amplitude, 25 mV; pulse width, 8 mV and frequency, 15 Hz. (B) Corresponding plots showing the peak area (1) and the peak shift (2) in the electro-decomposition potentials against the pHs.

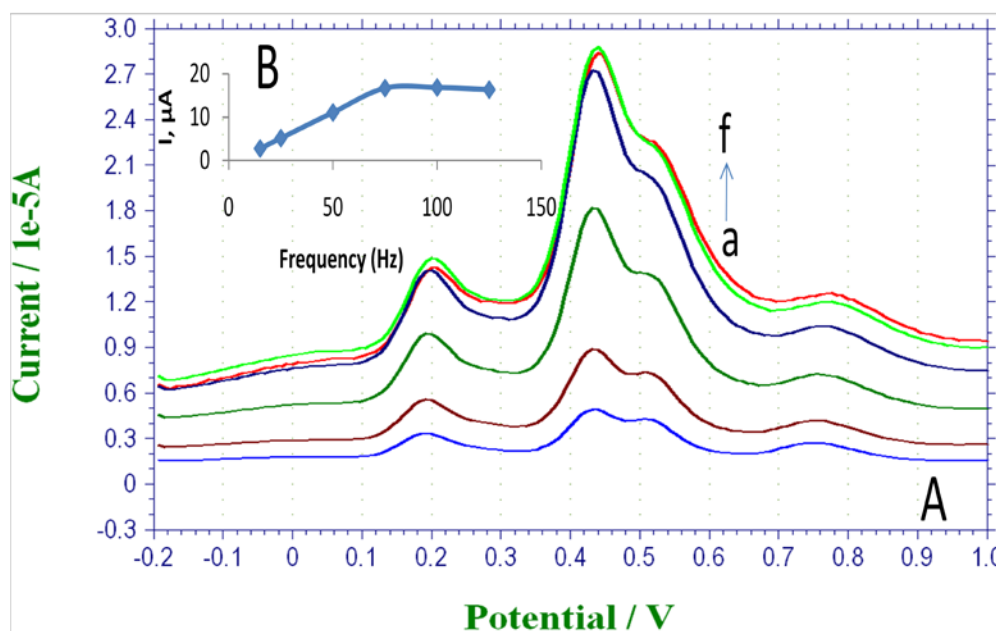


**Figure 4.46:** (A) Square wave stripping voltammograms for 30  $\mu\text{M}$  2-chlorophenol in 0.1 M PBS of pH 5.00 for different frequency values: (a) 15 Hz, (b) 25 Hz, (c) 50 Hz, (d) 75 Hz, (e) 100 Hz and (f) 125 Hz. Other working conditions as in Figure 4.45. (B) Corresponding plots of Current ( $\mu\text{A}$ ) vs. Frequency (Hz).

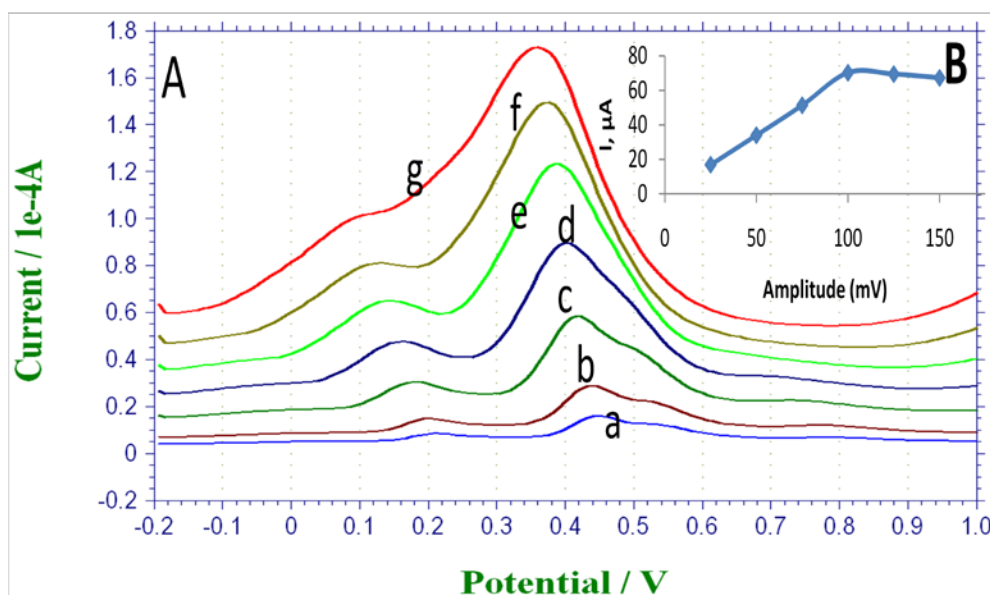


**Figure 4.47:** (A) Square wave stripping voltammograms for 30  $\mu\text{M}$  2-chlorophenol at 100 Hz frequency for different amplitudes: (a) 15 mV, (b) 25 mV, (c) 50 mV, (d) 75 mV, (e) 100 mV (f) 125 mV and (g) 150 mV. Other working conditions as in Figure 4.45. (B) Corresponding plots of Current ( $\mu\text{A}$ ) vs. Amplitude (mV).

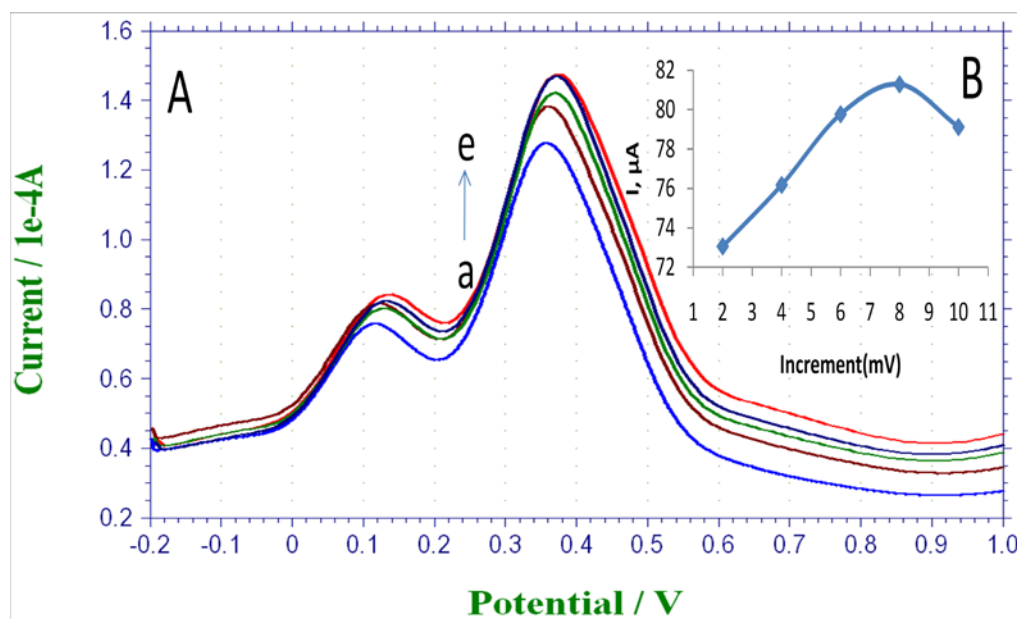


**Figure 4.48:** (A) Square wave stripping voltammograms for 30  $\mu\text{M}$  2-chlorophenol at 100 mV amplitude for different pulse width: (a) 2 mV, (b) 4 mV, (c) 6 mV, (d) 8 mV, and (e) 10 mV. Other working conditions as in Figure 4.45. (B) Corresponding plots of Current ( $\mu\text{A}$ ) vs. Increment, pulse width (mV).



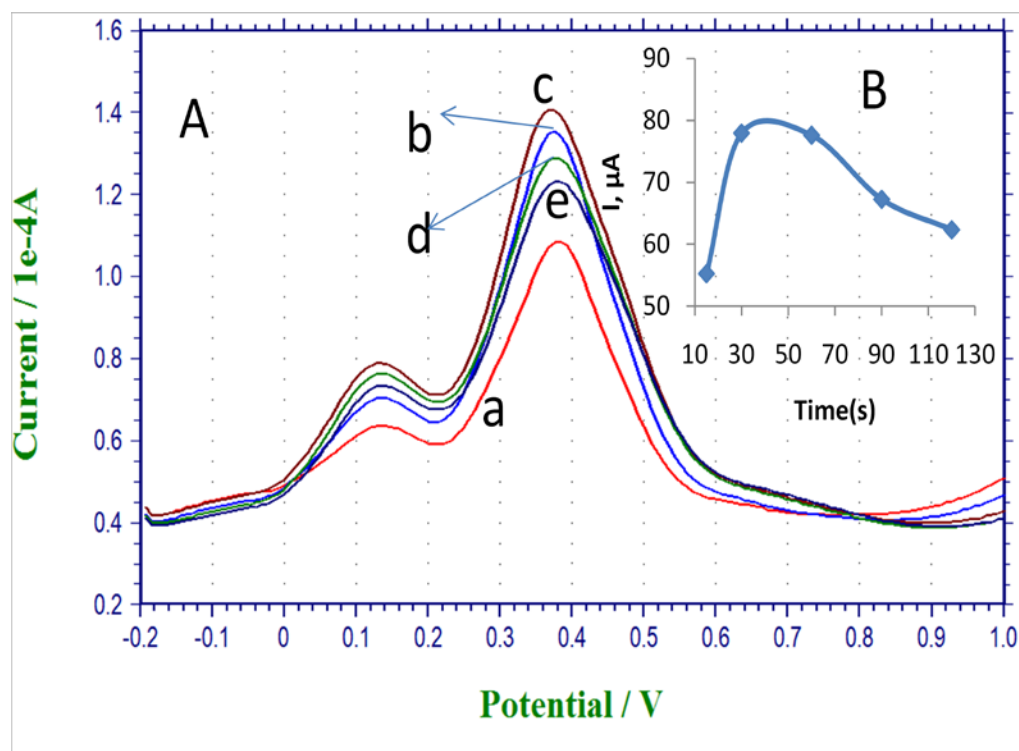


**Figure 4.49:** (A) Square wave stripping voltammograms for 30  $\mu\text{M}$  2-chlorophenol at 8 mV pulse width for different accumulation times: (a) 15 s, (b) 30 s, (c) 60 s, (d) 90 s and (e) 120s. Other working conditions as in Figure 4.45. (B) Corresponding plot of Current ( $\mu\text{A}$ ) vs. accumulation time (s).

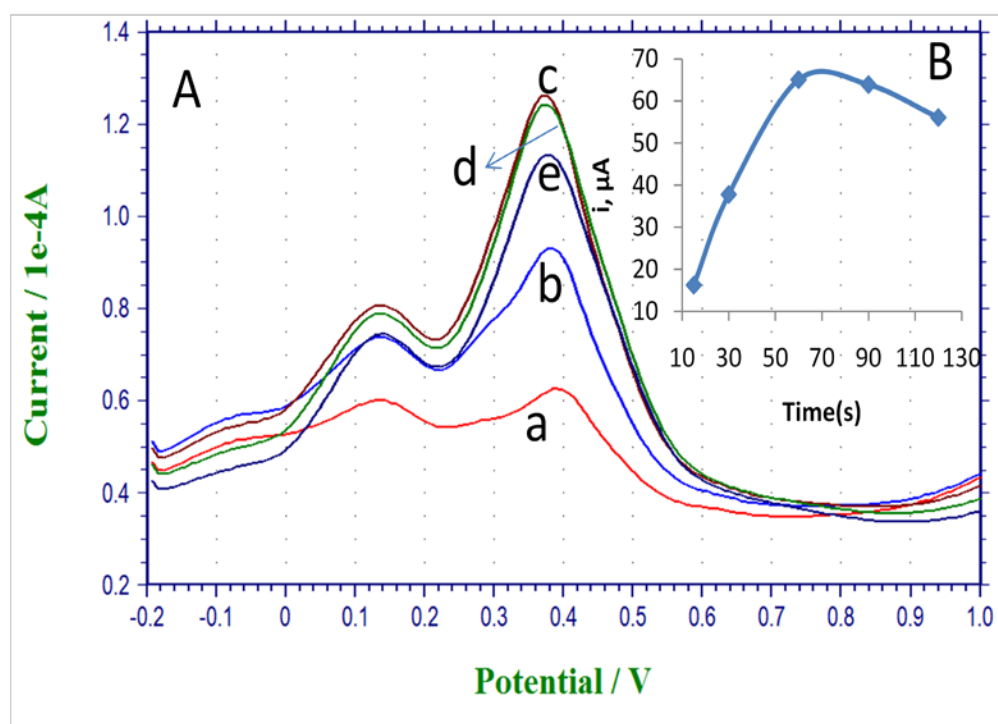


**Figure 4.50:** (A) Square wave stripping voltammograms for 10  $\mu\text{M}$  2-chlorophenol at 8 mV pulse width for different accumulation times: (a) 15 s, (b) 30 s, (c) 60 s, (d) 90 s and (e) 120 s. Other working conditions as in Figure 4.45. (B) Corresponding plot of Current ( $\mu\text{A}$ ) vs. accumulation time (s).

**Table 4.4: Optimized Conditions for Peak One (P1) and Peak Two (P2) of 2-Chlorophenol.**

2-chlorophenol	pH	Acc. Pot.	Acc. Time	Freq.	Amp.	Incr.
P1	7.00	400 mV	60s	100 Hz	50 mV	8 mV
P2	5.00	1100 mV	60s	100 Hz	100 mV	8 mV

### 4.2.3 Analytical Performance of Peak One (P1) and Peak Two (P2)

The analytical performances of both peaks (P1 and P2) were investigated under the optimum parameters summarized in Table 4.4 with seven repeated measurements of the same concentration of 30 $\mu$ M (Figure 4.51). The relative standard deviations for peak one (P1 at +0.40 V) and peak two (P2 at +1.10 V) were calculated to be 1.31% and 1.84% respectively.

### 4.2.4 Calibration Curves for Peak One (P1) and Peak Two (P2)

The optimization parameters (Table 4.4) obtained for both peaks were used to construct calibration curves. The voltammograms for peak one was from 10 $\mu$ M to 60 $\mu$ M as shown in Figure 4.52A. The limit of detection (LOD) for peak one was 18.99  $\mu$ M (2.44 ppm).

However, the limit of detection for peak one was surprisingly higher than the upper limit of detection for peak two and voltammograms with a dynamic range of 2 $\mu$ M to 12 $\mu$ M with a limit of detection of 1.11  $\mu$ M (140 ppb) as shown in Figure 4.52B.

The corresponding plots for both voltammograms are shown in Figure 4.53 along with their respective linear regressions and limit of detections as obtained from the following equations:

**Equation: Sigmoidal, Hill, 4 Parameter for Peak one (P1)**

$$F = y^0 + a * x^b / (c^b + x^b)$$

$a = 2141233.7922$ ,  $b = 1.3796$ ,  $c = 460372.1066$ ,  $y^0 = 0.1307$  and  $F$  is average plus 3 standard deviation of the blank.

**Equation: Sigmoidal, Chapman, 4 Parameter for peak two (P2)**

$$f = y^0 + a * (1 - \exp(-b * x))^c$$

$a = 59.5595$ ,  $b = 0.2482$ ,  $c = 3.8838$ ,  $y^0 = 1.4586$   $F$  is average plus 3 standard deviation of the blank.

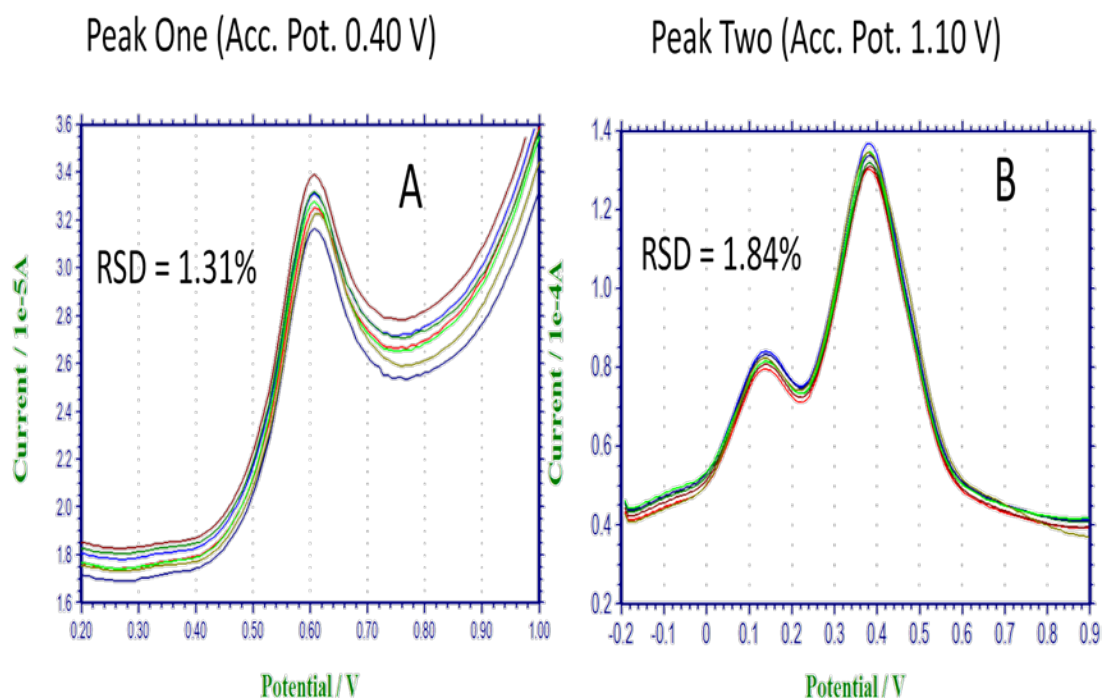


**Figure 4.51:** (A) Square wave stripping Voltammograms for analytical performance of seven repeated measurements for 30  $\mu$ M 2-chlorophenol of Peak One (P1 at +0.40 V) in 0.1 M PBS pH 7.00. Working conditions: accumulation time, 60 s; amplitude, 50 mV; pulse width, 8 mV and frequency, 100 Hz. (B) Square wave stripping Voltammograms for analytical performance of seven repeated measurements for 30  $\mu$ M 2-chlorophenol of Peak Two (P1 at +1.10 V) in 0.1 M PBS pH 5.00. Working conditions: accumulation time, 60 s; amplitude, 100 mV; pulse width, 8 mV and frequency, 100 Hz.

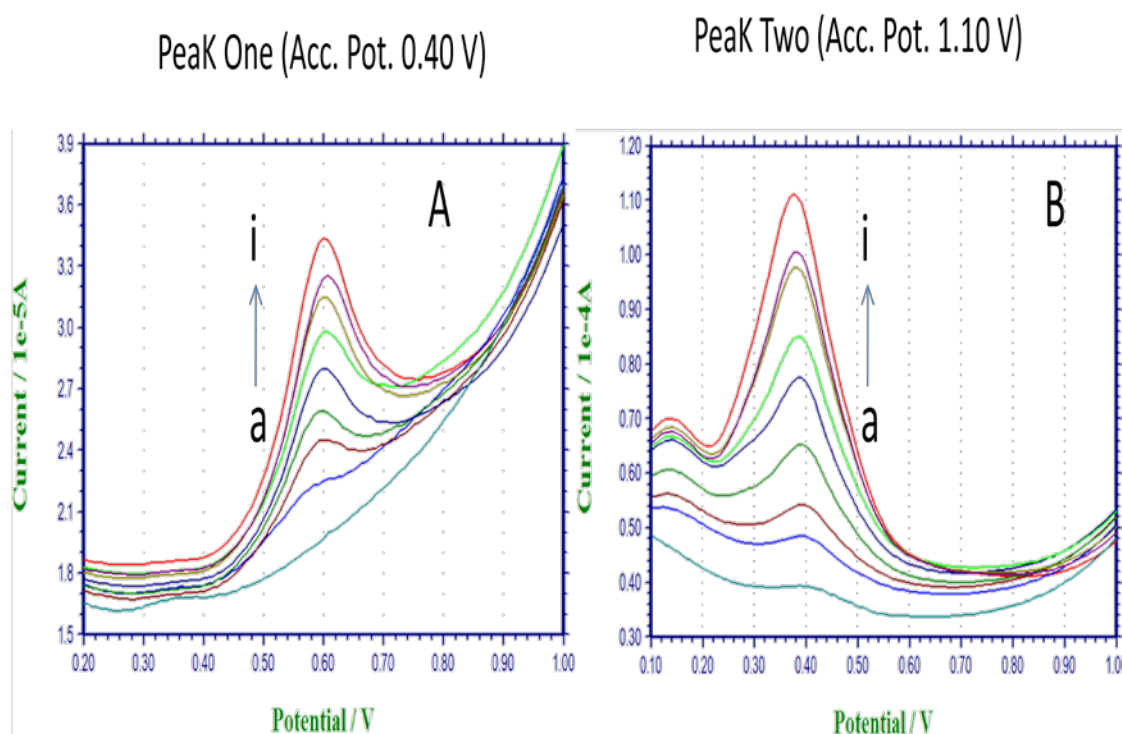


**Figure 4.52:** (A) Square wave stripping Voltammograms for 2-chlorophenol at different concentrations for Peak One (P1 at +0.40 V) in 0.1 M PBS pH 7.00 (a) blank, (b) 10  $\mu$ M, (c) 20  $\mu$ M, (d) 25  $\mu$ M, (e) 35  $\mu$ M, (f) 40  $\mu$ M, (g) 50  $\mu$ M, (h) 55  $\mu$ M and (i) 60  $\mu$ M. Working conditions: accumulation time, 60 s; amplitude, 50 mV; pulse width, 8 mV and frequency, 100 Hz. (B) Voltammograms for 2-chlorophenol at different concentration for peak two (P2 at +1.10V) in 0.1 M PBS pH 5.00 (a) blank, (b) 2  $\mu$ M, (c) 3  $\mu$ M, (d) 4  $\mu$ M, (e) 5  $\mu$ M, (f) 6  $\mu$ M, (g) 7  $\mu$ M, (h) 9  $\mu$ M and (i) 11  $\mu$ M. Working conditions: accumulation time, 60 s; amplitude, 100 mV; pulse width, 8 mV and frequency, 100 Hz.

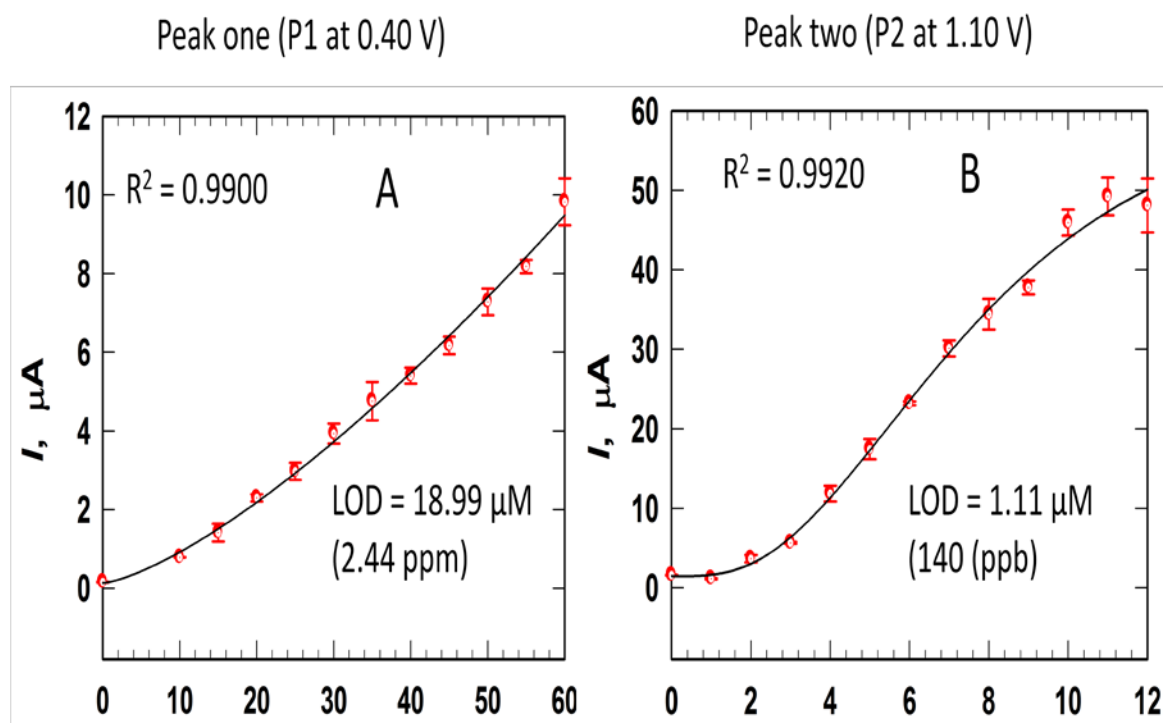


**Figure 4.53:** Corresponding plots for calibration curves (A) Peak One (P1) and (B) Peak Two (P2).



## CHAPTER 5

### 5.0 CONCLUSIONS AND FUTURE PROSPECTIVES

#### 5.1 CONCLUSIONS

Electrochemical techniques (Cyclic voltammetry and square wave stripping voltammetry) were successfully used to study the oxidation and reduction pathways of phenol and chlorophenol derivatives. We were able to confirm the isomerize product peaks of phenol and chlorophenol derivatives at their respective optimized pH of 0.1M phosphate buffer solution. The pentachlorophenol sodium salt was found to have no isomerized product peaks due to the absence of the exchange protons in the five positions of benzene ring. This clarifies the misconception reported by Ureta-Zanartu et al. 2002 (57) that pentachlorophenol does not passivate (foul) the surface of glassy carbon electrode (GCE) despite the adsorption control process of the electrode that leads to polymerization reaction. Hence phenol and studied chlorophenol derivatives with no exception passivate the surface of GCE due to irreversibility of the oxidized product that isomerize to ortho- and the para-isomerize's products at low concentration except pentachlorophenol. With the effect of the accumulation potential, in addition to the first irreversible anodic peak, other peaks were obtained as well. By optimizing these peaks, more sensitive analytical method than reported Sun D. and Zhang H. 2006 (51) was successfully developed.

Our results indicated that phenol and all studied chlorophenol derivatives with no exception passivate the surface of glassy carbon electrode due to the irreversible first oxidized product (phenoxy radicals), and that all of the phenol and chlorophenol derivatives isomerize at low concentration except pentachlorophenol. That allows us to predict six schemes (I – VI) for oxidation and reduction reactions pathways for phenol and chlorophenol derivatives.

Furthermore, we were able to obtain peaks other than the irreversible well-known conventional anodic peak at a single scan utilizing of accumulation potential effect. We have also optimized the obtained peaks for possible analytical determination at a lower detection limit.

## **5.2 FUTURE PROSPECTIVES**

All attempts to characterize the surface of glassy carbon electrode after accumulation of the oxidized phenols were proved abortive. The problem was the extraction of the product from the surface of the electrode since it is an interfacial reaction.

There is a need for surface characterization of the GCE using other techniques with an integrated system to monitor the electrical properties that can be utilized to study the intermediate and final product of the electrochemical redox reaction of phenol and chlorophenol derivatives.

Besides, simultaneous determinations of chlorophenol, aminophenol and nitrophenol should be considered.

## REFERENCES

1. Holler, F. James; Skoog, Douglas A.; West, Donald M. (1996). Fundamentals of analytical chemistry. Philadelphia: Saunders College Publishers. ISBN 0-03-005938-0.
2. Nieman, Timothy A.; Skoog, Douglas A.; Holler, F. James (1998). Principle of Instrumental Analysis. Pacific Grove, CA: Brooks/Cole ISBN 0-03-002078-6.
3. Wang J. (2001). Analytical Electrochemistry, Second Edition, VCH Publishers, New York ISBN 0-471-22823-0
4. Harvey David (2000). Modern Analytical Chemistry. McGraw-Hill Company ISBN 0-07-237547-7
5. Barker G. C.; Jenkins. International Congress on Analytical Chemistry, 1952, 77, 685 – 696.
6. O’Dea J. J.; Osteryoung, J.; Osteryoung, R.A., Anal. Chem., 1981, 53, 695 – 701.
7. Updike S. J.; Hicks, G. P., Nature, 1967, 214, 986 -988.
8. Bard A. J. (2001). Electrochemical Methods Fundamentals and Applications, Second Edition, John Wiley and Sons, Inc., New York.
9. Harris P. J. F., Philosophical Magazine, 2004, 84, 3159 -3167.
10. Almeida C. M. V. B.; Giannetti, B. F., Electrochemistry Communication, 2002, 4, 985 – 988.

11. Wang J.; Kirgoz, A.U.; Mo, J.; Lu, J.; Kawde, A.; Muck, A., *Electrochemistry Communication*, 2001, 3, 203 – 208.
12. Bond A. M.; Mahon, P. J.; Schiewe, J.; Vicente-Beckett, V., *Analytica Chimica Acta*, 1997, 345, 67 -74.
13. Wang J., *Electroanalysis*, 1991, 3, 255 – 259.
14. Baldwin R. P.; Thomsen, K. N., *Talanta*, 1991, 38, 1, 1 – 16.
15. Ortega F.; Dominguez, E.; Burestedt, E.; Emneus, J.; Gorton, L.; Marko-Varga, G., *J. Chromatography A*, 1994, 675, 1 – 2, 65 – 78.
16. Castillo M.; Domingues, R.; Alpendurada, M. F.; Barcelo, D., *Analytica chimica Acta*, 1997, 353, 133 – 142.
17. Agency for Toxic Substances and Disease Registry (ATSDR), 4770 Buford Hwy NE, Atlanta, GA 30341.
18. World Health Organization. Environmental health criteria for Chlorophenols other than pentachlorophenol. Supplement, Draft. July 31, 1986.
19. World Health Organization. Environmental health criteria for pentachlorophenol. Supplement, Draft. July 31, 1986.
20. Grazyna B. *J Chromatography B*, 1996, 682, 167 - 172.
21. Zafra-Gomez A; Luzon-Toro B; Jimenez-Diaz I; Ballesteros O; Navalon A. J. *Pharmaceutical and Biomedical Analysis*, 2010, 53, 103 - 108.
22. Faraji H; Tehrani M S; Husain S W. *J. Chromatography A*, 2009, 1216, 8569 - 8567.
23. Proestos C; Sereli D; Komaitis M. *Food Chemistry*, 2006, 95, 44 - 52.

24. Di Corcia A; Bellioni A; Madbouly M D; Marchese M. J. Chromatography A, 1996, 733, 383 - 393.
25. Angelino S; Gennaro M C. Analytical Chimica Acta, 1997, 346, 61 - 67.
26. Zakeri-Milani P; Barzegar-Jelali M; Tajerzadeh H; Azarmi Y; Valizadeh H. J. Pharmaceutical and Biomedical Analysis, 2005, 39, 624 - 630.
27. Jakopic J; Petkovsek M M; Likozar A; Solar A; Stampar F; Veberic R. Food Chemistry, 2011, 124, 1100 - 1106.
28. Zhang P; Shi Z; Feng Y. Talanta, 2011, 85, 2581 - 2586.
29. Correia C F; Nunes P M; Borges dos Santos R M; Martinho Simoes J A. Thermochimica Acta, 2004, 420, 3 - 11.
30. Alonso M V; Olier M; Perez J M; Rodriguez F; Echeverria J. Thermochimica Acta, 2004, 419, 161 - 167.
31. Chaghi R; de Menorval L; Charnay C; Derrien G; Zajac J. J. Colloid and Interface Science. 2008, 326, 227 - 234.
32. Fiamegos Y C; Stalikas C D; Pilidis G A; Karayannis M I. Analytical Chimica Acta, 2000, 403, 315 - 323.
33. Vieira I. C. and Fatibello-Filho O. Analytical Chimica Acta, 1998, 366, 111 - 118.
34. Nolan L.C and O'Connor K. E. Analytical Biochemistry, 2005, 344, 224 - 231.
35. Ni Y; Xia, Z and Kokot S., J Hazardous Mat., 2011, 192, 722 - 729.
36. Shaghghi M; Manzoori J L; Jouyban A. Food Chemistry, 2008, 108, 695 - 701.
37. Kang C; Wang Y; Li R; Du Y; Li J; Zhang B; Zhou L; Du Y. Microchemical Journal, 2000, 64, 161 - 171.

38. Fiamegos Y C; Stalikas C D; Pilidis G A. *Analytical Chimica Acta*, 2002, 467, 105 - 114.
39. Rahman N; Hoda M. *II Farmaco*, 2002, 57, 435 - 441.
40. Hemmateenejad B; Akhond M; Samari F. *Spectrochimica Acta Part A*, 2007, 67, 958 - 965.
41. Galindez-Mayer J; Ramon-Gallegos J; Ruiz-Ordaz N; Juarez-Ramirez C; Salmero-Alcocer A; Poggi-Varaldo H M. *Biochemical engineering Journal*, 2008, 38, 147 - 157.
42. Roy J J; Abraham T E; Abhijith K S; Kumar P V S; Thakur M S. *Biosensors and Bioelectronics*, 2005, 21, 206 - 211.
43. Korkut S; Keskinler B; Erhan E. *Talanta*, 2008, 76, 1147 - 1152.
44. Anh T M; Dzyadevych S V; Soldatkin A P; Chien N D; Jaffrezic-Renault N; Chovelon J M. *Talanta*, 2002, 56, 627 - 634.
45. Wang P; Liu M; Kan J. *Sensors and actuators B*, 2009, 140, 577 - 584.
46. Adamski J; Nowak P; Kochana J. *Electrochimica Acta*, 2010, 55, 2363 - 2367.
47. Zhao J; Wu D; Zhi J. *Bioelectrochemistry*, 2009, 75, 44 - 49.
48. R N Adams "Electrochemistry at Solid Electrode" Marcel Dekker, New York, 1969, Pg. 363.
49. Spataru T; Spataru N. *J Hazardous Mat.*, 2010, 180, 777 - 780.
50. Yang H; Zheng X; Huang W; Wu K. *Colloid and Surface B: Biointerphases*, 2008, 65, 281 - 284.
51. Sun D; Zhang H. *Water Research*, 2006, 40, 3069 - 3074.
52. Wang J; Deo R P; Musameh M. *Electroanalysis*, 2003, 15, 23-24, 1830 - 1834.

53. Zhao Q; Guan L; Gu Z; Zhuang Q. *Electroanalysis*, 2005, 17, 1, 85 - 88.
54. Wang X; Wu Q; Ding Y. *Colloid and Surface A: Physicochem. Eng. Aspect*, 2008, 329, 119 - 124.
55. Pera-Titus M; Garcia-Molina V; Banos M A; Gimenez J; Esplugas S. *Applied Catalysis B: Environmental*, 2004, 47, 219 - 256.
56. Ezerskis Z; Jusys Z. *Pure Appl. Chem.*, 2001, 73, 12, 1929 - 1940.
57. Ureta-Zanartu M S; Bustos P; Berrios C; Diez M C; Mora M L; Gutierrez C. *Electrochimica Acta* 2002, 47, 2399 - 2406.
58. Enache T A; Oliveira-Brett A M. *J Electroanalytical Chemistry*, 2011, 655, 9 - 16.
59. Codognoto L; Machado S. A. S.; Avaca L. A., *Portugaliae Electrochimica Acta*, 2005, 23, 225 -246.



## VITAE

❖ NURUDEEN ADEWALE ODEWUNMI

❖ Born in Lagos, Nigeria

❖ Received Bachelor of Technology (B.Tech) degree in Industrial Chemistry from the Federal University of Technology, Akure (FUTA), Ondo State, Nigeria in June, 2005.(FUTA), Ondo State, Nigeria in June, 2005.

❖ Worked as an Assistant Quality and Process Controller at Amigos Technologies from 2006 – 2007.

❖ Joined KFUPM in February, 2010 as a Research Assistant along with the pursuance of Master Degree in Chemistry.

❖ Awarded M.S Degree in Chemistry in June 2012 with a specialization in Analytical Chemistry (Electroanalytical)

❖ An oral Presenter of a Paper “Electrochemical Investigation and Analytical Determination of Ciprofloxacin in pure and drug Formulation Forms” at the third student conference in Saudi Arabia.

❖ Present Address: KFUPM, Dhahran, 31261, KSA.

E-mail: g200903830@kfupm.edu.sa

❖ Permanent Address: 6, Akinola Street, Shasha, Ajako B/S, ALimosho LGA, Lagos Niageria.

**E-mail: mailwale32@yahoo.com**